

國立臺灣大學生物資源暨農學院生物科技研究所

博士論文



Institute of Biotechnology
College of Bioresources and Agriculture
National Taiwan University

Doctoral Thesis

病毒抑制子 HC-Pro 對於 HEN1 功能及甲基轉移酶活性之
研究

HEN1 functional characterization and evaluation of
methyltransferase activity under viral suppressor HC-Pro

沙妮妲

Neda Sanobar

指導教授：林詩舜 博士

Advisor: Shih-Shun Lin, Ph.D.

中華民國 111 年 5 月

May 2022

Acknowledgment



In deep reverence and thankfulness, I bow my head to ALLAH for making this task reach its completion.

I wish to express my sincere gratitude and thankfulness to Prof. Shih-Shun Lin for his constant support, encouragement and guidance throughout these four years. I would also like to thanks Dr. Wu, Dr. Chiou, Dr. Chen and Dr. Yang for their time and willingness to be my committee members.

My sincere thanks are owed to the PMBV lab of IOB for providing me facilities which made it possible to achieve desired targets during my Ph.D. work. I express my deep sense of gratitude to all the lab members for their cooperation, keen interest, constructive attitude, everlasting moral support and encouragement which helped me a lot to acquire the fabulous experience of my Ph.D. work.

This lab has given me wonderful friends like Arthuro, Veny, Phuong Anh, Abigail, Thanh Ha and Pookiie who filled this journey with memories. I will always be grateful for their encouragement, moral support and constant care.

Above all, words would be inadequate to express the indefinite gratitude to my mother, Mrs. Qaisra Parveen and my husband, Najim Akhtar for their guidance and enormous amount of moral support throughout the journey. There are many more people to thank for their help, but words are not enough for them.

Neda Sanobar

中文摘要

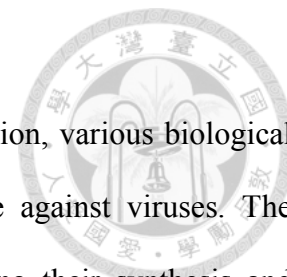


植物基因靜默系統在基因調控、各種生物和發育過程以及諸如防禦病毒等逆境反應中發揮著廣泛的作用。該系統的小核糖核酸 (sRNA) 含量藉由調整其合成和代謝率來嚴格調節。3' 末端核糖的 2'-O-甲基化是為小核糖核酸提供穩定性的主要過程，甲基轉移酶 (HEN1) 扮演此至關重要的角色。在本論文中，我們比較並分析被子植物阿拉伯芥 HEN1 (AtHEN1) 和苔蘚植物地錢 (*Marchantia polymorpha*) HEN1 (MpHEN1) 的異同處。我們的體內及體外結果顯示 MpHEN1 活性與 AtHEN1 相當，並且它們對雙鏈體微型核糖核酸 (miRNA duplex) 的特異性保持一致。此外，系統發育樹和多重氨基酸序列比對凸顯了不同植物家族 HEN1 之間保守區域的分子。另外我們也分析在不同物種界中 HEN1 的 MTase 區域以了解蛋白質的相關性。蕪菁嵌紋病毒 (TuMV) 的 P1/HC-Pro 是一種已知的 RNA 靜默抑制因子，也已知可抑制 HEN1 對於 sRNA 的甲基化。在本研究中，我們發現 HC-Pro 可與 AtHEN1 物理性交互作用並抑制其甲基化活性。此外，HC-Pro 上的 FRNK 是兩個蛋白相互作用和抑制能力重要的區域。體外 EMSA 數據顯示 TuMV 的 GST-HC-Pro 缺乏 sRNA 雙鏈體結合能力。令人驚訝的是，隨著 TuMV HC-Pro 劑量提升可增加對 MpHEN1 活性的抑制。未來可針對 HEN1 和不同種病毒 HC-Pros 的相互作用機制研究，增進我們對病毒抑制因子的認識。

關鍵字：小核糖核酸、HEN1 甲基轉移酶、P1/HC-Pro、HEN1- HC-Pro 交互作用



Abstract



Plant gene silencing system plays a broad role in gene regulation, various biological and developmental processes, and stress responses such as defense against viruses. The system's small RNA (sRNA) levels are tightly regulated by adjusting their synthesis and turnover rates. The 2'-*O*-methylation of the 3' terminal ribose is a major process that provides stability to the small RNAs which is facilitated by HEN1. In this thesis, we analyzed the *Arabidopsis thaliana* HEN1 (AtHEN1), an angiosperm as well as *Marchantia polymorpha* HEN1 (MpHEN1) which is a bryophyte at different levels. Our in vivo and in vitro data have shown MpHEN1 activity being comparable with AtHEN1, and their substrate specificity towards duplex miRNA remained consistent. Furthermore, the phylogenetic tree and multiple alignment highlighted the conserved molecular evolution among HEN1 of different plants family. The MTase domain of HEN1 which is found across different kingdom of species is analyzed to understand the relatedness of the protein. The P1/HC-Pro of the turnip mosaic virus (TuMV) is a known RNA silencing suppressor and is also known to inhibit the HEN1 mediated methylation of sRNAs. In this study, we have found that HC-Pro physically interacts with AtHEN1 inhibiting the methylation activity of the latter. Moreover, the FRNK motif of HC-Pro plays a significant role in this interaction and inhibition ability of the protein. The in vitro EMSA data indicates that GST-HC-Pro of TuMV lacks sRNA duplex-binding ability. Surprisingly, TuMV HC-Pro also inhibits MpHEN1 activity in a dosage-dependent manner. Further investigations on understanding interaction mechanism of HEN1 and various potyviral HC-Pros can advance our knowledge of viral suppressors.

Keywords: sRNA, HEN1, methylation, P1/HC-Pro, HEN1-HC-Pro interaction.

Publications



1. **Neda Sanobar***, Pin-Chun Lin*, Zhao-Jun Pan, Ru-Ying Fang, Veny Tjita, Fang-Fang Chen, Hao-Ching Wang, Huang-Lung Tsai, Shu-Hsing Wu, Tang-Long Shen, Yan-Huey Chen and Shih-Shun Lin. "Investigating the viral suppressor HC-pro inhibiting small RNA methylation through functional comparison of HEN1 in angiosperm and bryophyte." *Viruses* 13, no. 9 (2021): ;1837 (Co-first author).
2. Sin-Fen Hu, Wei-Lun Wei, Syuan-Fei Hong, Ru-Ying Fang, Hsin-Yi Wu, Pin-Chun Lin, **Neda Sanobar**, Hsin-Ping Wang, Margo Sulistio, Chun-Ta Wu, Hsiao-Feng Lo, Shih-Shun Lin. "Investigation of the effects of P1 on HC-pro-mediated gene silencing suppression through genetics and omics approaches." *Botanical Studies* 61, no. 1 (2020): 1-18.
3. (*Under Communication*) Syuan-Fei Hong, Ru-Ying Fang, Wei-Lun Wei, Zhao-Jun Pan, Yu-Ling Hung, **Neda Sanobar**, Yen-Hsin Chiu¹, Li-Yu Daisy Liu, Tang-Long Shen, Ho-Chun Yang, Mei-Yeh Jade Lu, Shih-Shun Lin. "Counteraction between host defense and turnip mosaic virus (TuMV) infection through the viral RNA and AGO1 degradations."

Conferences

1. **Neda Sanobar**, Pin-Chun Lin and Shih-Shun Lin. “The study of interactive region of HEN1 with HC-Pro.” Poster Presentation, *Taiwan Society of Plant Biologists*, 2020, Taiwan.
2. **Neda Sanobar**, Pin-Chun Lin and Shih-Shun Lin, “The involvement of autophagic genes in AGO1 degradation along with HC-Pro and study of interactive region of HEN1 with HC-Pro.” Poster presentation, *Japan-Taiwan Plant Biology*, 2019, Japan.



Abbreviations



sRNA	Small RNA
HEN1	HUA ENHANCER 1
AGO1	Argonaute 1
AtHEN1	<i>Arabidopsis thaliana</i> HUA ENHANCER 1
MpHEN1	<i>Marchantia polymorpha</i> HUA ENHANCER 1
TuMV	Turnip mosaic virus
PTGS	Post-transcriptional gene silencing
TGS	Transcriptional gene silencing
dsRNA	Double stranded RNA
miRNA	MicroRNA
siRNA	Short-interfering RNA
piRNA	PIWI-interacting RNA
tsRNA	Transfer RNA-derived small RNA
nt	Nucleotide
hc-siRNA	Heterochromatic siRNA
phasRNAs	Phased secondary siRNA
easiRNA	Epigenetically activated siRNA
DCL1	Dicer-like RNA III endonuclease 1

HYL1	HYPONASTIC LEAVES 1
RdDM	RNA-directed DNA methylation
DRM2	Domains Rearranged Methylase 2
RDR	RNA dependent RNA polymerase
SE	SERRATE
TE:	Transposable elements
TCV	Turnip crinkle virus
CaLCuV	Cabbage leaf curl virus
CMV	Cucumber mosaic virus
HESO1	HEN1 SUPPRESSOR 1
MTase:	Methyltransferase
dsRBD:	Double-stranded RNA binding domain
PLD	PPIase-like domain
SDN1	Small RNA degrading nuclease 1
PAGE	Polyacrylamide gel electrophoresis
VSR	Viral suppressor of RNA silencing
RSS	Suppressor of RNA silencing
HC-Pro	Helper component proteinase
PVC	Potato virus C



TVMV	Tobacco vein mottling virus
PVY	Potato virus Y
TEV	Tobacco etch virus
rgs-CaM:	Regulator of gene silencing calmodulin-like protein
PVA	Potato virus A
SAMS:	S-adenosyl-L-methionine synthetase
SAHH:	S-adenosyl-L-homocysteine hydrolase
AA	Amino acid
LMV	Lettuce mosaic virus
ZYMV	Zucchini yellow mosaic virus
GFP	Green fluorescence protein
PPV	Plum pox virus
vsRNA	Virus derived siRNA
CIRV	Carnation Italian ringspot virus
TYMV	Turnip yellow mosaic virus
AdoMet	S-adenosyl-L-methionine
AdoHcy	S-adenosyl-L-homocysteine
Pimet	piRNA MTase
Pnkp:	Polynucleotide kinase-phosphatase



IPTG	Isopropyl β -D-1-thiogalactopyranoside
PMSF	Phenylmethylsulfonyl fluoride
SDS-PAGE	Sodium dodecyl sulfate-polyacrylamide gel electrophoresis
PVDF	Polyvinylidene difluoride
ECL	Enhanced chemiluminescence
GMQE	Global Model Quality Estimation
QMEAN	Qualitative Model Energy Analysis
ss-miR159:	Single stranded miR159
ds-miR159	Double stranded miR159
HENN1	Nematode HEN1
DmHEN1	<i>Drosophila melanogaster's</i> HEN1
mHen1	Mouse Hen1
FPLC	Fast Protein Liquid Chromatography
ML	Maximum likelihood
CHLM	MAGNESIUM-PROTOPORPHYRIN IX METHYLTRANSFERASE
Sm	<i>Selaginella moellendorffii</i>
At	<i>Arabidopsis thaliana</i>
Os	<i>Oryza sativa</i>
Atr	<i>Amborella trichopoda</i>



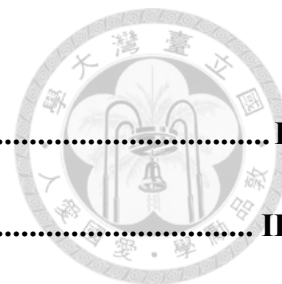
Pab	<i>Picea abies</i>
Mp	<i>Marchantia polymorpha</i>
Pp	<i>Physcomitrella patens</i>
Kf	<i>Klebsormidium flaccidum</i>
Cr	<i>Chlamydomonas reinhardtii</i>
Vc	<i>Volvox carteri</i>
Zm	<i>Zea mays</i>
Sf	<i>Sphagnum fallax</i>
Sl	<i>Solanum lycopersicum</i>
Pt	<i>Populus trichocarpa</i>
Gr	<i>Gossypium raimondii</i>
Tc	<i>Theobroma cacao</i>
Cpa	<i>Carica papaya</i>
Vv	<i>Vitis vinifera</i>
WT	Wild type
MS	Murashige and Skoog
TAK	Takaragaike
Nb	<i>Nicotiana benthamiana</i>
RISC	RNA induced silencing complex



Dpi	Days post inoculation
EMSA	Electrophoresis mobility shift assay
TuCP	Turnip mosaic virus coat protein
ORMV	Oilseed rape mosaic tobamovirus
Me	Methylated
UnMe	Unmethylated
Unt	Untreated
Y2H	Yeast two-hybrid screening
Co-IP	Co-immunoprecipitation



Contents



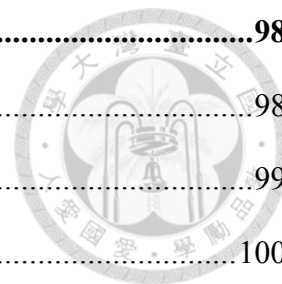
Acknowledgment	I
中文摘要.....	II
Abstract.....	IV
Publications.....	V
Conferences.....	VI
Abbreviations.....	VII
Contents	XIII
Chapter 1.	1
Literature Review	1
1.1. Post-transcriptional gene silencing in plants.....	1
1.1.1. miRNA pathway.....	2
1.1.2. siRNA pathway	3
1.2. miRNA stability in plants.....	6
1.2.1. HEN1 mediated methylation maintains miRNA stability	6
i. HEN1 structure studies.....	7
ii. HEN1 substrate specificity.....	8
iii. HEN1 antagonistic HESO1 destabilizes unmethylated miRNAs.....	9
iv. siRNA competes with miRNA for HEN1 mediated methylation.....	10
v. Analysis of methylation status of small RNAs.....	10
1.3. PTGS induced during virus infection.....	11

1.3.1. Suppressor of RNA silencing (RSS)	11
1.3.2. Suppression of virus induced PTGS.....	12
1.3.3. Role of RSS in plant pathogenicity	13
1.4. Potyvirus.....	14
1.4.1. Turnip mosaic virus (TuMV).....	15
1.4.2. Helper Component Protease (HC-Pro).....	15
i. Multiple functions of HC-Pro.....	18
ii. Structural characterization of HC-Pro.....	19
iii. Critical FRNK motif of HC-Pro.....	20
1.4.3. ZYMV HC-Pro.....	21
1.4.4. TEV HC-Pro	22
1.4.5. TuMV HC-Pro	25
1.4.6. HC-Pro in antiviral RNA silencing pathway	26
1.5. Conclusion and thesis organization	27
1.6. Figures and legends.....	29
Chapter 2.	33
Plant's HEN1 functional/characteristics evaluation.....	33
2.1. Abstract	33
2.2. Introduction.....	34
2.3. Material and methods	37
2.3.1. Plasmid construction	37
2.3.2. Recombinant protein purification.....	37
2.3.3. The α -AtHEN1 and α -MpHEN1 IgG Production	38

2.3.4. Western blotting	39
2.3.5. In vitro HEN1 Methylation assay.....	39
2.3.6. β -elimination and northern blot.....	40
2.3.7. MpHEN1 Structure Modeling.....	40
2.3.8. Sequence Identity, Similarity, and Phylogenetic Analysis	41
2.4. Results.....	42
2.4.1. The α -AtHEN1 antibody production and evaluation	42
2.4.2. The methylation activity and substrate specificity of recombinant HEN1.....	43
2.4.3. HEN1 mediated methylation of individual strands of RNA duplex	44
2.4.4. AtHEN1 and MpHEN1 Functional Domain Comparison.....	45
2.4.5. HEN1 Orthologs in Plant Species	46
2.4.6. The MTase comparison in various species	47
2.5. Discussion	48
2.5.1. HEN1 antibody production.....	48
2.5.2. AtHEN1 and MpHEN1 substrate specificity.....	48
2.5.3. Methylation of individual strands of duplex miRNA by HEN1	49
2.5.4. HEN1 like protein in Arabidopsis.....	50
2.5.5. Evolution of methyltransferase	51
2.6. Figures and legends.....	52
Chapter 3.	70
HC-Pro suppresses the methyltransferase activity of HEN1	70
3.1. Abstract	70
3.2. Introduction.....	71
3.3. Materials and methods.....	74

3.3.1. Plant growth conditions	74
3.3.2. Mechanical inoculation of virus	74
3.3.3. Fluorescent microscopy	75
3.3.4. Western blot	75
3.3.5. In vivo and in vitro methylation assay	76
3.3.6. In vitro pull down and in vivo IP	76
3.3.7. EMSA	77
3.3.8. β -elimination and northern blot.....	77
3.4. Results.....	78
3.4.1. TuGK and TuGR virus inoculation and titre check	78
3.4.2. HEN1 activity is inhibited by the TuMV HC-Pro suppressor	78
3.4.3. HC-Pro ^R suppresses the activity of the HEN1, in vitro.....	79
3.4.4. HC-Pro ^R interacts with HEN1 and inhibits miRNA methylation.	80
3.5. Discussion	82
3.5.1. Variation in suppression activity among different HC-Pros.....	82
3.5.2. HC-Pro alone, without any accessory protein mediates HEN1 inhibition	83
3.5.3. TuMV HC-Pro also can inhibit bryophyte HEN1.....	83
3.5.4. Silencing suppressors interfere with distinct sRNA processes in different ways	84
3.6. Figures and legends.....	85
Chapter 4.	96
Conclusion and future direction.....	96
4.1. Overview.....	96
4.2. Angiosperm and bryophyte HEN1 characteristics study	96
4.3. HC-Pro suppressing HEN1 methyltransferase activity studies.....	97

4.4. Future directions	98
4.4.1. HEN1 and TuMV HC-Pro interaction studies	98
4.4.2. HEN1 inhibition studies under various potyviral HC-Pros	99
4.4.3. Virus derived siRNA methylation status evaluation	100
References	101



Chapter 1.

Literature Review

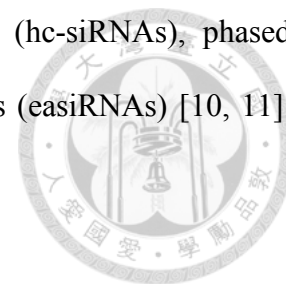


1.1. Post-transcriptional gene silencing in plants

Over the last few years, scientists have made significant progress in understanding the mechanism of RNA silencing, also known as RNA interference in animals, post-transcriptional gene silencing (PTGS) in plants, and quelling in fungi, a process that results in the degradation of homologous mRNAs [1-4]. The phenomena of RNA inhibition was first characterized as 'co-suppression' in *petunia* [5]. The functional analysis of genes in *Caenorhabditis elegans* has been studied in more detail [6]. The presence of an underlying mechanism that appears to be identical in diverse species shows that RNA silencing has had a biological function that has been conserved throughout the evolution of organisms. Transcriptional gene silencing (TGS), on the other hand, limits transcription via methylation and chromatin remodeling at the DNA level, whereas RNA silencing has no effect on gene locus transcription and only causes sequence-specific degradation of target mRNAs [7]. The presence of double-stranded RNA (dsRNA), which is subsequently cleaved into short RNAs to become functional in a multitude of epigenetic gene-silencing processes, is a common trait shared by RNA silencing and TGS [8]. In plants, RNA silencing, as an efficient component of gene silence, not only functions as a key component of the defensive mechanism against transposable elements and viral infection, but it also regulates endogenous gene expression [9].

In most eukaryotes, RNA silencing, which is mediated by short non-coding RNAs of 20–35 nucleotide (nt) in length, is a critical and necessary form of gene control. Small RNAs are categorized into four types based on their origin, processing mechanism, and effector protein association: microRNA (miRNA), short-interfering RNA (siRNA), PIWI-interacting RNA (piRNA, animals only), and transfer RNA-derived small RNAs (tsRNAs) [10, 11]. Different

sub-categories of siRNAs exist, including heterochromatic siRNAs (hc-siRNAs), phased secondary siRNAs (phasiRNAs), and epigenetically activated siRNAs (easiRNAs) [10, 11]. Some of the majorly found small RNA in plants are discussed below.



1.1.1. miRNA pathway

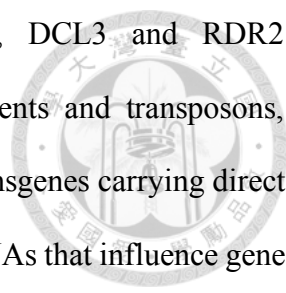
Plants, animals, and certain viruses encode miRNAs, which are 20-24 nt in length and are distinguished from other small RNAs by their very accurate excision from stem-loop present in original miRNA transcripts (pri-miRNAs) [12]. miRNAs restrict gene expression in plants primarily via facilitating target RNA cleavage or translational inhibition [13, 14]. The majority of plant miRNAs are encoded by intergenic region genes (*MIRs*), however other miRNAs are produced from protein-coding gene introns and other non-coding RNAs [14-16]. The DNA-dependent RNA polymerase II (Pol II) generates pri-miRNA from the bulk of plant *MIRs* [14, 17]. The Dicer-like RNase III endonuclease 1 (DCL1) recognizes and processes the imperfect stem-loop structure of pri-miRNA into a short precursor (pre-miRNA) with the assistance of the dsRNA-binding protein HYPONASTIC LEAVES 1 (HYL1) and the zinc finger protein SERRATE (SE) (Figure 1.1). In the nucleus, DCL1 further processes pre-miRNAs to produce miRNA/miRNA* duplexes, which have a duplex region and 2-nt 3' overhangs at either end [13, 18]. After processing, the small RNA methyltransferase HUA ENHANCER 1 (HEN1) performs 2'-*O*-methylation on each strand of the duplex miRNA at the 3' end, protecting miRNAs against degradation [19]. The guide strand of the miRNA/miRNA* duplex is then chosen (miRNA) and loaded into Argonaute 1 (AGO1) to form the miRNA-induced silencing complex (miRISC), while the passenger strand or star strand (miRNA*) is removed [18] (Figure 1.1). It should be emphasized that in plants, certain miRNAs are loaded into

AGO1 homologs rather than AGO1 [20-22]. miRISC assembles in the nucleus and is exported to the cytoplasm in a CRM1(EXPO1)/NES-dependent manner, according to recent research [23, 24]. However, another research found some unloaded miRNAs in the cytoplasm, indicating that miRISC assembly can potentially take place in the cytoplasm [25].

Hundreds of miRNAs have been discovered in plants to date. These miRNAs influence plant development and physiology, including seed, root, shoot, and flower development, phase transitions, and responses to biotic and abiotic stresses [14, 17, 26, 27]. miRNA accumulation has been found to induce developmental abnormalities or diseases, suggesting that miRNA production is a tightly regulated process.

1.1.2. siRNA pathway

siRNAs are small interfering RNAs with a length of 21–24 nt that are made from lengthy dsRNAs or single-stranded RNAs (ssRNAs) which ultimately produces duplex RNA that build longer and more perfect hairpin structures as compared to miRNA precursors. While a single miRNA precursor produces only one miRNA, siRNA precursors create numerous siRNAs. Through sequence-specific interactions with their targets, siRNAs initiate TGS or PTGS and guide the enzymatic action of their effector proteins [28, 29]. Endogenous siRNAs in plants are divided into two groups: hc-siRNAs and ta-siRNAs. Exogenous sources, like viruses and transgenes, can also produce siRNAs [28, 29]. siRNAs are distinct from miRNAs in that they are made up of double-stranded RNA, which needs the activity of RNA-dependent RNA polymerases (RDRs) in some situations such as RDR1, RDR2, and RDR6 [30-35]. Moreover, DCL2, DCL3 and DCL4 are all known to have a role in siRNA biogenesis in Arabidopsis [30-35]. For



example, in the heterochromatin-associated RNAi pathway, DCL3 and RDR2 collaborate to produce 24-nt siRNAs from different retroelements and transposons, ribosomal arrays, endogenous direct and inverted repeats, and transgenes carrying direct repeats [34, 36, 37]. het-siRNAs or hc-siRNAs are 24 nt long siRNAs that influence gene expression in plants by RNA-directed DNA methylation (RdDM). The RdDM pathway is only found in plants, and it is responsible for de novo DNA methylation and transcriptional silencing in the nucleus [38-41]. RdDM is governed by 24-nt siRNAs produced by a combination of the plant-specific RNA polymerase IV (PolIV), RDR2, and DCL3 functions. In summary, PolIV generates aberrant RNA by transcribing methylated and highly repetitive DNA, and RDR2 transforms this ssRNA into dsRNA, which is then processed by DCL3 into 24-nt siRNAs, which are then methylated at the 3' hydroxyl group of the terminal nucleotides by HEN1 [42]. To construct RISC, the 24-nt siRNAs are loaded onto AGO4 in a process that involves both nuclear and cytoplasmic steps [43]. The AGO4-siRNA complex then interacts with long non-coding RNA generated from target DNA by another plant-specific RNA Polymerase V (PolV) to recruit other components, such as Domains Rearranged Methylase2 (DRM2), resulting in direct de novo DNA cytosine methylation. A non-canonical RdDM mechanism has been discovered, which is triggered by 21-nt siRNAs [43, 44]. RdDM's primary job is to silence the transposable elements (TEs) and repetitive DNA in order to ensure genomic integrity.

The tasiRNAs, like miRNAs, are a family of 21-nt sRNAs derived from non-coding transcripts generated by RNA polymerase II from *TAS* genes [32, 33, 45]. Specific miRNAs guide the cleavage of TAS precursor RNA to start tasiRNA synthesis. RDR6 converts TAS transcript miRNA cleavage fragments to long dsRNA, which is then processed by DCL4 into 21-nt siRNAs with 21-nt phasing beginning at the miRNA

cleavage site [32, 46-49]. The size of miRNAs is critical for triggering tasiRNA synthesis, with only 22-nt miRNAs being found to do so [50, 51]. HEN1 methylates tasiRNAs same as it methylates miRNA, which interact with AGO1 or AGO7 to guide the degradation of target mRNAs [42]. ta-siRNAs have been discovered to target auxin response factors involved in the phase transition from juvenile to reproductive stages in *Arabidopsis* [52]. In *Arabidopsis* and other plant species, a huge number of ta-siRNA-like siRNAs, commonly termed as phased siRNAs or phasiRNAs, have been identified [53-56]. These phasiRNAs are 21-nt in size and need 22-nt miRNAs as in case of 1510, a soybean miRNA, AGO1, RDR6, and DCL4 for synthesis, just as the previously described ta-siRNAs [53-56].

Antiviral RNA silencing is dependent on a number of key variables involved in the production and function of endogenous siRNAs [57]. DCL4 is a protein that catalyzes the synthesis of 21-nucleotide siRNAs from a variety of RNA and DNA viruses. [58-61]. In the absence of DCL4, DCL2 and DCL3 create 22- and 24-nucleotide-long virus-derived siRNAs, respectively [58-61]. DCL1 may act as a negative regulator of DCL4 in an indirect manner [62] and as a catalyst in the synthesis of siRNAs produced from geminiviruses and cauliviruses [58, 62]. RDR1, RDR2, and RDR6 have also been demonstrated to be required for siRNA biogenesis or antiviral silencing [31, 61-64, 65, 62, 66]. From inverted-repeat transgenes, DCL4 creates siRNAs [67], DCL2 generates viral siRNAs derived from the turnip crinkle virus (TCV) or the cabbage leaf curl virus (CaLCuV), whereas DCL3 produces CaLCuV-derived siRNAs [34, 58]. RDR1 and RDR6 are required for the amplification of cucumber mosaic virus (CMV)-derived siRNAs in *Arabidopsis* for systemic RNA silencing [66]. Because RDR1 is triggered by salicylic acid, it may interact with other defensive responses [35, 68, 69].

1.2. miRNA stability in plants

At many levels, the accumulation of miRNAs in vivo can be regulated. miRNA levels are affected by mechanisms that lead to RNA degradation, including as 3' uridylation and 3' truncation, in addition to miRNA production. Plant miRNAs, on the other hand, are protected from truncation and uridylation by 2'-*O*-methylation. The discovery of HEN1 SUPPRESSOR1 (HESO1) as the primary enzyme responsible for miRNA uridylation in Arabidopsis was a first step toward a complete understanding of miRNA turnover mechanisms [70].

1.2.1. HEN1 mediated methylation maintains miRNA stability

The rates of biogenesis and degradation of a miRNA determine its abundance in cells. The first insight into pathways that lead to miRNA degradation came from research on one of the synthesis stages in plants, miRNA 2'-*O*-methylation. Almost all miRNAs in Arabidopsis are completely 2'-*O*-methylated at its 3' ends in vivo. Northern blots were used to evaluate multiple miRNAs in wild type and *hen1* mutants in order to better understand the function of miRNA methylation. When miRNAs are unmethylated, they are shown to be less abundant and more diverse in size. Primer extension experiments revealed that the size heterogeneity is present in the 3' ends of miRNAs [42]. miR173 and miR167 were cloned and sequenced (by the standard Sanger technique) in wild type and *hen1* mutants, revealing that miRNAs are 3' truncated and 3' uridylated, resulting in the addition of a short U-rich tail [42]. This led to the idea that the 2'-*O*-methyl moiety in plant miRNAs protects them against 3'-to-5' exonucleolytic activity and uridylation activity, hence promoting their stability [42]. High-throughput sequencing was used to evaluate a large number of miRNAs in wild type and *hen1* mutants in a recent study. In the absence of methylation, all identified miRNAs found in the libraries undergo 3'

truncation and 3' uridylation, confirming the findings of the earlier investigation [42, 71]. In addition to miRNAs, *HEN1* or *HEN1* orthologs also 2'-*O*-methylate siRNAs in plants and *Drosophila*, and piRNAs in mammals [42, 72-79]. Lack of small RNA methylation is frequently linked to small RNA instability in both plants and mammals, as evidenced by lower accumulation, 3' truncation, and 3' uridylation [42, 70, 72, 79-81].

i. HEN1 structure studies

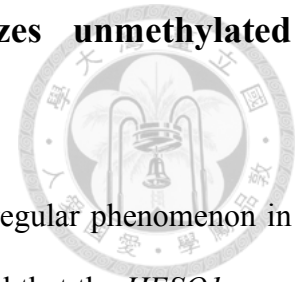
HEN1 was discovered to be required for Arabidopsis miRNA accumulation in vivo after being discovered as a floral patterning gene in a genetic screen [82, 83]. According to evolutionary study, the plant HEN1 and its animal homologues possess a highly conserved methyltransferase (MTase) domain that is not closely linked to any known RNA 2'-*O*- MTases [84]. In the amino-terminal region of HEN1, two potential RNA binding modules, a double-stranded RNA binding domain (dsRBD), and a La motif have been identified [84]. In another study the authors determined the crystal structure of full-length Arabidopsis HEN1 in complex with a small RNA duplex in the presence of the cofactor product adenosyl-L-homocysteine to better understand the specific recognition of small RNA substrates and the molecular mechanism of the 3' end 2'-OH-specific methylation by HEN1 and its homologues (AdoHcy). At 3.1Å, the crystal structure was identified (Figure 1.2). According to the structure, Arabidopsis HEN1 binds to the small RNA substrate as a monomer, which is verified by gel filtration data [85]. The ternary complex structure of the short RNA substrate has an A-form conformation, and both duplex termini are particularly recognized by HEN1 [85]. With the exception of the PPIase-like domain (PLD), which has a high degree of

structural similarity to well-characterized FK506-binding proteins, the HEN1 protein has five structural domains, four of which directly interact with the short RNA substrate [86]. Two dsRNA-specific binding domains, dsRBD1 and dsRBD2, bind to the A-form duplex of the short RNA substrate [87]. Treatment with increasing amounts of EDTA, which chelates Mg^{2+} in the process, results in the loss of HEN1 activity, indicating that HEN1 is a Mg^{2+} -dependent small RNA methyltransferase [85] (Figure 1.2).

ii. HEN1 substrate specificity

The structure of the HEN1-small RNA complex revealed that many HEN1 domains work together to bind small RNA substrates, elucidating HEN1's RNA substrate selectivity [85]. In plants, the N-terminal domain dsRBD1 in HEN1 may first bind the RNA substrate, allowing HEN1 to only operate on double-stranded RNAs [19]. A typical dsRBD recognizes an RNA duplex over a 16-bp distance [88]. As a result, the small RNA duplexes generated in plants, which are around 21–24 nucleotides long, are highly targeted during initial recognition. LCD's end-capping interaction is aided by dsRBD2, which, together with dsRBD1, establishes a tight grip on the duplex region of the short RNA substrate, allowing the other duplex terminal to be positioned towards the MTase domain. The distance between the active site of the MTase domain and the 5'-end-capping site in the LCD determines the desired length of short RNA substrates identified by HEN1 [85]. Animal HEN1 homologues exclusively work on single-stranded small RNAs, and contact with AGO proteins stimulates their small RNA methyltransferase activity [75, 77, 78].

iii. HEN1 antagonistic HESO1 destabilizes unmethylated miRNAs



In plants and animals, miRNA 3' uridylation is a regular phenomenon in *hen1* mutants [42, 70, 72-81]. In Arabidopsis, studies found that the *HESO1* gene is important for small RNA uridylation in *hen1* mutants [70, 80]. The *hesol* mutation dramatically lowers uridylation, according to high-throughput sequencing of miRNAs in *hen1 hesol* and *hen1*. In vitro, HESO1 has nucleotidyl transferase activity that adds tens of non-templated poly-U to an RNA oligonucleotide, and 2'-*O*-methylation on the RNA's 3' terminal ribose entirely inhibits this activity. HESO1 has preference towards U compared to the other three nucleotides. These biochemical features align with genetic evidence that miRNAs acquire a U-rich tail in the absence of methylation. Although the *hesol-1* mutation is most likely a null allele, still uridylation, predominantly monouridylation, is observed in this mutant, suggesting that another nucleotidyl transferase is capable of uridylating unmethylated miRNAs. As the miRNA levels are higher in *hen1 hesol* than in *hen1*, uridylation causes miRNA degradation. Worth to note that although miRNAs in *hen1 hesol* are not methylated, the higher quantities of miRNAs result in more efficient repression of miRNA target genes in *hen1 hesol* than in *hen1* [70, 80, 89]. This suggests that unmethylated miRNAs can still regulate their targets. As a result, methylation of miRNAs is likely to serve merely to stabilize them rather than to affect their functioning. It is unknown if HESO1 is also involved in the degradation of 2'-*O*-methylated miRNAs at this time. In the wild-type HEN1 background, loss of function in HESO1 had no effect on miRNA accumulation, suggesting that HESO1 has no effect on miRNA stability in the wild type, where miRNAs are completely methylated. This is in accordance with the

finding that 2'-*O*-methylation of HESO1's substrate fully inhibits its action. However, it's plausible that HESO1 collaborates with other enzymes to degrade miRNAs in the wild type. It might, for example, work in tandem with SMALL RNA DEGRADING NUCLEASE (SDN1), which truncates short RNAs, or with another nucleotidyl transferase that can operate on 2'-*O*-methylated miRNAs [90].

iv. siRNA competes with miRNA for HEN1 mediated methylation

In structure, biosynthesis, and function, siRNAs are similar to miRNAs. In contrast to miRNAs, which are made up of hairpin pre-miRNAs, siRNAs are made up of lengthy dsRNA precursors [91, 92]. Plants have a 2'-*O*-methyl group on the 3'-terminal nucleotide of both miRNAs and siRNAs, a modification mediated by the methyltransferase HEN1 [19, 42]. When HEN1 function is impaired in Arabidopsis, siRNAs compete with miRNAs for methylation [93, 94]. Mutations in DNA-dependent RNA polymerase IV or RNA-dependent RNA polymerase II, both of which are required for the synthesis of endogenous 24-nt siRNAs, led to this result [34, 95, 96]. The deficiencies in miRNA methylation of *hen1-2*, a weak *hen1* allele, may be rescued by these mutations, indicating the negative impact of siRNAs on HEN1-mediated miRNA methylation [19].

v. Analysis of methylation status of small RNAs

The sRNA methylation reaction which is catalyzed by HEN1 in plants is analyzed by techniques like β -elimination followed by northern blotting [251].

Periodate oxidation followed by β -elimination treatment is capable of removing the 3' terminal nucleoside of unmethylated RNAs, leaving a phosphate group at 3' end and resulting in an approximately 1.5 nt faster migration on polyacrylamide gel electrophoresis (PAGE). Upon methylation the 3' terminal nucleoside becomes resistant to the β -elimination treatment.

1.3. PTGS induced during virus infection.

A number of tests conducted since the discovery of PTGS have demonstrated a complicated relationship between PTGS and viral infection/resistance. Indeed, viruses can act as PTGS targets, inducers, or inhibitors. In eukaryotes, PTGS is critical for gene expression control throughout development [97, 98], stress feedback and genome stability maintenance [99]. It's also triggered by the invasion of molecular parasites like viruses, as well as other elements with comparable structure and biological capabilities (viroids, satellite RNAs, defecting RNAs, and defecting-interfering RNAs) [100]. Plants use PTGS to efficiently and specifically recognize and remove molecular invaders, despite the fact that no antibodies (that would preserve persistent immunological memory against viruses) have been discovered in plants so far. Viruses take use of cellular biochemical machinery to proliferate in infected host cells since they lack their own machinery. Importantly, all plant viruses (DNA, RNA, ssRNA or dsRNA, with positive or negative polarity in their genomes) must overcome the RNA stage, which is a source of PTGS-inducing chemicals (dsRNA) [101].

1.3.1. Suppressor of RNA silencing (RSS)

Virus infection and replication in the host trigger a variety of antiviral defense responses. RNA silencing is one of the most well-studied antiviral defense mechanisms.

Several viral suppressors of RNA silencing (VSRs) or suppressor of RNA silencing (RSS) have been found in practically all plant virus genera, despite the fact that they are very varied within and between kingdoms, with no obvious sequence commonalities. By interacting with critical components of the cellular silencing machinery and frequently imitating their normal cellular activities, RSSs effectively block host antiviral responses. Recent research has demonstrated that the influence of RSSs on endogenous pathways is significantly more complicated and extensive than previously thought [102]. The presence of such a counter-defense strategy in viruses serves as a model for the mechanical complexity of RNA silencing in plants under various biotic stressors.

1.3.2. Suppression of virus induced PTGS

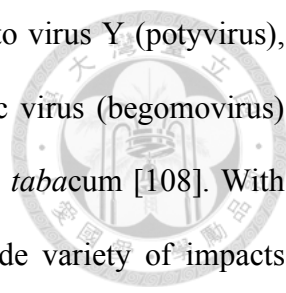
Following the delivery of viral genetic material into the plant, the PTGS machinery identifies pathogenic RNA and degrades it. Only an immediate viral response to PTGS would allow the virus to propagate systemically at this point. In reality, this viral defense might be based on: (1) long dsRNA binding and protection against DCL processing, (2) siRNA sequestration and/or degradation, (3) deactivation of functioning RISCs, and (4) prevention of short- and long-distance silencing signal propagation. Indeed, viral suppressors can stop the PTGS from activating at least one of the pathways indicated [250]. Importantly, viral proteins' suppressive effect is linked to their other biological roles that are required during the virus replication cycle. This is consistent with viruses' overall genetic skills, which include the ability to encode just the most important genes with relatively tiny genomes. Potyviral HC-Pro, for example, is both an RSS and a helper component of viral proteinase, both of which are essential for virus

transmission and systemic mobility [103], P38 of TCV, on the other hand, inhibits PTGS and is a part of the viral capsid [104].

RNA silencing has been documented in plant and animal systems across all kingdoms, and as a result, suppression of it has been characterized for plant and animal viruses. Young et al. (2012), found that related Potyviridae viruses may suppress PTGS utilizing three separate proteins and perhaps three different suppressing pathways: P1 (*tritimoviruses*), P1 or P1b (*ipomoviruses*), and HC-Pro (*potyviruses*) [105]. In recent study, the authors found that ectopically introduced P1 did not have same effect as the one expressed naturally as fusion form with HC-Pro [106]. The viral RSSs have a wide range of biological variety in terms of structure, mechanism of action, and influence on the host plant. Despite the fact that knowledge in the field of RSS is regularly validated and updated, it appears that the underlying mechanism of this specific virus–host interaction is still unknown. The notion of RSS functional complexity has been broadened and deepened by new experimental evidence. At least at the PTGS level, it places a lot of emphasis on the occurrence of several layers of plant defense and viral counter-defense relationships [58, 107].

1.3.3. Role of RSS in plant pathogenicity

The route of action of known viral RSSs is complex: it targets highly sensitive plant metabolic pathways and affects cellular regulatory signal homeostasis based on small regulatory RNA distribution. As a result, it's not unexpected that the presence of RSS in plant cells is linked to macroscopic alterations that emerge as disease-like symptoms, such as leaf deformity, stem stunting, or local and necrotic lesions. P1 of Rice yellow mottle virus (sobemovirus), P1 of cocksfoot mottle virus (sobemovirus), P19 of

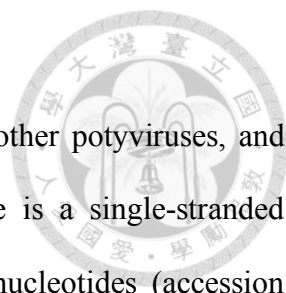


TBSV (tombusvirus), P25 of PVX (potexvirus), HC-Pro of potato virus Y (potyvirus), 2b of CMV (cucumovirus), and AC2 of African cassava mosaic virus (begomovirus) were used to study phenotypic effects in *N. benthamiana* and *N. tabacum* [108]. With reference to tobacco species, the authors determined that a wide variety of impacts manifested differently depending on the expression of certain RSSs. Further, Soitamo and colleagues wondered if and how the phenotypic effect of RSS expression in plants is linked to alterations in the transcriptome and proteome [109]. The authors demonstrated that expression of PVY HC-Pro in transgenic plants activated defense, stress, and photosynthesis-related genes using both high-throughput transcriptomic (microarray) and proteomic (2-DE) approaches. When the authors compared the amounts of changed transcripts in plants expressing HC-Pro and AC2, they discovered that around 500 and 300 transcripts, respectively, were up- and downregulated. It was also fascinating to see if viral RSS may influence AGO expression and miRNA-dependent regulation. Plant viruses activate miR168, which inhibits antiviral AGO1 [110]. It was shown that viral suppressors of PTGS can interfere with miRNA-mediated silencing pathways, resulting in developmental abnormalities, when the interactions between miRNAs and RSS were considered [111-114].

1.4. Potyvirus

Potyvirus particles are 700–750 nm long and contain one copy of the genome, which is a single-stranded, positive-sense RNA molecule with a length of around 10 kb. Untranslated regions surround each end of the open reading frame in the genome.

1.4.1. Turnip mosaic virus (TuMV)



TuMV particles are filamentous and flexuous, just like other potyviruses, and have an average length of 720nm [115, 160]. TuMV genome is a single-stranded positive-sense RNA molecule with a length of about 10,000 nucleotides (accession number NC 002509). TuMV, a member of the *Potyviridae* family, is one of the world's top five plant-pathogenic viruses affecting vegetable crops. TuMV causes mottling in regions that are wide, yellow, round, and irregular. The oldest leaves frequently turn a brilliant yellow color all throughout. The lamina is often necrotic. Veins do not become green, and leaves do not grow brittle. Aphids spread the virus through sap in a non-persistent way. This virus infects at least 318 species across 156 taxa and 43 families of plants. TuMV infects most cruciferous plants, although Chinese cabbage, turnip, mustard, and radish are the most susceptible. Beets, spinach, and tobacco are additional targets. TuMV infects economically important Brassica crops, yet it causes developmental abnormalities in *A. thaliana*'s vegetative and reproductive organs. P1, HC-Pro, and nuclear inclusion a protein (NIa), three virus-encoded proteinases, proteolytically convert TuMV polyproteins into at least ten mature protein products [116]. P1 and HC-Pro, in particular, autocatalytically cleave their respective C-termini, whereas NIa is in charge of the remaining seven junctions. P1 has a strong affinity for secondary structure and can bind ssRNA and ssDNA [117].

1.4.2. Helper Component Protease (HC-Pro)

Potyviruses, like all other viruses, are constantly subjected to selection pressure in order to make their genomes as compact and efficient as necessary for their survival.

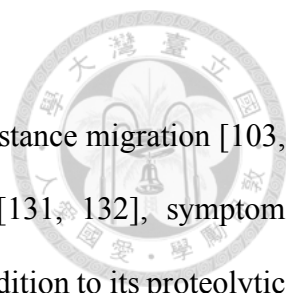
As a result, potyviral proteins are frequently multifunctional, with helper component proteinase (HC-Pro) being the greatest example.

Studies on the aphid transmissibility of co-infecting viruses provided the first evidence of a need for a particular protein in the potyvirus transmission mechanism. Two naturally aphid non-transmissible viruses, potato potyvirus C (PVC) and potato aucuba mosaic potexvirus, have been demonstrated to be transferred by aphids from plants co-infected with an aphid transmissible potyvirus, such as potato virus A or Y [118]. When aphids first probed or fed on plants infected with an aphid transmissible potyvirus, transmission of these non-transmissible viruses was restored, but not when aphids probed healthy plants or plants infected with the non-transmissible virus alone [119]. These early findings led to the hypothesis that a specific helper factor was able to facilitate non-transmissible potyvirus transmission through aphids. Two additional lines of evidence suggested that the helper activity was linked to a component present in infected plants rather than the virus particle itself: (i) the virus's lack of aphid transmissibility after purification, despite its high level of infectivity when mechanically inoculated, and (ii) the restoration of aphid transmissibility when purified virus was mixed with extracts of potyvirus-infected plants (depleted of virus particles) [120]. Surprisingly, aphids that had first obtained purified virus before probing extracts of infected plants for the helper factor were unable to increase transmission [121]. Govier et al. were the first to isolate and describe the helper component (HC) from infected plants. The findings were crucial in proving the proteinaceous origin of HC. Antibodies against a partly purified sample of HC from tobacco vein mottling virus (TVMV) infected tobacco plants were used to selectively immunoprecipitate a 75kDa polypeptide from cell-free translation products directed by the genome of the TVMV [122]. Thornbury & Pirone (1983) demonstrated that loss of HC activity was associated with the removal of a 53 kDa or 58 kDa

polypeptide (as detected by SDS-PAGE) from active fractions of TVMV or potato virus Y (PVY) HC preparations from infected plants using a TVMV HC antiserum in immunosorption chromatography assays. Because biological activity was connected with a protein with an apparent size of 100 to 150 kDa in a later experiment under non-denaturing conditions, this technique effectively identified the monomeric form of HC as a 53 kDa to 58 kDa protein [123]. As a result, it's now commonly assumed that the physiologically active form of HC is a homodimer.

Carrington et al. presented the first evidence of a proteolytic activity associated with HC [124]. A proteolytically active domain was discovered in the C-terminal half of the tobacco etch potyvirus (TEV) HC using deletion analysis and clustered point mutations of Cys residues. As a result, the protein was given the name HC-Pro. The *in vitro* cleavage site, determined by sequencing the cleavage product's N terminus, was found at a conserved Gly-Gly dipeptide at the C terminus of HC-Pro, near the junction with P3. Further, *in vitro* tests that failed to establish catalytic activity *in trans*, backed up this conclusion. This all suggested that HC-Pro acted autocatalytically [125]. Furthermore, when produced in *E. coli*, this proteinase domain was completely active, indicating that no host components were necessary for HC-Pro's proteolytic activity [125]. Different findings support the hypothesis that HC-Pro is a papain-like proteinase with an active Cys rather than a Ser [126]. Carrington et al. (1990) demonstrated autocatalytic cleavage by HC-Pro in transgenic plants expressing a polyprotein corresponding to the TEV proteins P1, HC-Pro, and part of P3 [127], as well as in insect cells bearing a construct containing the N-terminal three cistrons of the TVMV polyprotein [127]. In protoplasts or plants, potyvirus genomes bearing mutations that affect HC-Pro proteolytic processing are not infectious [128, 147].

i. Multiple functions of HC-Pro



HC-Pro is involved in viral cell-to-cell and long-distance migration [103, 129], genome replication [130], aphid transmission [131, 132], symptom development [133], and viral synergism [134-136], in addition to its proteolytic activity. Other roles of HC-Pro include inhibiting endonuclease activity [137] and 20S proteasome protease activity [138], as well as enhancing viral particle yield [139]. HC-Pro also interacts with a number of host factors, including the regulator of gene silencing calmodulin-like protein (rgs-CaM), an endogenous suppressor of RNA silencing [140], the ethylene-inducible transcription factor RAV2 [141], translation initiation factors eIF4E/iso4E [142], RING-finger protein HIP1 [143], microtubule-associated protein HIP2 [144]. The capacity of HC-Pro to suppress RNA silencing is perhaps its most well-known and investigated characteristic [145-147]. Despite substantial investigation, the molecular mechanism that underpins this capacity is not fully understood. The most widely accepted theory is that HC-Pro suppresses RNA silencing by directly binding and sequestering sRNA duplexes [148, 149]. Inhibition of sRNA methylation is a possible alternative or complementary mechanism [150, 151] leading to polyuridylation and degradation [42, 90]. This might be accomplished by HC-Pro inhibiting HEN1, the enzyme responsible for sRNA methylation [19, 151]. In vitro, it has been observed that the HC-Pro of the zucchini yellow mosaic virus physically interacts with HEN1 and inhibits its methyltransferase function [152]. In another study the authors demonstrated that potato virus A (PVA) HC-Pro interacts with S-adenosyl-L-methionine synthetase (SAMS) and S-adenosyl-L-homocysteine hydrolase (SAHH), two

key proteins in HEN1 methionine cycle, resulting in disruption of the cycle [153].



ii. Structural characterization of HC-Pro

According to mutagenesis studies and sequence alignments, HC-Pro may be separated into three regions: an N-terminal section required for transmission, a C-terminal portion containing the proteinase activity, and a central region involved in all other activities (Figure 1.3). Two conserved motifs are involved in the transmission function. The N-terminal KITC motif with amino acid (AA 52–55; numbering based on HC-Pro from lettuce mosaic virus (LMV) is important in binding to the stylets of the aphid vector [154]. The other is the C-terminal PTK motif (AA 310–312), which is thought to help HC-Pro connect to the viral capsid protein's N-terminal DAG motif [155, 156]. The proteinase domain has been identified as a cysteine protease-like activity containing Cys344 and His417 residues in the active site, and it has been localized to the C-terminal 155 AA [126]. This area could also overlap with a cell-to-cell movement domain, as in bean common mosaic necrosis virus HC-Pro, a C-terminal deletion of 87 and 293 AA, respectively, partially or fully eliminated cell-to-cell movement of heterogeneously expressed protein in microinjection studies [129]. The core region of HC-Pro (AA 100–300) is thought to have a role in genome amplification (IGN motif, AA 260–262), viral synergism, and systemic transport within the host plant (CC/SC motif, AA 292–295) [157, 158]. Non-specifically binding nucleic acids with a propensity for single-stranded RNA were characterized as two

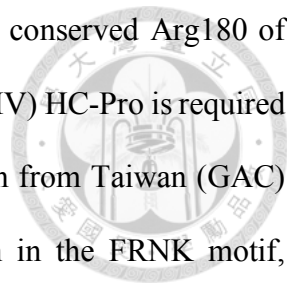
domains (A and B) encompassing the whole central region (Figure 1.3). The B domain is homologous to that of ribonucleoproteins [159, 160].

HC-Pro has been discovered to be a suppressor of PTGS and virus-induced gene silencing [161, 162]. In plants, the phloem transmits an unidentified silencing signal throughout the plant, suppressing the expression of the relevant gene throughout the entire plant. Many plant viruses have evolved anti-PTGS tactics, such as encoding PTGS suppressors like HC-Pro. HC-Pro does not disrupt the mobile silencing signal, but it does prevent the accumulation of short interfering RNA via an unknown mechanism [163]. The central region of HC-Pro is thought to be involved in suppressor function, and it coincides with the area linked to genome amplification and viral movement [164] (Figure 1.3). Although mutagenesis experiments have characterized several of HC-Pro's actions, little is known about the molecular processes involved and the connections between the numerous activities.

In size exclusion chromatography, Thornbury et al. and Wang and Pirone previously established that the HC-Pro of tobacco vein mottling virus, PVY, and TuMV behave like dimers or trimers [123]. Other findings were confirmed for the LMV his-HC-Pro, and they show that this is a common property of potyviral HC-Pro molecules. [165].

iii. Critical FRNK motif of HC-Pro

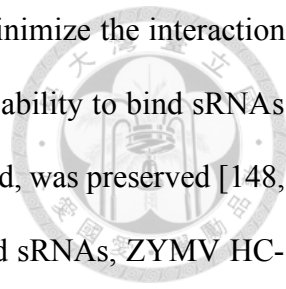
The potyvirus HC-Pro is a multifunctional protein with three different regions: N-terminal, central, and C-terminal. The central region which is responsible for pathogenicity has conserved FRNK motif among various



potyviruses. Previous research has shown that the highly conserved Arg180 of the FRNK motif of the zucchini yellow mosaic virus (ZYMV) HC-Pro is required for viral pathogenicity [166, 167]. The ZYMV mild strain from Taiwan (GAC) and Israel (AG), which contains an Arg180Ile mutation in the FRNK motif, induces modest symptoms in infected zucchini squash plants with a moderate viral titer and provides 100% cross-protection [166, 167]. Furthermore, the Arg of HC-Pro's FRNK motif is required for the suppression of the miRNA-mediated host response, which controls many genes throughout plant growth [148, 168]. In another study the authors employed the TuMV strain YC5 harboring a green fluorescence protein (GFP) gene as a model virus (denoted as Tu-GR) to develop attenuated mutants to further investigate mechanisms of cross-protection [169, 170]. In *Arabidopsis thaliana* (Col-0), a mutant Tu-GK with an Arg182Lys substitution in HC-Pro (HC-Pro^K) induces symptomless infection and it provided complete cross-protection against Tu-GR in Col-0 [171].

1.4.3. ZYMV HC-Pro

A mutation in the highly conserved FR180NK box (phenylalanine, arginine180, asparagine, lysine) of the ZYMV to FI180NK (isoleucine180) produced mitigation of symptoms in multiple cucurbit species without impacting viral accumulation or silencing suppressor function [148]. In the conserved FRNK box, amino acid alteration from R to I resulted in reduced viral infection [166]. Furthermore, total protein isolated from plant-produced HC-Pro^{FINK} was shown to poorly bind a 21-bp siRNA duplex [148]. Many RNA-binding proteins, for example, have an R-rich domain that is required for RNA binding. R's positively charged side chains may interact with the RNA's phosphate



backbone. As a result, replacing R with non-charged AA may minimize the interaction [172]. The results showed that HC-Pro^{FINK} of ZYMV has lost its ability to bind sRNAs in vitro. It's in vivo silencing suppressor activity, on the other hand, was preserved [148, 173]. These findings showed that, in addition to its ability to bind sRNAs, ZYMV HC-Pro has other activities that are not dependent on the FRNK box. The HEN1 methyltransferase is thought to catalyze sRNA methylation in *A. thaliana*. As a result, it's possible that HC-Pro interacts with HEN1 or other variables that are essential for HEN1 action, causing sRNA methylation to be disrupted. Another finding reveals that HC-Pro^{FRNK/FINK} suppressed *A. thaliana* HEN1 (AtHEN1) methyltransferase activity in vitro, but not the truncated proteins with lower in vitro affinity for AtHEN1 binding. It was postulated that HC-Pro covers the 3' overhangs of sRNAs, preventing HEN1 access to sRNA and hence inhibiting 3' modifications. Alternatively, it's been suggested that HC-Pro is in competition with HEN1 [174]. In vitro and in vivo, however, HC-Pro^{FINK} of ZYMV lost its sRNA-binding activity while retaining its silencing suppressor function. As a consequence, the study clearly suggests that HC-Pro^{FRNK/FINK} of ZYMV inhibits AtHEN1 activity by a direct contact between the two proteins. As a result, it may be established that HC-Pro mediated HEN1 inhibition and sRNA-binding actions are independent [152].

1.4.4. TEV HC-Pro

TEV, like many other viruses, has a suppressor protein called HC-Pro encoded in its genome [145, 157]. TEV is one potyvirus that appears to be more tolerant to changes on the HC gene. Full-length TEV clones with foreign sequences inserted upstream of or as mutations within the HC-Pro region were stable and produced the foreign protein in

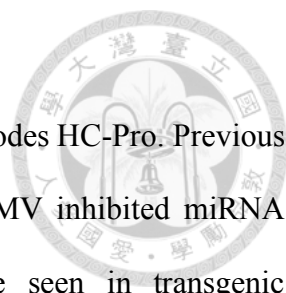
infected plants, while deletions in the N-terminal region of HC-Pro were tolerated [175-177]. Similar mutants of the TVMV and the plum pox virus (PPV) were either non-infectious or unstable, and the foreign sequence was lost during plant infections [178]. TEV may be the best potyvirus for researching the functional domains of the HC-Pro protein, based on these findings.

TEV HC-Pro transgenic *Arabidopsis thaliana* plants displayed developmental abnormalities. The occurrence of severe phenotypes was closely linked to the amount of HC-Pro expression [179]. The molecular mechanism by which HC-Pro interferes with anti-viral silencing was unknown until Lakatos et al (2006) discovered that, similar to the well-known tombusviral RSS P19, the TEV HC-Pro prevents the loading of virus derived siRNA (vsiRNAs) into the silencing effector complexes by direct binding to these molecules in a size-specific manner. Other research (Lozsa et al., 2008) found that different RNA silencing suppressors have different effects on siRNA 3' modification in *Nicotiana benthamiana* plants infected with viruses that express RNA silencing suppressors, such as the p19 protein of carnation Italian ringspot virus (CIRV) and the HC-Pro of TEV [174]. TEV had a considerable inhibitory impact on si/miRNA alterations, but CIRV had just a little effect. The HC-Pro produced by TEV and PVA have both been shown to interfere with AGO-containing effector complexes. In the first example, TEV HC-Pro takes use of the host RNA silencing pathway's homeostatic self-regulation capabilities to boost miR168 expression, resulting in downregulation of its endogenous targets, which include the antiviral AGO1 mRNA [180, 181]. In the second example, PVA HC-Pro interacts directly with AGO1 in ribosomal complexes, indicating that this RSS is able to counteract the putative translational suppression of the potyviral genome caused by RNA silencing [153]. Host factors have a role in HC-Pro-mediated silencing suppression as well. The tobacco rgs-CaM, a calmodulin-related protein that

binds directly with TEV HC-Pro and functions as an endogenous RSS, is one example (eRSS) [140].

It's still up for dispute whether HC-Pro interference with various RNA silencing modules is a side consequence of silencing suppression or an intentional viral effort to favor the infection process. Synthetic evolution studies provide an appealing chance to investigate these two approaches in this regard. For example, Torres-Barcelo et al. (2008) introduced numerous mutations in TEV HC-Pro and investigated not only the impact of these modifications on RNA silencing suppression activity, but also on TEV infection of tobacco plants, the natural TEV host [182]. As a result, they discovered that HC-Pro hypersuppressor variants rapidly evolved towards variants with moderate, wild-type-like anti-silencing capacity, implying that HC-Pro activity is fine-tuned during TEV infection to minimize the negative effects of silencing blockage on normal plant developmental patterns. Surprisingly, Lakatos et al. (2006) discovered that TEV HC-Pro's RNA silencing suppression activity was dependent on siRNA binding, and the conserved FRNK motif, which overlaps with the RNA-binding domain A, was subsequently discovered to be important for HC-Pro–siRNA interaction [148, 168]. Additional structural studies using TEV HC-Pro isolated from infected plants and viewed under an electron microscope corroborated the oligomerization states. Although HC-Pro dimers, tetramers, and hexamers were seen in solution, an amended model suggested that, at least in the case of TEV, monomer self-interaction occurred on a V-shaped conformation with HC-Pro in an antiparallel orientation [183].

1.4.5. TuMV HC-Pro



Same as previously discussed two viruses TuMV also encodes HC-Pro. Previous research showed that the *P1/HC-Pro* genes of ZYMV and TuMV inhibited miRNA regulation [171]. Serrated and curled leaf phenotypes were seen in transgenic Arabidopsis expressing P1/HC-Pro of ZYMV (*P1/HC^{Zy}* plant) as well as P1/HC-Pro of TuMV (*P1/HC^{Tu}* plant), which are linked to miRNA misregulation and viral symptom development [168, 171]. In TuMV HC-Pro the Arg of FRNK motif is required for miRNA-mediated gene regulation and viral pathogenicity [171]. The authors created TuMV recombinant wild type virus by inserting a GFP gene (TuGR) into the genome sequence of a turnip mosaic virus (TuMV) infectious clone, as well as the mutant mild strain of TuMV (TuGK) that caused milder symptoms in Arabidopsis and *Nicotiana benthamiana* [171, 184]. A serrated and curled leaf phenotype was seen in transgenic Arabidopsis expressing the TuGR *P1/HC-Pro^R* gene (*P1/HC-Pro^R* plant). The transgenic Arabidopsis expressing the *P1/HC-Pro^K* gene (*P1/HC-Pro^K* plant), on the other hand, had a normal developmental phenotype [171]. The findings of subsequent investigation revealed that HC-Pro^K had lost its capacity to inhibit the miRNA pathway [171, 185]. In other study the researchers show that transgenic plants can make two amiRNAs from pre-amiRNAs: amiR-P69¹⁵⁹ and amiR-HC-Pro¹⁵⁹, which have complementary sequences to two RSS, the P69 of turnip yellow mosaic virus (TYMV) and HC-Pro of TuMV coding sequences, respectively [170]. Furthermore, even at low temperatures that prevent post-transcriptional gene silencing, these plants demonstrated particular resistance when infected with the specific virus [170]. Furthermore, resistance to both viruses was provided by production of a dimeric amiRNA precursor that can create both amiR-P69¹⁵⁹ and amiRHC-Pro¹⁵⁹ [170]. NBR1 which is a cargo adaptor protein associated with autophagosome specifically targets TuMV accumulation by selectively targeting HC-pro

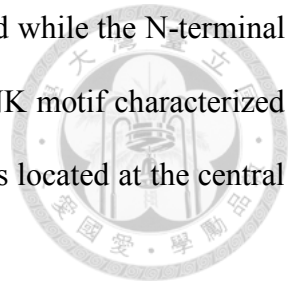
in the presence of virus-induced RNA granules [186]. TuMV proteins appear to impede the antiviral potential of the NBR1-dependent autophagy pathway during infection [186]. Finally, the authors show that NBR1-independent autophagy delays cell death and increases virus production time, implying a possible epidemiological trade-off between viral interference with autophagy and host survival [186]. Another study found that P1 of polyprotein P1/HC-Pro enhances the serrated leaf phenotype mediated by HC-Pro of TuMV [106]. TuMV HC-Pro Inhibits SA-Mediated Defense Responses by Interacting with SA-Binding Protein 3 [187]. TuMV HC-Pro interacted with itself in yeast cells, plant cells, and insect cells, according to yeast two-hybrid experiments and bimolecular fluorescence complementation [188]. It was also discovered that the HC-Pro's central and C-terminal domains were involved in these self-interactions. TuMV HC-Pro was found in the cytoplasm and formed aggregates along the ER, according to fluorescence microscopy [188].

1.4.6. HC-Pro in antiviral RNA silencing pathway

The three most extensively studied potyviral HC-Pros namely TEV, TuMV and ZYMV have found to be involved in sequestration of vsiRNA with the targeted step of vsiRNA uploading. [148, 149, 189, 190]. ZYMV HC-Pro has effector effect where it binds and inactivates the methylation activity of HEN1 [152] while TEV HC-Pro also has effector effect as it causes down-regulation of AGO1 [181]. Induction of endogenous silencing suppressor also found to be mediated in case of TEV and TuMV HC-Pros as they interact with rgs-CaM and RAV2 [140, 141].

The amino acid sequence alignment of the three HC-Pros allowed us to create a figure depicting the conserved amino acid positions (Figure 1.4). As expected, the

protease C-terminal region has shown more conserved amino acid while the N-terminal region shows less conserved amino acid across species. The FRNK motif characterized as essential for HC-Pro mediated suppression of RNA silencing is located at the central position of the protein (Figure 1.4).



1.5. Conclusion and thesis organization

Because RNA viruses have such little genomes, they offer a unique chance to examine how evolution works to make the most use of limited genetic data. The production of proteins with diverse functions is a common viral technique for resolving the coding space problem. Members of the *Potyviridae* family, the most common RNA virus family in plants, provide numerous appealing examples of viral components that play roles in a variety of infection-related pathways. HC-Pro is a multifunctional protein that is necessary and well-known. Furthermore, plenty of host variables have been shown to interact with HC-Pro. Surprisingly, the majority of these partners have not been assigned to any of the HC-Pro activities during the infectious cycle, indicating that this protein may have even more functions than those previously known.

In *Arabidopsis*, the RNA methyltransferase HEN1 is responsible for the 2'-*O*-methylation of sRNAs at the 3'-terminus. TuMV P1/HC-Pro suppressed the methylation of miRNAs in transgenic *Arabidopsis* plants [185]. HC-Pro may inhibit HEN1 from engaging with duplexes or accessing the 2'-OH of the 3'-terminal nucleotide, according to one theory. Alternatively, HC-Pro might bind to HEN1 directly and block its action [19]. In one study, the authors used ELISA binding assay to demonstrate that ZYMV HC-Pro directly binds and inhibits the methyl transferase activity of HEN1 [152]. The ZYMV HC-Pro^{FINK} mutant, which lacks small RNA-binding capability, was shown to inhibit HEN1 activity, but truncated proteins and total soluble bacterial proteins did not [152]. They showed that both the wild-type

HC-Pro^{FRNK} and HC-Pro^{FINK} bound to HEN1, with HC-Pro^{FRNK} binding being stronger than HC-Pro^{FINK} [152].

This thesis is organized into four different chapters. Each chapter is formatted according to the requirement. The chapter 1, “Literature Review” gives us the background knowledge regarding our overall study. Chapter 2, “Plant’s HEN1 functional/characteristics evaluation” was conducted to understand the methyltransferase activity of HEN1 from both angiosperm and bryophyte. For this, we designed experiments which helped us to understand the methyltransferase activity of the two HEN1s. The chapter also deals with other concepts, for instance, knowing the substrate specificity, the structural and functional similarity between the two HEN1s. Also, this chapter helps us to compare and understand the evolution of MTase domain of HEN1 across different species of diverse kingdoms.

Chapter 3, titled as “HC-Pro suppresses the methyltransferase activity of HEN1” focused on severe and milder strain of TuMV infection onto Arabidopsis and their study. We designed this chapter to understand the TuMV HC-Pro mediated HEN1 suppression in detail. The chapter tells us about the molecular mechanism of HEN1 methyltransferase activity suppression under TuMV HC-Pro influence. This chapter sheds light on how a critical amino acid substitution can lead to loss of suppression activity of viral suppressor HC-Pro. This chapter also discusses the variation of function among different HC-Pros, belonging to diverse potyviruses and also the ability of TuMV HC-Pro inhibiting the *M.polymorpha* HEN1 (MpHEN1) despite not being a host of the latter. The last chapter, chapter 4 “Conclusion and future direction” summarizes the overall work from different chapters and provides future directions which would provide deeper knowledge and understanding of the subject.

1.6. Figures and legends

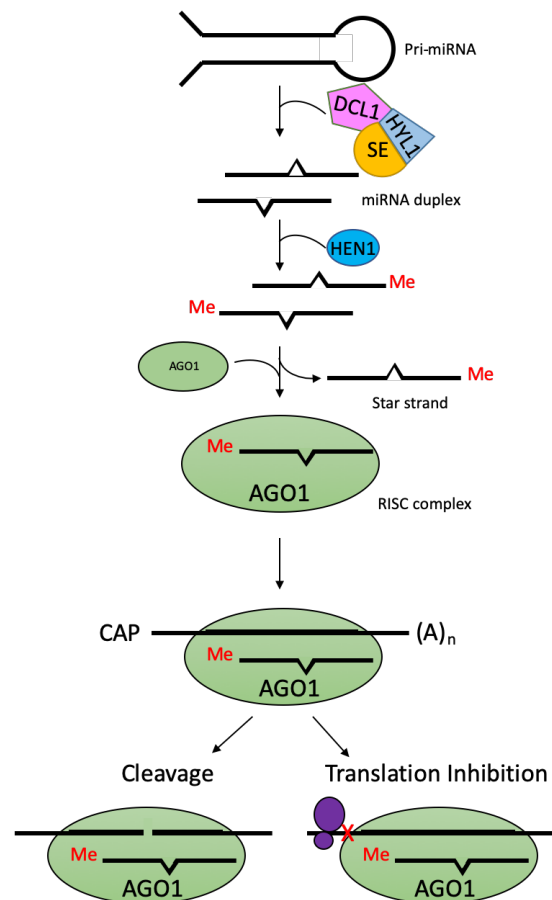


Figure 1.1. The various steps involved in miRNA pathway. The RNase III enzyme DCL1 and its associated RNA-binding cofactors HYL1 and SE process the primary miRNA transcript to generate a miRNA, which is then methylated by HEN1, exported to the cytoplasm, and incorporated into the AGO1 containing RISC to silence mRNA targets important for development, diseases, and stress responses.

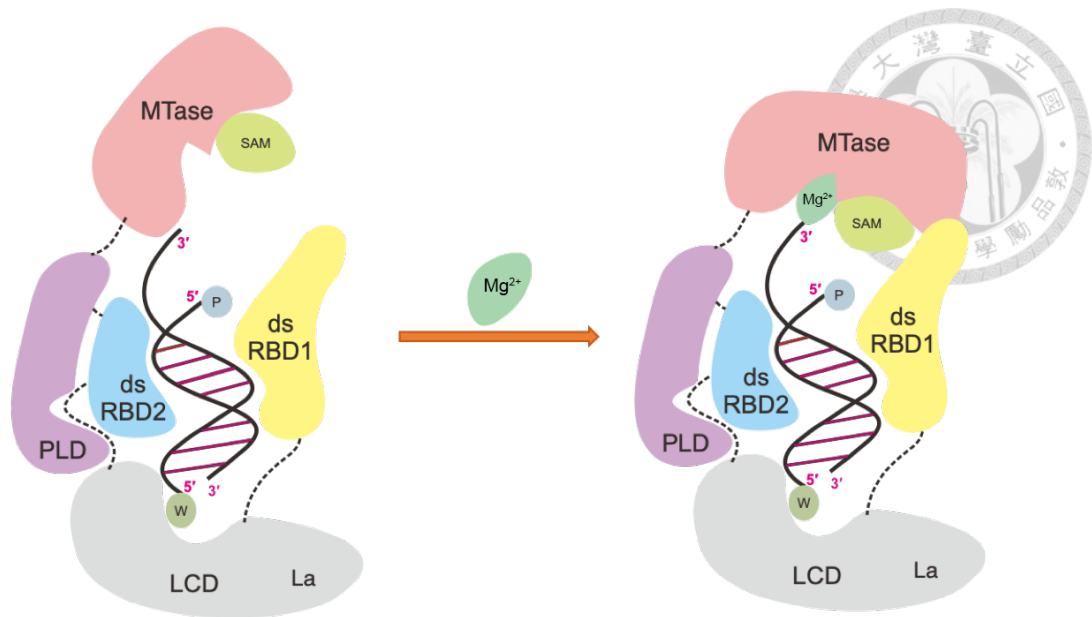


Figure 1.2. Proposed model for AtHEN1 depicting domains interacting with dsRNA with Mg^{2+} and SAM as co-factors. Multiple RNA binding domains in HEN1 target the small RNA substrate. dsRBD1 and dsRBD2 grasp the duplex region, and the critical tryptophan residue in LCD interacts with the other end of the methylating strand. The MTase domain preferentially detects the 2-nucleotide 3' overhang on the 20–24 nucleotide long small RNA substrate and methylates the 2'-hydroxyl of the 3'-terminal nucleotide.

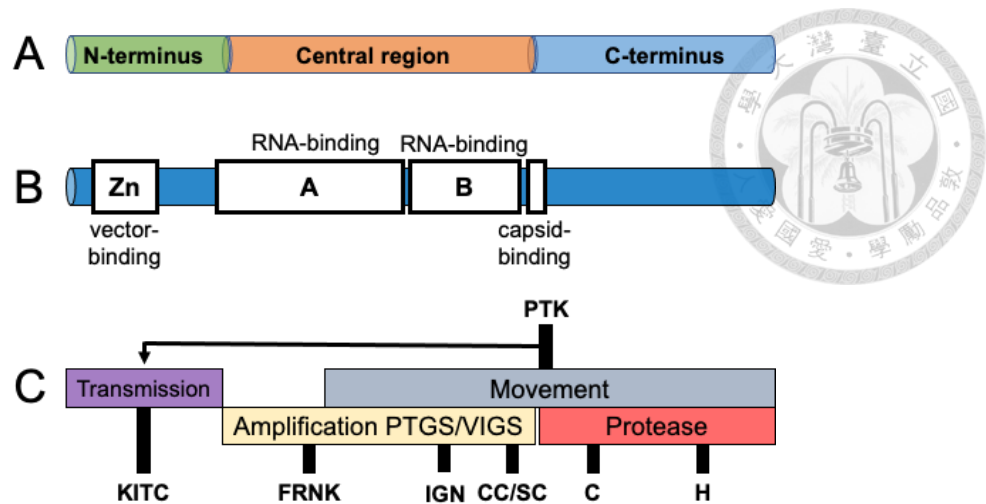


Figure 1.3. Functional regions of HC-Pro. **A.** HC-Pro can roughly divided into three regions. **B.** Location of stylets of the aphid vector binding, RNA binding, and capsid-binding regions in the HC-Pro sequence. **C.** Biological functions of different HC-Pro regions and position of conserved motifs. The C-terminal domain has cysteine protease-like activity containing conserved Cys (C) and His (H). This area overlaps with a cell-to-cell movement domain. The central region has role in genome amplification (IGN motif), viral synergism, and systemic transport within the host plant and suppression of PTGS. The arrow indicated that PTK is also involved in transmission.

```

TEV : -----SDKSISEAFETIPSKMFEELRPGISHGCTRGVSVERCGEVAAILTGAISFGGKITCKRCVVEPDIVEGEGGSVIN-QGKILAMLEQYEFEMA-- : 96
TuMV : -----AAGNNFVKETIRGPIAMRSNREHTCYSELDVTCGEVAALMGIAMFPGKITGPGVTDSELSQGAASEPSMKRIAQIRELIKSSYERFKA-- : 95
zymv : SEVDHYSQPEVQFPGGWRREMDKERE-SLTHVCKVDHINEECGELAAIFCCALFEVVKLSCQHCREKLSRISFEEFKUSINA----NFIIHDEWDSFREGSH : 99

TEV : EKILIRFLCQKSLVNTINLTACVSVKQLIGTRKCAPITHVLAVSELTFRGNKITADLEASTHMLEIARFTNNRTENMRICHLGFRNKISSKAHVNNALMCDN : 200
TuMV : VOILIRMECSLSGANENYQDFAIQSLTDGMEKZADPHANKLIATLLKGATATEEPEYCATKHLLEITHYMNRTENIEKCSLKSFRNKISSKAHINPTLMCDN : 199
zymv : YDNIRKILKQVATQATONIKLSSEVMKLVQHTSTHMKQIQDINRAIMKGSINVDQEDIALAQCLEMTQVFNNHMLTGEETAMFRNKSSKAMINPSLLCDN : 203

TEV : QLDKNGNFIWGLRGCAHAKRRLGFFTEIDPNEGYSKYVIRKHIRGSRKLAIGNLIMSTDFTLRQQICGELIERKETGNECISMNGNYVYPCCCVTLEDGKAQ : 304
TuMV : QLDKNGNFIWGERGWHAKRRESNYFEIIDPKGYTCYETRLVPNGSRKLAIGKLVPTNFEVLREQMKGEEVEPHEITVBCVSKSQGDFVHACCCVTESGDPV : 303
zymv : QLDKNGNEVWGERGMHSKRLEKNFFEEVIESEGYTRYVVRNFPNGTRKLAIGSLIVHLNLDRAITALLGESIEKKPLTSACVSQQNGNYIHS CCCVTDDGTEM : 307

TEV : YSLKHPTRKHLVIGNSGDSKYLDLEVNEEKMYIANEGYCYMNIFFALLVNVVEELAKFTKRTIRFTIVEMLGAWPTMODVATACYYLSILFPDVLSAELPRI : 408
TuMV : LSEIRMPTRKHLVIGNSGDEPKYVDLEEDENKMYIAEGYCYINIFTAMLVNVRESIAKEFTKVVRKLVGELGWPTLLDVATACYYELRVFPDVANAEPRM : 407
zymv : YSELKSPTKRLHLVIGASGDEPKYIDLEASAEARMYIAEGYCYLNIFTAMLVNVNENIAKFTKNIRVLIEMLGQWPSIMDVATAAYILGVHPEETRAELPRI : 411

TEV : LVDHDKTTHHVLDYSYGSSTTGYPHMLKMNITSLIEFVHSGLESSEMKTYIVG : 459
TuMV : LVDHDKTTHHVLDYSYGSLSRGYHILKNTTVEQLIRETRQNLESSLKHYIVG : 458
zymv : LVDHDKTTHHVLDYSYGSSTTGYPHVLKACTVNHLEQASNMQSSEMKHYIVG : 462

```

Figure 1.4. Sequence alignment of TEV, TuMV and ZYMV HC-Pros. Pink box represents the four conserved amino acids, the FRNK motif of the respective potyviral HC-Pros. The yellow box represents the conserved PTK motif while the two green boxes indicate the two catalytic residues of the cysteine protease domain.

Chapter 2.

Plant's HEN1 functional/characteristics evaluation



2.1. Abstract

sRNAs perform a variety of roles in eukaryotes' biological processes as important components of RNA silencing. Small RNA levels that are abnormally low or high are linked to a variety of developmental and physiological defects. Small RNA levels in the system are finely controlled by altering their synthesis and turnover rates. A significant mechanism that enhances the stability of small RNAs is 2'-*O*-methylation on the 3' terminal ribose. miRNAs and siRNAs in plants, piRNAs in mammals, and siRNAs in *Drosophila* are all methylated by the small RNA methyltransferase HEN1 and its homologs. In plants, the *hen1-1* mutant of the well-studied *Arabidopsis* HEN1 (AtHEN1) displayed a developmental phenotypic deficiency, demonstrating the significance of sRNA methylation. Furthermore, a HEN1 ortholog gene (MpHEN1) has been discovered in *Marchantia polymorpha*, although its function is unknown. By using in vitro analysis this study has demonstrated the methylating ability and the substrate specificity of MpHEN1 being comparable with the AtHEN1 ortholog, establishing the fact that in plants the duplex sRNA is being methylated by HEN1, and not the single stranded RNA. Furthermore, in this study we analyzed the HEN1 orthologs as well as the MTase domain of orthologous HEN1 among plantae as well as kingdom Animalia. The data suggests that plants' HEN1 shares a common ancestor and has conserved critical amino acid in the MTase domain. In case of HEN1 orthologs analysis from diverse kingdom, the amino acid alignment revealed particular conserved residues in the MTase domain of HEN1 orthologs, and the phylogenetic tree showed plant's HEN1 relatedness. These findings revealed that HEN1-mediated miRNA methylation is a conserved mechanism across plant species, offering up new avenues for research into the small regulatory RNA silencing pathway.

2.2. Introduction

Plants, unlike animals, necessarily require HEN1 to methylate both miRNA and siRNA. It was shown that siRNA competes with miRNA for this alteration, which is important since the 2'-OH of the 3'-end ribose post methylation protects the sRNA against tailing and trimming effects [19, 191, 192].

The HEN1 methyltransferase catalyzes the transfer of a methyl group from the cofactor S-adenosyl-L-methionine (AdoMet) to the 2'-hydroxyl of the 3'-terminal nucleotide of small RNAs like miRNA and siRNA [185, 193]. The ternary complex containing double-stranded miRNA/miRNA* and cofactor product S-adenosyl-L-homocysteine (AdoHcy) was X-ray crystallographically studied, revealing five structural domains of Arabidopsis HEN1 [85]. The N-terminal region of 2'-O-methyltransferase, which contains two dsRBDs, dsRBD1 and dsRBD2, as well as a La-motif-containing domain, LCD domain, is assumed to be responsible for target RNA strand binding and size. These domains work together to bind the central and non-target ends of dsRNA and aid in the appropriate placement of the bound duplex in the catalytic domain at the C-terminus. The functions of the second RNA-binding motif dsRBD2 and the central region of HEN1, which is similar to FK506-binding proteins, are yet unknown [85]. In a Mg^{2+} -dependent manner, HEN1 methylates the 2' OH of the 3'-terminal nucleotide [85]. In the absence of any additional proteins, kinetic investigations revealed that HEN1 is catalytically effective. To complete the methylation of the duplex, the enzyme changes individual strands one by one [194]. The role of the N-terminal region of HEN1 is to stabilize the catalytic complex because the C-terminal portion of HEN1 (residues 666-942) effectively modifies small RNA duplexes in vitro but has poorer affinity for both small RNA duplexes and AdoMet (the methyl donor) [194].

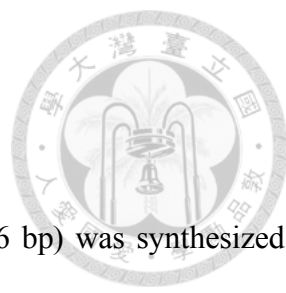
Phylogenetic analysis revealed that the N-terminal three-fourths of Arabidopsis HEN1 is conserved only among plant homologs, and the C-terminal domain, which makes up about one-fourth of HEN1 and contains a recognizable S-adenosyl methionine (AdoMet)-binding motif is conserved among bacterial, fungal, and metazoan homologs [19, 84]. The MTase catalytic domain of HEN1 is closely linked to small molecule MTases, according to bioinformatics study [84]. Recombinant Arabidopsis HEN1 operates on 21-24-nt short RNA duplexes and deposits a methyl group onto the 2' OH of the 3'-terminal nucleotides of each strand, according to in vitro activity experiments. Two essential properties of Arabidopsis HEN1 substrates are the 2-nt overhang of the duplex and the 2' and 3' OH of the 3' nucleotide [151].

Animal germlines express piRNAs, which direct Piwi proteins to silence TEs. Animal Hen1 proteins are smaller than plant HEN1 proteins because they lack the plant-specific N-terminal region [72, 75-78]. Mouse piRNAs and Piwi proteins, as well as Hen1, are only found in the testis. Single-stranded piRNAs are methylated in vitro by recombinant mouse Hen1 [76, 195]. The Hen1 gene in zebrafish is expressed in both female and male germ lines, although it is only required for oocyte development and is not required for testis development [72]. The 3' termini of piRNAs and AGO2-associated siRNAs in Drosophila are 2'-O-methylated [77, 78, 196]. The study revealed that in Drosophila, the HEN1 homolog Pimet (piRNA MTase) causes the 2'-O- methylation of piRNAs [77]. In vitro, recombinant Pimet methylates single-stranded small RNA oligos and interacts with the Piwi protein physically [77]. A two-gene operon that also codes for polynucleotide kinase-phosphatase (Pnkp), an RNA repair enzyme, encodes bacterial Hen1. [82, 197, 198]. Bacterial Hen1 methylates the 3'-terminal nucleotide of the 5' segment of a damaged tRNA in a Mn^{2+} -dependent way to prevent it from further damage by a trans-esterifying endonuclease, and subsequently Pnkp in the Hen1-Pnkp complex repairs the RNA substrate via end healing and sealing [82, 197, 198].

The liverwort, *Marchantia polymorpha*, is a member of the basal land plant lineage [199] *M. polymorpha* has become one of the most studied liverwort species due to its short life cycle and other advantages like as ease of multiplication and crossover, high transformation efficiency, small genome size, and lower genetic redundancy [200, 201]. *M. polymorpha* has a copy of the RNA silencing system, which includes DCL1, AGO1, HEN1, and other proteins [202-204]. Our earlier research showed that *M. polymorpha* miRNAs were methylated; however, no biological evidence for *Marchantia polymorpha* HEN1 (MpHEN1) activity has been found thus far [203].

2.3. Material and methods

2.3.1. Plasmid construction



Codon-optimized full-length of the *AtHEN1* gene (2826 bp) was synthesized (GeneDireX, Inc., Taoyuan, Taiwan), and was cloned into the pET28 vector to generate pET28-syn-AtHEN1. The pET28-syn-AtHEN1 plasmid was employed as a template for MTase domain amplification by KOD with the P-syn-MTase (5'-CAGCCATATGAGCGAGGAACGTATGGAAGCGGCGTTCTTT-3')/M-syn-MTase (5'-GGTGCTCGAGCAGGTCGGTCTTCTTCTTCTCAACATCTTC-3') primer set. pET28-syn-his-MTase was created by cloning the amplified MTase domain DNA fragment into pET28a. Similarly, the Codon-optimized full-length of the *MpHEN1* gene (3053 bp) was synthesized (GeneDireX, Inc., Taoyuan, Taiwan), and was cloned into the pET28 vector to generate pET28-syn-MpHEN1.

2.3.2. Recombinant protein purification

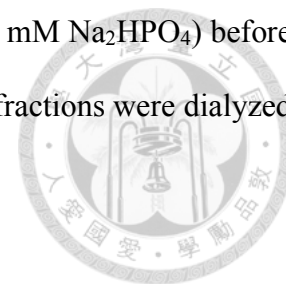
The proteins were purified with the same protocol where the vector pET 28a-syn HEN1 and pET 28a-syn MTase of HEN, and His-MpHEN1 were transformed in *E.coli* BL21, a single colony was then picked and inoculated in 10ml LB at 30°C with shaking for overnight. The next morning, it was subcultured with 400ml LB (50ug/μl kanamycin) for 1-2 hours in a 2 liters flask at 37°C shaking. The culture then was allowed to cool down at room temperature and 0.125 mM Isopropyl β-D-1-thiogalactopyranoside (IPTG) was added and incubated at 18°C with 90 rpm overnight. Collected the cell by centrifugation at 5000 rpm for 10 minutes and suspended the pellet with 150ml of lysis buffer (50 mM Tris-HCl pH 8.0, 300 mM NaCl, 1 mM DTT, and 10 mM imidazole) with freshly prepared 1 mM phenylmethylsulfonyl fluoride (PMSF).

Lysed the cell at 15,000-18,000 psi using a high-pressure cell lyser until the solution became clearer. Later, centrifuged at 13,000 rpm for 30 minutes at 4°C collected the supernatant and passed it by the filter. The filtered solution was then passed through a HisTrap column of 1ml volume capacity (GE Healthcare, Chicago, IL, USA). After this binding step, the column was subjected to FPLC (GE Healthcare, Chicago, IL, USA) where it was washed with washing buffer (50 mM Tris-HCl pH 8.0, 300 mM NaCl, 1 mM DTT, and 20 mM imidazole) for around 80-100 minutes and then subjected to elution using elution buffer (50 mM Tris-HCl pH 8.0, 300 mM NaCl, 1mM DTT and 200 mM imidazole) where the elution buffer was increased gradually. The collected fractions were checked on Sodium dodecyl sulfate-polyacrylamide gel electrophoresis (SDS-PAGE) and protein collected was dialyzed twice with dialysis buffer (10 mM Tris-HCl pH 8.0, 100 mM NaCl, 1 mM DTT, 0.1 mM EDTA 2 mM MgCl_2).

2.3.3. The α -AtHEN1 and α -MpHEN1 IgG Production

The his-MTase recombinant protein was employed as an antigen for the generation of AtHEN1 antibodies. The complete length of his-MpHEN1 was used as antigen for the generation of α -MpHEN1 antibodies. For a month, a New Zealand rabbit was given 1 mg of recombinant protein once a week. The recombinant protein was injected with Freund's complete adjuvant (1:1 v/v) for the first week, followed by Freund's incomplete adjuvant for the next three weeks. Sera from the 5th to the 8th week, as well as blood from the last week, were used to purify IgG by loading 10 mL of antiserum into a HiTrap Protein A column (GE Healthcare, Chicago, IL, USA) with 10 mL of PBS buffer (137 mM NaCl, 2.7 mM KCl, 8.1 mM Na_2HPO_4 , 1.5 mM KH_2PO_4 , pH 7.4, 1:1 v/v). The column was then attached to the FPLC machine and

washed with 20 mM phosphate buffer (7.8 mM NaH₂PO₄, 12.2 mM Na₂HPO₄) before being eluted with 0.1 M citric acid, pH 3.0 buffer. The protein fractions were dialyzed using a 1 × PBS buffer and 200 L of 1M Tris-HCl, pH 8.0.



2.3.4. Western blotting

The protein samples were mixed with 2× sampling buffer (2% SDS, 10% glycerol, 1% β-mercaptoethanol, 0.005% bromophenol blue, 50 mM Tris-HCl, pH 6.8) at 1:1 v/v, cooked at 100 °C for 10 min. SDS-PAGE was used to separate the samples, which were then blotted onto a methanol-pretreated polyvinylidene difluoride (PVDF) membrane (GE Healthcare, Chicago, IL, USA). At 4°C, the PVDF membrane was incubated with the primary antibody overnight while shaking. The membrane was washed, and the secondary antibody used was commercial HRP-conjugated anti-rabbit IgG (GE Healthcare, Chicago, IL, USA). The membrane was washed again after 2 hours of incubation, and immunostained proteins were stained with PerkinElmer's enhanced chemiluminescence (ECL) Western blot detection reagent (Waltham, MA, USA) and exposed using X-ray film.

2.3.5. In vitro HEN1 Methylation assay

The single-stranded synthetic miR159a was annealed for 5 minutes at 95°C in 5× annealing buffer (300 mM KCl, 30 mM HEPES, pH 7.5, 1 mM MgCl₂) before cooling to room temperature. 8 µl pure his-AtHEN1 or his-MpHEN1 protein, 10 µl NEB Cutsmart buffer, and 3.2 mM SAM were used to methylate a total of 0.4 ng of ds-syn-miR159a.



2.3.6. β -elimination and northern blot

The periodate oxidation technique was used to investigate HEN1's methylation activity [19]. The RNA pellet was dissolved in 176 μ l of 0.06 M borax/boric acid (pH 8.6) and then 24 μ l of 0.2 M sodium periodate was added. The reaction was oxidized in the dark at room temperature for an hour and then was passed through the G25 beads. 1/10 volume of glycerol was added to the reaction product for around 30 minutes to stop the reaction. After that, RNA was precipitated at 4°C for 10–15 min at 13,000 rpm. β -elimination was performed by dissolving the precipitated RNA in 100 μ l of 0.055 M borax/boric acid/NaOH (pH 9.5) and incubating for 90 min at 45°C. The RNA was precipitated in the same way as previously and then submitted to northern blot analysis, where it was separated on a 20% polyacrylamide gel with 8 M urea and hybridized with 32 P labeled As-miR159a (5'-TAGAGCTCCCTTCAATCCAAA-3'). The X-ray film was used to expose the miR159a signal on the membrane.

2.3.7. MpHEN1 Structure Modeling

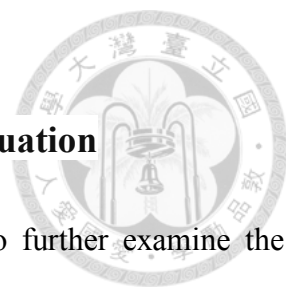
SWISS-MODEL, www.expasy.org/resources/swiss-model, was used to develop a protein model for MpHEN1. GMQE (Global Model Quality Estimation) and QMEAN (Qualitative Model Energy Analysis) factors were used to assess the accuracy of the final model [205]. The MpHEN1 model's GMQE and QMEAN scores (0.60 and 4.09 respectively) are close to the SWISS-MODEL website's recommended indicator values. This signifies that the model supplied can be used as a reference. We didn't make any changes to the default settings for any of the algorithms' parameters.

2.3.8. Sequence Identity, Similarity, and Phylogenetic Analysis

SIAS, imed.med.ucm.es/Tools/sias.html, was used to assess the pairwise sequence identity and similarity of the MTase domain of HEN1 and HEN1 orthologs. Using an Emboss needle, [www.ebi.ac.uk/Tools/psa/ emboss needle/](http://www.ebi.ac.uk/Tools/psa/emboss_needle/), the various domains of AtHEN1 were also examined for amino acid identity and similarity. In order to create a phylogenetic tree, HEN1 and HEN1-like orthologs were chosen [206]. Protein sequences were identified through BLAST and searched from Phytozome v12.1 (phytozome.jgi.-doe.gov), the Gymno PLAZAv1.0 (bioinformatics.psb.ugent.be/plaza/versions/gymno-plaza), the algae genome project (www.plantmorphogenesis.bio.titech.ac.jp/~algae_genome_project/ klebsormidium,), TAIR (www.arabidopsis.org), and NCBI (www.ncbi.nlm.nih.gov, accessed on 31 July 2021). CLUSTAL W v2.1 (www.genome.jp/tools-bin/clustalw) was used to align multiple sequences. ETE3 v3.1.1's function "build," as implemented on GenomeNet (www.genome.jp/tools/ete), was used to generate phylogenetic reconstructions [207]. Fasttree with slow NNI and MLACC = 3 was used to build the tree (to make the maximum-likelihood NNIs more exhaustive) [208]. At nodes, values are SH-like local support. We didn't make any changes to the default settings for any of the algorithms' parameters.

2.4. Results

2.4.1. The α -AtHEN1 antibody production and evaluation



The AtHEN1 antibody to detect endogenous HEN1 to further examine the HEN1 characterization was developed. First, the *E. coli* BL21 was used to purify the full-length recombinant his- AtHEN1. On the coomassie blue staining page, about 130 kDa his-AtHEN1 was found, and the size of the protein was comparable with the anticipated size (Figure 2.1.A). However, the quantity of purified his- AtHEN1 required for rabbit immunization was found not to be enough (Figure 2.1.A). As a result, the assessment of the expression of all five AtHEN1 domains in order to determine the optimum domain for expression and immunization was done. For dsRBD1 (1–86 aa), LCD domain (95–357 aa), dsRBD2 (387–500 aa), PLD (535–683 aa), and MTase domain (690–940 aa), we examined the recombinant domain expressions (Figure 2.1.B–E). The results shown that the his-MTase can produce a large amount of recombinant protein (Figure 2.1.F) hence, the antibody was produced by immunizing mice with recombinant his-MTase. To test the antibody's efficiency, different dilutions of his-AtHEN1 were used, and the results showed that the antibody can detect his-AtHEN1 at 130 kDa position, the same as the corresponding signal detected with commercial α -His antibody (Figure 2.2.A), which is consistent with the protein's predicted molecular weight. As a result, this antibody produced by his-MTase classifies as a α -AtHEN1 antibody.

In parallel, MpHEN1 antibody was produced using full length his-MpHEN1 (Appendix figure 2.1.A). The result shows that even at 1200 \times dilution, the full-length produced α -MpHEN1 antibody recognized his-MpHEN1 while it showed no cross-detection for his-AtHEN1 (Figure 2.2.B). This result shows that antibody production

for the full-length his-MpHEN1 antigen is more sequence selective. Interestingly, at 300× dilution, the α-AtHEN1 can detect both his-AtHEN1 as well as his-MpHEN1 (Figure 2.2.C). The efficacy of α-AtHEN1 to identify endogenous HEN1 was then tested. The results showed that α-AtHEN1 can identify exogenous AtHEN1 in the transgenic Arabidopsis expressing the *HA-AtHEN1* gene (*HA-AtHEN1* plant), but no signal was observed in the Col-0 and *hen1-8* mutants, indicating that α-AtHEN1 may be less effective at detecting endogenous AtHEN1 (Figure 2.2.D). The endogenous MpHEN1 protein in wild type *M. polymorpha*, TAK1 could also not detectable by α-MpHEN1 (Appendix figure 2.1.B).

Furthermore, the alignment between AtHEN1 and MpHEN1 showed that the MTase domain of AtHEN1 and MpHEN1 have 42% amino acid identity (Figure 2.3), which might explain why the α-AtHEN1 antibody can cross-react with his-MpHEN1.

2.4.2. The methylation activity and substrate specificity of recombinant HEN1

The methylation activity and substrate specificity for his-AtHEN1 were determined using an in vitro experiment to further examine the HEN1 characteristics. All double stranded syn-miR159a samples were methylated in the presence of AtHEN1, as evidenced by the signal at 21-nt position (upper band), whereas syn-miR159a remained unmethylated in the absence of his-AtHEN1, as evidenced by the signal at 20-nt position (lower band) (Figure 2.4.A). Similarly, in vitro methylation of his-MpHEN1 revealed that syn-miR159a was 67% methylated, demonstrating that MpHEN1 plays a role in miRNA methylation (Figure 2.4.B). The different domains of

HEN1 interacts with dsRNA and with the aid of Mg^{2+} and SAM as co factors facilitate the methyltransferase activity (Figure 1.2).

HEN1 orthologs in various species have distinct RNA substrates, according to previous research. Some orthologs can only methylate single-stranded RNA, whereas others can methylate duplex RNA [78, 151, 209]. Therefore, to evaluate the substrate specificity of AtHEN1 and MpHEN1 we performed in vitro methylation and β -elimination assays where single stranded syn-miR159 (ss-miR159) and double-stranded syn-miR159 (ds-miR159) were employed as substrates. His-AtHEN1 and his-MpHEN1 can methylate ds-miR159 but not ss-miR159, suggesting that HEN1 in bryophytes and angiosperm has substrate selectivity when it comes to miRNA duplex methylation (Figure 2.4.C).

2.4.3. HEN1 mediated methylation of individual strands of RNA duplex

To better understand how the duplex miRNA gets methylated we performed an experiment where we used hemi-methylated synthetic miRNA. After the methylation assay and β -elimination treatment, the probe was designed to bind with the other non-methylated strand of the duplex miRNA. The result demonstrated that neither of the strand being sensitive to sodium periodate treatment, confirming the assumption that both strands are fully methylated (Figure 2.5).

2.4.4. AtHEN1 and MpHEN1 Functional Domain Comparison

Our study showed that MpHEN1 facilitates a similar activity by methylating its miRNA at the 3' end ribose as discussed above. Next, we evaluated the amino acid identity and similarity of AtHEN1 and MpHEN1 for five domains (dsRBD1, LCD, dsRBD2, PLD, and MTase) (Figure 2.6). The dsRBD1 domains of AtHEN1 and MpHEN1 were shown to have 30% identity and 49% similarity, respectively (Figure 2.6). Furthermore, the MTase domain between AtHEN1 and MpHEN1 has the best conservation, with 42% identity and 57% similarity (Figure 2.6).

In addition, we compared the AtHEN1 structure (PDB code 3HTX) to the proposed MpHEN1 model, and the results show that MpHEN1 has the same functional domains as AtHEN1 and may play comparable functions in *M. polymorpha* (Appendix figure 2.2). Moreover, there are five RNA-binding motifs (RBM1 to RBM5) present on two dsRBDs of AtHEN1 in a pairwise amino acid alignment of AtHEN1 and MpHEN1 and we found the other four out of five, with the exception of RBM4, are not conserved in MpHEN1 (Figure 2.7). Furthermore, we discovered that five of the seven dsRNA-interacting residues on AtHEN1's LCD are conserved in MpHEN1 (Figure 2.7). Moreover, three SAM-binding residues and three metal-binding residues in AtHEN1 and MpHEN1 are significantly conserved (Figure 2.7). However, critical functional residues in the LCD and MTase domains of AtHEN1 and MpHEN1 are largely conserved. Finally, all of these findings show that MpHEN1 may act similarly to AtHEN1. Based on amino acid sequence homology model the α -helix and β -sheet arrangements among different domains of AtHEN1 are compared with MpHEN1 (Figure 2.8).

2.4.5. HEN1 Orthologs in Plant Species

To better understand the links between HEN1 and HEN1 orthologs from different green plant taxa, a phylogenetic tree was created. Green algae, lycophyte, bryophyte, gymnosperm, and angiosperm HEN1 and HEN1 orthologs were all shown to be monophyletic (Figure 2.9). Furthermore, bryophyte HEN1 orthologs constitute a monophyletic group that is sister to the lycophyte SmHEN1-like protein (Figure 2.9). Other species only have a single copy of HEN1 orthologs, with the exception of lineage-specific duplication occurrences within species such as *Sphagnum fallax*, *Populus trichocarpa*, and *Arabidopsis*. This suggested that HEN1 may have had a conserved function in sRNA duplex methylation throughout plant history.

Plant species had an MTase domain identity of 11.63-62.62%, whereas bryophytes had an MTase domain identity of 30.69-58.9% (Table 2.1). The divergence of the AtHEN1-like ortholog from other HEN1s resulted in a larger difference in sequence identity. The MTase domain of the AtHEN1-like ortholog had a significant deletion (Figure 2.10). This suggested that following duplication, one copy of the *Arabidopsis* HEN1 paralog (AtHEN1) may retain its primary RNA MTase activity, whereas another copy (AtHEN1-like) would have the same or divergent function. The conserved residues of the MTase domain were then examined further. The alignment results revealed that several SAM-binding and metal-binding residues in the MTase domain were highly conserved (Figure 2.10). The FXPP motif in the N terminus of the MTase domain is required for eukaryotic HEN1 substrate recognition [209]. Plant HEN1s have an FXP(P/S/C) sequence at the relevant place, according to the alignment (Figure 2.10). These findings indicated that plant HEN1 had a common ancestor and exhibited highly conserved sequence characteristics, particularly in the MTase domain.

2.4.6. The MTase comparison in various species

We constructed a phylogenetic tree to understand the relatedness among HEN1 or HEN1 orthologs in different species, including Actinobacteria, *Arabidopsis thaliana*, *Marchantia polymorpha*, *Caenorhabditis elegans*, *Drosophila melanogaster*, *Mus musculus*, and *Homo sapiens*. The two clades shown on the phylogenetic tree, Actinobacteria, *A. thaliana*, and *M. polymorpha* were grouped in Clade I, whereas *C. elegans*, *D. melanogaster*, *M. musculus*, and *H. sapiens* were grouped as Clade II (Figure 2.11). These data suggested that the HEN1 of Actinobacteria is closer with land plants, and the methyltransferase in the animal kingdom has far from the plant kingdom that implied functional difference between HEN1 of plant and HEN1 orthologs in animals [78, 151, 209].

The HEN1 orthologs offer methylation activity irrespective of the species and kingdom highlighting the importance of the MTase domain. We compared the MTase domain of HEN1 orthologs in plant and animal kingdoms. The 7 species MTase identity and similarity comparison between different species are listed in Table 2.2. The HsMTase and mMTase domains showed 78% identity, whereas the AtMTase domain and MpMTase domains showed 42%. We further investigated the conserved residues of the MTase domain in various species. The alignment results revealed that several S-adenocyl-L-methionine binding residues and metal-binding residues, including as S726, D745, I798, E799, and H800, are highly conserved in the MTase domain based on *Arabidopsis* amino acid positions (Figure. 2.12).

2.5. Discussion

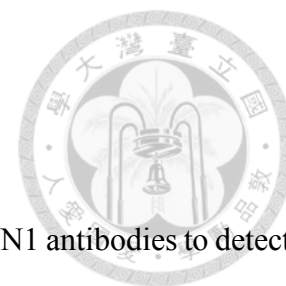
2.5.1. HEN1 antibody production

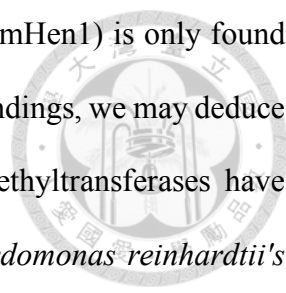
We were successful in creating α -AtHEN1 and α -MpHEN1 antibodies to detect recombinant proteins in this work. Furthermore, the exogenous HA-AtHEN1 in the *HA-AtHEN1* plant is detectable by the α -AtHEN1. α -AtHEN1 and α -MpHEN1 antibodies, on the other hand, are unable to detect endogenous HEN1 in *Arabidopsis* and *M. polymorpha* respectively. We speculated that this was due to low levels of endogenous protein expression or HEN1 expression in plant cells that was temporal and tissue dependent. Previous research has demonstrated that the expression pattern of HEN1 in *M. polymorpha* varies depending on developmental stage, corroborating our hypothesis [210].

The 42% amino acid similarity of the MTase domain between AtHEN1 and MpHEN1 may be the best explanation for α -AtHEN1's ability to cross-react with his-MpHEN1. The α -MpHEN1 antibody, on the other hand, was produced using the full-length recombinant protein and so became specific for his-MpHEN1 detection.

2.5.2. AtHEN1 and MpHEN1 substrate specificity

Two dsRBD domains in AtHEN1 and MpHEN1 can selectively bind to a duplex of miRNA/miRNA* or siRNAs but not single-stranded miRNAs or siRNAs. Animal HEN1 orthologs, unlike plant HEN1 orthologs, can operate on piRNAs or single-stranded siRNAs [209]. Furthermore, HEN1 orthologs do not methylate all small RNAs in mammals. The nematode HEN1 (HENN1) methylates Piwi-bound short RNAs in germlines of *Caenorhabditis elegans* [73]. *Drosophila melanogaster's* HEN1 ortholog





(DmHen1) targets single-stranded piRNAs [78]. Mouse Hen1 (mHen1) is only found in the testes and methylates piRNAs [76]. By combining these findings, we may deduce that while they all belong to the Animalia kingdom, their methyltransferases have different substrate discriminating ability. Interestingly, *Chlamydomonas reinhardtii*'s HEN1 ortholog has two dsRBD domains that can methylate miRNA/miRNA* and siRNA duplexes [211]. These findings lead to the intriguing conclusion that sRNA duplex methylation is a conserved trait in the plant and algal kingdoms. The method by which HEN1 orthologs differentiate between substrates is yet unknown. In this study, the in vitro findings revealed that AtHEN1 and MpHEN1, both belonging to the plantae, have stringent substrate specificity and only methylates RNA duplexes, but not ssRNA [19, 151, 194]. In conclusion, these findings imply that MpHEN1 and AtHEN1 have structural and functional similarities. Furthermore, the cross-substrate methylating efficiency of various orthologous HEN1 would be interesting to investigate.

2.5.3. Methylation of individual strands of duplex miRNA by HEN1

Early studies suggest that microRNA duplexes can be modified by HEN1 methyltransferase on either strand [19, 151]. However, structural changes on one strand of the duplex were found in the miRNA/ miRNA* substrates utilized in these experiments: atypical 1- or 3-nt overhangs at the 3'-terminus of the complementary strand [151] or a missing 2'-hydroxyl in the 3'-terminal nucleotide [19]. Hence, we conducted experiment using synthetic RNA structurally similar to the miR159/miR159* from *A. thaliana* since artificially structured substrates might possibly influence the nature of the protein-RNA interaction. The result revealed that both the strands of miR159 were fully methylated excluding the possibility that the

reaction mixture contains hemi-methylated as well as fully methylated miRNAs. Since we have designed probe detecting both non-methylated and hemi-methylated strands, our findings show that methylation of the 3'-terminal nucleotide on one strand does not prevent methylation on the other, indicating that HEN1 may fully methylate both strands of a miRNA duplex. Hence, considering the structure of AtHEN1 (Appendix figure 2.2) we hypothesize that one strand of the miRNA gets methylated first (based on the interaction with domains and critical amino acid) and then the orientation of the duplex miRNA might change, providing the other strand to be methylated making the duplex miRNA fully methylated.

2.5.4. HEN1 like protein in Arabidopsis

Tu et al. (2015) suggested that methylation at the 3' end protects miRNAs in plants against uridylation and degradation [89]. Furthermore, both the *hen1-1* mutant and the P1/HC-Pro^R plants displayed a severe developmental phenotype, emphasizing the relevance of HEN1-mediated miRNA methylation in plants. The accumulation of the most-tested miRNAs was either undetectable or drastically decreased in abundance in the *hen1-1* mutant [82]. This suggests that certain miRNAs in the *hen1* mutants are not completely eliminated. In the *hen1-4* mutant, certain siRNAs are still detectable [212]. It was hypothesized that methylation or stabilized sRNA duplexes may be created by a protein with similar capacities to HEN1. Because it is a duplicated copy of HEN1 and has a strong sequence similarity with HEN1, the HEN1-like heterologous protein is most likely the contender (Table 2.1). Several conserved amino acid residues for SAM binding and substrate binding may still be detected on the shortened MTase domain of the Arabidopsis HEN1-like protein, despite the loss at the C-terminus

(Figure 2.10). As a result, we believe that *Arabidopsis* has a HEN1-like protein that participates in a partial RNA interference process via 3'-end 2'-*O*-methylation. Animal miRNAs, on the other hand, are not methylated, and they can nevertheless play a role in RNA silencing. These findings back up the idea that plants and animals have different miRNA turnover rates.

2.5.5. Evolution of methyltransferase

The amino acid sequences of the RNA MTase domains are conserved throughout several kingdoms, including viridiplantae, bacteria, fungus, euglenozoan, metazoan, and others [84, 85]. HEN1 protects small RNA from degradation by methylating it at its 3' end in plants, and it plays a key role in controlling small RNA turnover [19, 151]. Animals have HEN1 as well, but their miRNAs are not methylated at their 3' ends; instead, their piwi-interacting RNA (piRNAs) and siRNA, which are single-stranded RNAs of 25-31 nt in length, get 3'-end 2'-*O*-methylation [76-78]. The existence of HEN1 in the bacterial system, despite the fact that they lack an RNA interference mechanism, participates in an RNA repair process that shields the RNA from future damage via 3'-end 2'-*O*-methylation [197].

2.6. Figures and legends

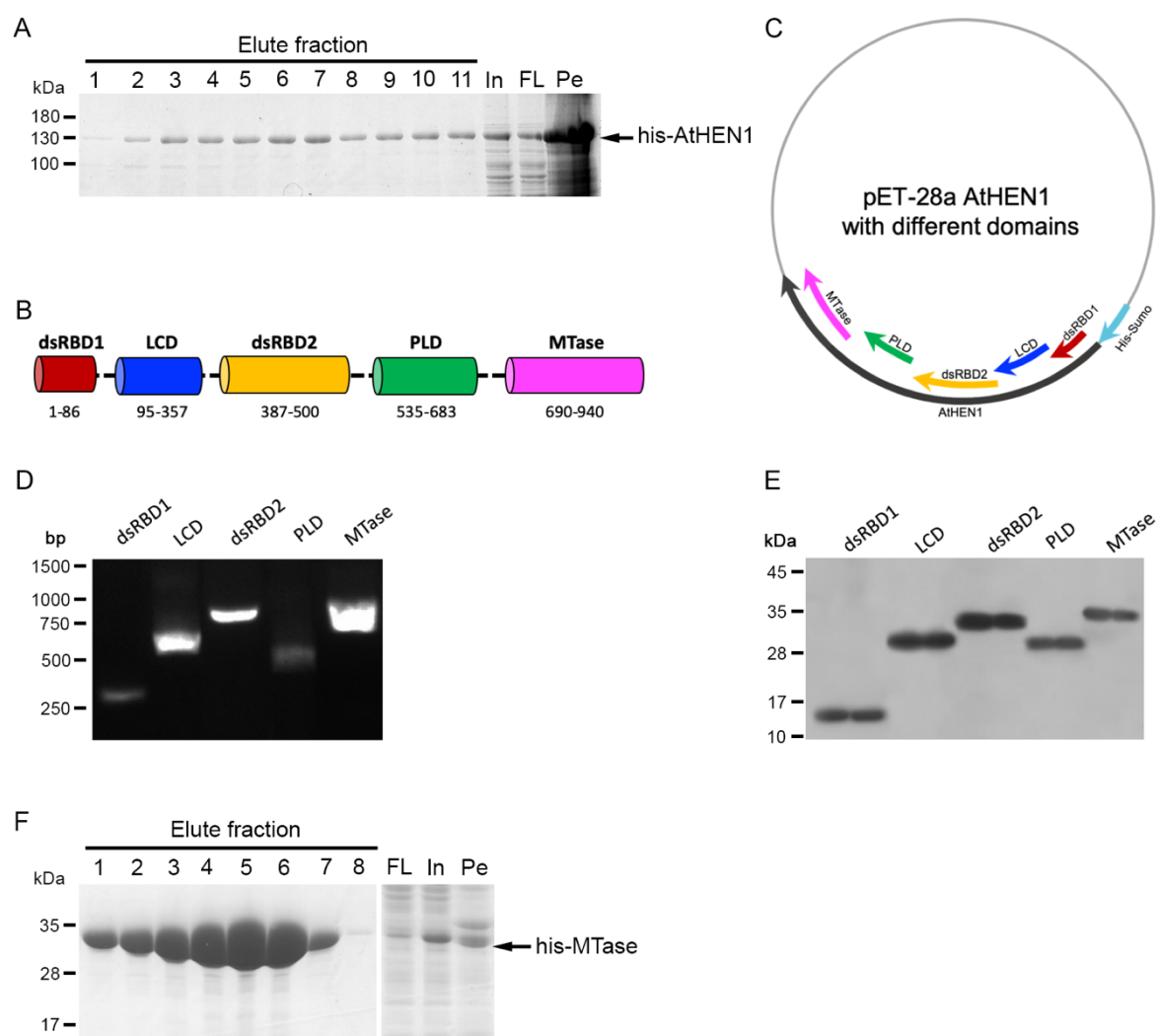
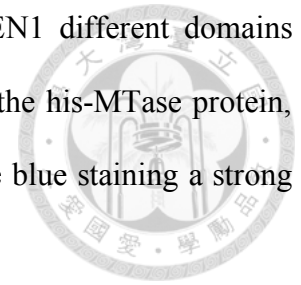


Figure 2.1. α -AtHEN1 production (A) Expression of the his- AtHEN1 protein using *E.coli* BL21 (DE3) cells, purified by Fast Protein Liquid Chromatography (FPLC) with His-TrapTM FF, Ni-NTA column of 1ml capacity, and the collected fractions were subjected to 7.5% SDS-PAGE. Upon Coomassie blue staining a band of 130 kDa was prominent in figure 1A which is consistent with the predicted protein size. In this result Pe, In, FL and M represents pellet, input, flow-through and marker respectively. (B) Schematic representation of domains in AtHEN1 with red, blue, yellow, green and magenta showing dsRBD1, LCD, dsRBD2, PLD and MTase domain respectively. (C) Schematic representation of construction of full length as

well as different domains of AtHEN1 using pET-28a vector. AtHEN1 different domains cloning **(D)**, and protein expression detection **(E)**. **(F)** Expression of the his-MTase protein, collected fractions were subjected to 10% SDS-PAGE. On Coomassie blue staining a strong band of 34 kDa corresponds to his-MTase as expected.



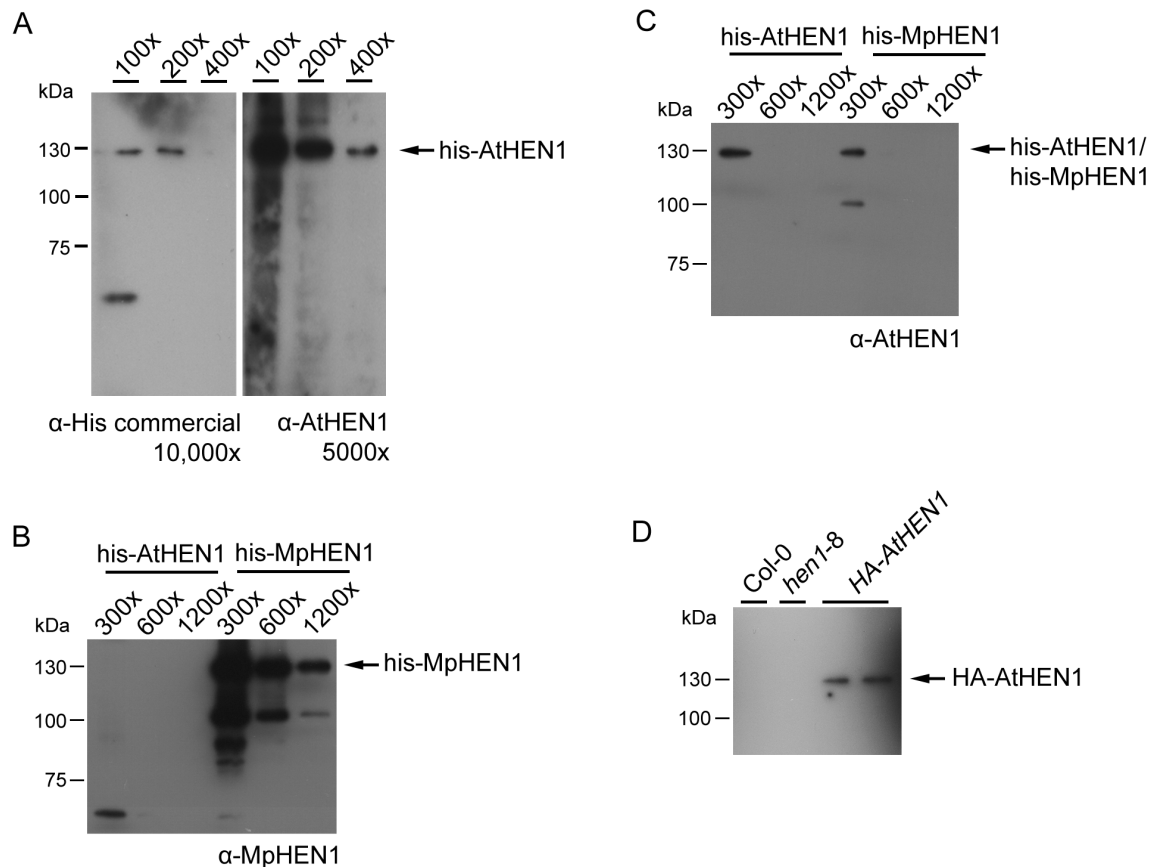


Figure 2.2. Antibody sensitivity evaluation. (A) The sensitivity of α -AtHEN1 (5000 \times dilution) was compared to his-monoclonal antibody (10,000 \times dilution) in this study. The evaluation of antibody cross-reaction between α -AtHEN1 (B) and α -MpHEN1 (C) antibodies at different dilutions of his-AtHEN1 and his-MpHEN1. Both antibodies were diluted at 10,000 \times . (D) α -AtHEN1 antibody sensitivity check using different tissues including *Arabidopsis thaliana* ecotype Col-0 (WT), HEN1 mutant as *hen1-8* and, two transgenics overexpressing HEN1 lines as HEN1 O.E.

```

AtHEN1 : MAGGGKHPTTPKAIHOKFGAKASYTVBEVHDSSQSGCLGTAIE-----QKGPCLYRCHLCLP-EESVVSNVFKKKKSECSAAE : 79
MpHEN1 : ----MTTPKAKLYQIEQFGEGLKFQTEFVINTSKVEADVLPGSTAFFKPNHAVQFRCTLSPFGGLTVVSDLFPRKKDAEQHASK : 80

AtHEN1 : LALDKLCTIRPQN--DLTVDBARDEIVGRITKYIFSDSELSAEHPLGAHLRAALRRDGRGCSVPVSVIATVDAKINSCKKIINS : 162
MpHEN1 : QALEQMSVQLAKSEDLTTDEKWNLRARIATFTDKNVQNYNPLRCHFKAAVKREGSRMCOVPLSATVTLDDTKIESLCKLIDRK : 165

AtHEN1 : VESDPFLAISYVMKAAAKLADYTVASPHGLR-RKNAYSEIVEADAT--HVSDSIHSR-----EVAAYVIPCIDEVEVELD : 235
MpHEN1 : AETNPAAHAAALLCKAAARNCPVKIDDTLCLSRREEFSPSELVQCLVVKTRYNEETEAASEKPEETNLQEVAVHIPCSTDTGGFV : 250

AtHEN1 : TLYTSSNRHYLDSIAERLGLKDGNOVMISRMFGKASCGSECRLYSEIPKKYLDNS---S--D-ASGTS----- : 297
MpHEN1 : NLIVKPEEYVLDVIARELGVKDCGRVVFESRPVGHGTHP--SMRMVWCAPKELPQVQGGSDSEVNIITGGDVGDSVVADEDLRLYSLK : 333

AtHEN1 : -N-EDSSHIVKSRNARASYTGGQDIHGDAILASVGYRWKSD-DIDYDDVTNVSFYRICCGMSFNGIYKISRCAVIAAQLPFAFTT : 379
MpHEN1 : QQPEESNGLQYFKNVRASLIMGYAVHGEVILLAAVGGDWTSHGKIYALDITESTFYRMLLQREFCGSYKVSRCAILATKLENVFSS : 418

AtHEN1 : KSNWRCPLEPRLGLFCHRIAPFLLSSSTAPVKSLS-----DIFRSHKRLKVSQVDDANENLSROKEDTFGLCHGER-CEVKI : 458
MpHEN1 : RACWKMSPRALLIEFCQYHRLPEPVFALTAIGTSTTEPPGTPPESSDVRLDVGVEPKDTSSESDDFECGSDTRNDDESN : 503

AtHEN1 : FTKSCDLVLVLCSEKRFYRK-----ENDAHQNASLKALLWFSEKFFADLDVDEGSCDTPDDQDKTSSSPNVFAAPPI : 529
MpHEN1 : AAGNCGGFEFTKVRVVEWQKGSFVEFESDGPYRNRRHDAQSASLKALHCFDSWFESCMNGAYEEVLAKTKTNGDVDKDPLITDADDE : 588

AtHEN1 : LQKEHSS--ESKNTNVLSAPKRVOSITNGSVVSIQYSLSLAVDPEYSSDGESFREDNESNEEMESEYSAANCESSEVELIESNEEIE : 612
MpHEN1 : AGIDIRDCWDFADGGFFEAEEVEDISQTDKTPPAGSMVTVRYTVRYNDADCE-----ESVSNLLEKHEKE : 656

AtHEN1 : FEVGTGSMNPHISEVTQMTVGEMASFRMTTFDAAEALILAVGSDTVRIRSLLSERPOLNYNILLGVKGPSERMEAAEFKPSI : 697
MpHEN1 : FELGGGAVIGALDSLVSRMSVGPACVTTESPAIGLLSALAYDIGDKRVLMESGS---VMYTVRLMKYVEAPEERMEAAHFKPSI : 738

AtHEN1 : SKORVEYALKHIRESSASTLVDFGCGSGSLLESLLDYPTSLQTLIGVDISEKGLARAAMLVKIN-KEACN---VKSATLYDGS : 778
MpHEN1 : SKORVEYALQVIKQORAKSLIDLCCGSGSLLESLELQPTDLRELVGVDVSEKSLTAAKLLTLKLNKEMAGKESLEKIDLYEGS : 823

AtHEN1 : ILRFDSRLHVDVITCTCLEVIEHMEEDQACEFGERVLSLEFEPKLLIVSTPNYEFNTILCRSTPETQE-----E-- : 845
MpHEN1 : IADYDRLGGADVAVCIEVVEHMDPELEKFGSTVLEMLRQVLLIVSTPNFEYNELILQGLEWDESTNSLKSQVEVIDGLESVDVKQ : 908

AtHEN1 : -----NNSFPQLKFRNHDKHFEWTRFOENQWASKICKRNNYSVEFSGVGGSC-EVEPGFASQIALETRERASSVENV : 916
MpHEN1 : IRLSDHELNGCNSDLSLRSVKFRNEDHRFEWTRSERVWASNMAYHSHSYVRFSGVGGSCDEGCPGYASQIALETRRKQQS-L : 992

AtHEN1 : AESSMOFYKVIWEWKEDVEKKKIDL- : 942
MpHEN1 : ANGCPQSKGIAADEVHLKLVHWASGP- : 1018

```

Properties among amino acids	Full length AtHEN1 and MpHEN1	MTase domain of AtHEN1 and MpHEN1
Identity	32%	42%
Similarity	49%	57%

Figure 2.3. Amino acid sequence alignment of AtHEN1 and MpHEN1. The entire proteins hold the sequence identity as 32% and the similarity as 49% while the MTase domain of the two HEN1s shows sequence identity as 42% and the similarity among sequences as 57%. The defined MTase region of AtHEN1 is highlighted and being compared in magenta colored box.

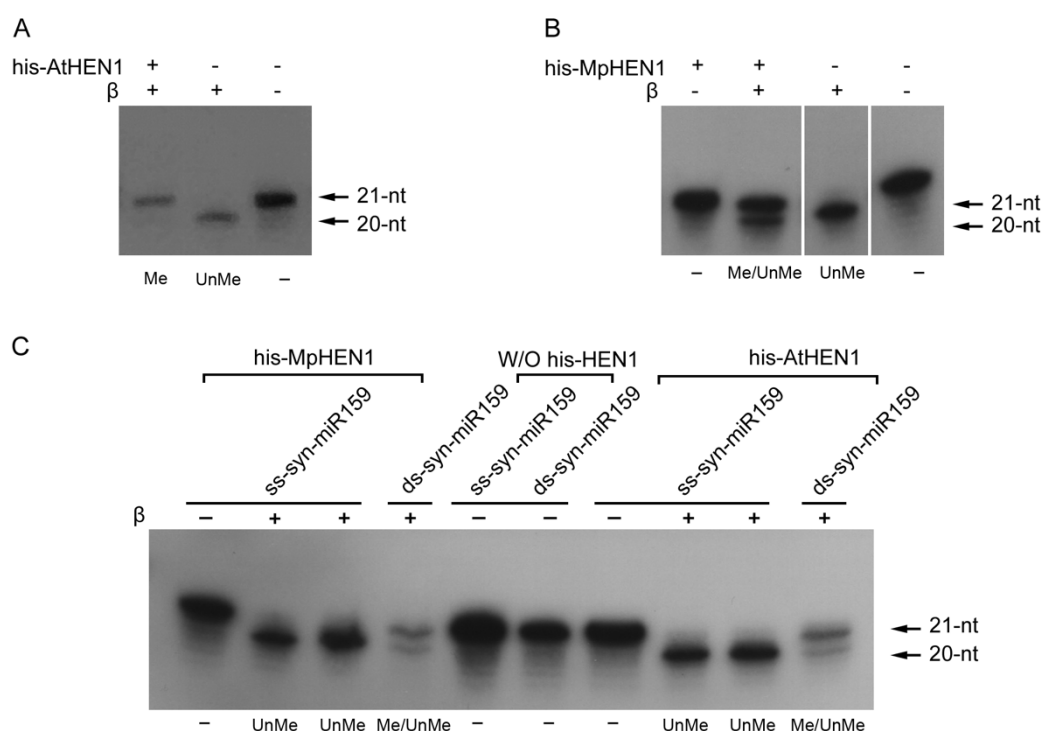


Figure 2.4. In vitro his-AtHEN1 and his-MpHEN1 methylation activity and substrate selectivity. The methyltransferase activity of recombinant his-AtHEN1 (**A**), and his-MpHEN1 (**B**) were evaluated by checking methylation status of synthetic miRNA by oxidation reaction followed by β -elimination, further subjected to small RNA northern assay. The methylated miRNA is represented by Me at the 21-nt location, whereas the unmethylated miRNA is represented by UnMe at the 20-nt position. – symbolizes untreated samples located at the 21-nt position. The sample having a mix of both methylated and unmethylated is represented by Me/UnMe. (**C**) The substrate specificity of AtHEN1 and MpHEN1 was assessed using single stranded as well as double stranded synthetic miRNA.

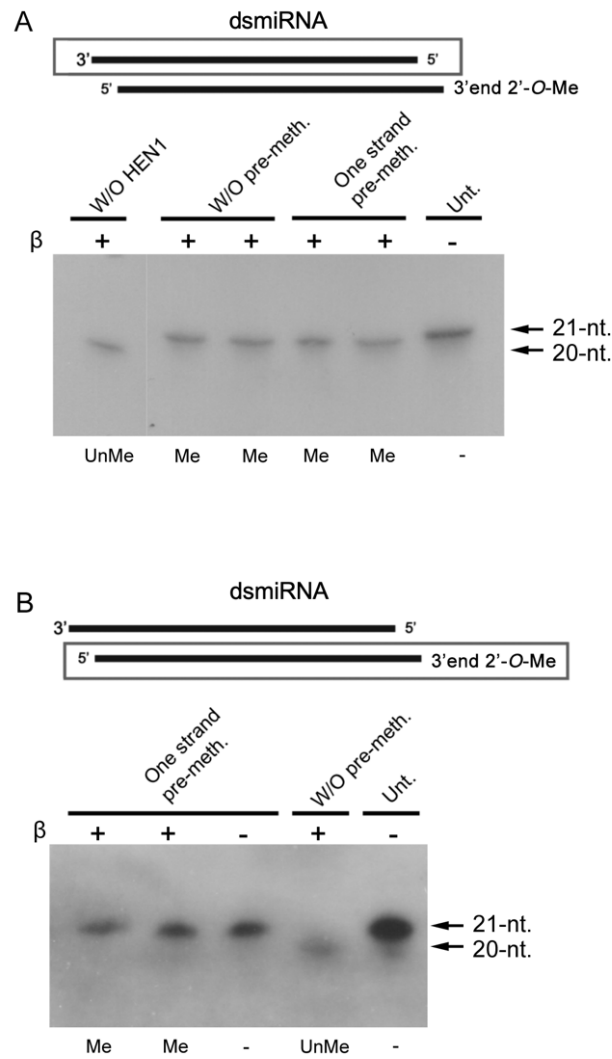


Figure 2.5. HEN1 methylates duplex RNA. (A) Probe used to detect the non-hemimethylated strand of duplex miRNA. The methylated miRNA is represented by Me at the 21-nt location, whereas the unmethylated miRNA is represented by UnMe at the 20-nt position. – symbolizes untreated samples located at the 21-nt position. Pre-meth means one strand of the synthetic duplex RNA is pre-methylated while Unt. means untreated synthetic duplex miRNA samples. **(B)** Probe detecting the hemi-methylated strand of the duplex miRNA.

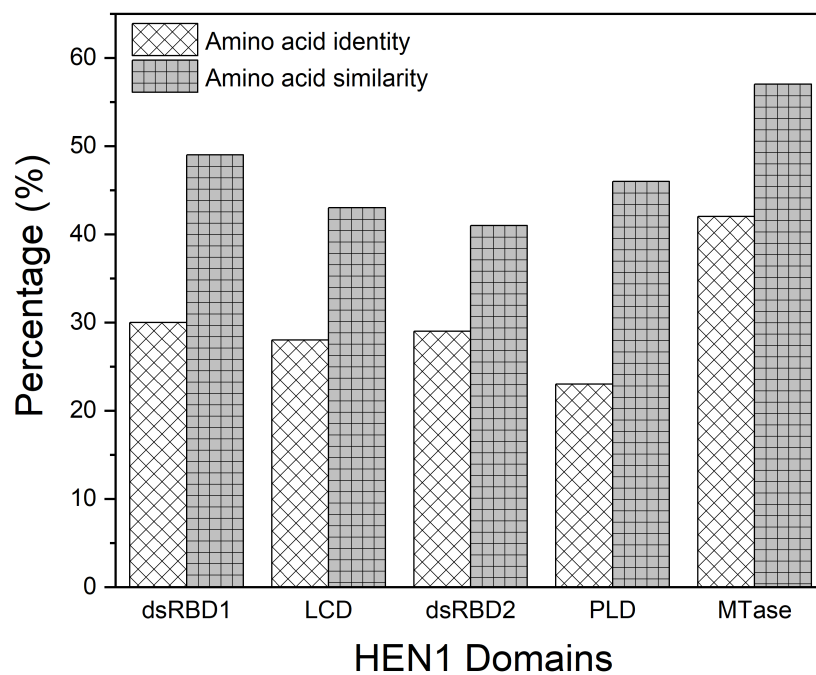


Figure 2.6. AtHEN1 and MpHEN1 domain comparison. The five different domains corresponding different functions are analyzed for their amino acid identity as well as similarity. The Y-axis represents the percentage of similarity and/or identity while the X-axis represents the specific domains.

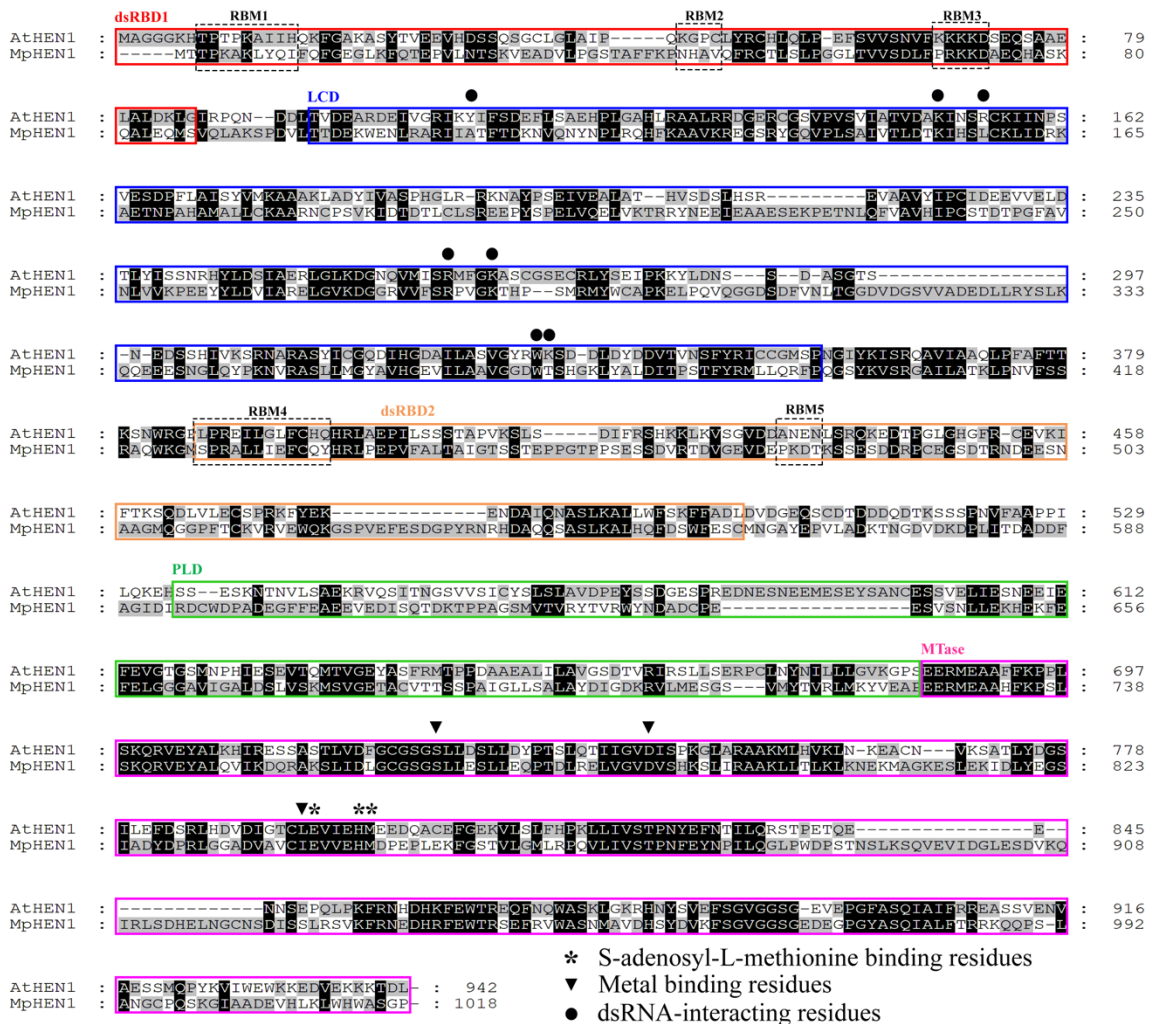


Figure 2.7. Amino acid sequence alignment for AtHEN1 and MpHEN1. Based on AtHEN1 structural studies, the five domains are highlighted in various colors and compared with the MpHEN1 sequence. The dsRBD1, LCD, dsRBD2, PLD and MTase domains are highlighted in boxes of color red, blue, yellow, green and magenta respectively. The arrowheads and the asterisks indicate the metal-binding residues and S-adenosyl-L-methionine binding residues respectively while the dots indicate the dsRNA-interacting residues. Five different RNA binding motifs (RBM) have been highlighted in black boxes.

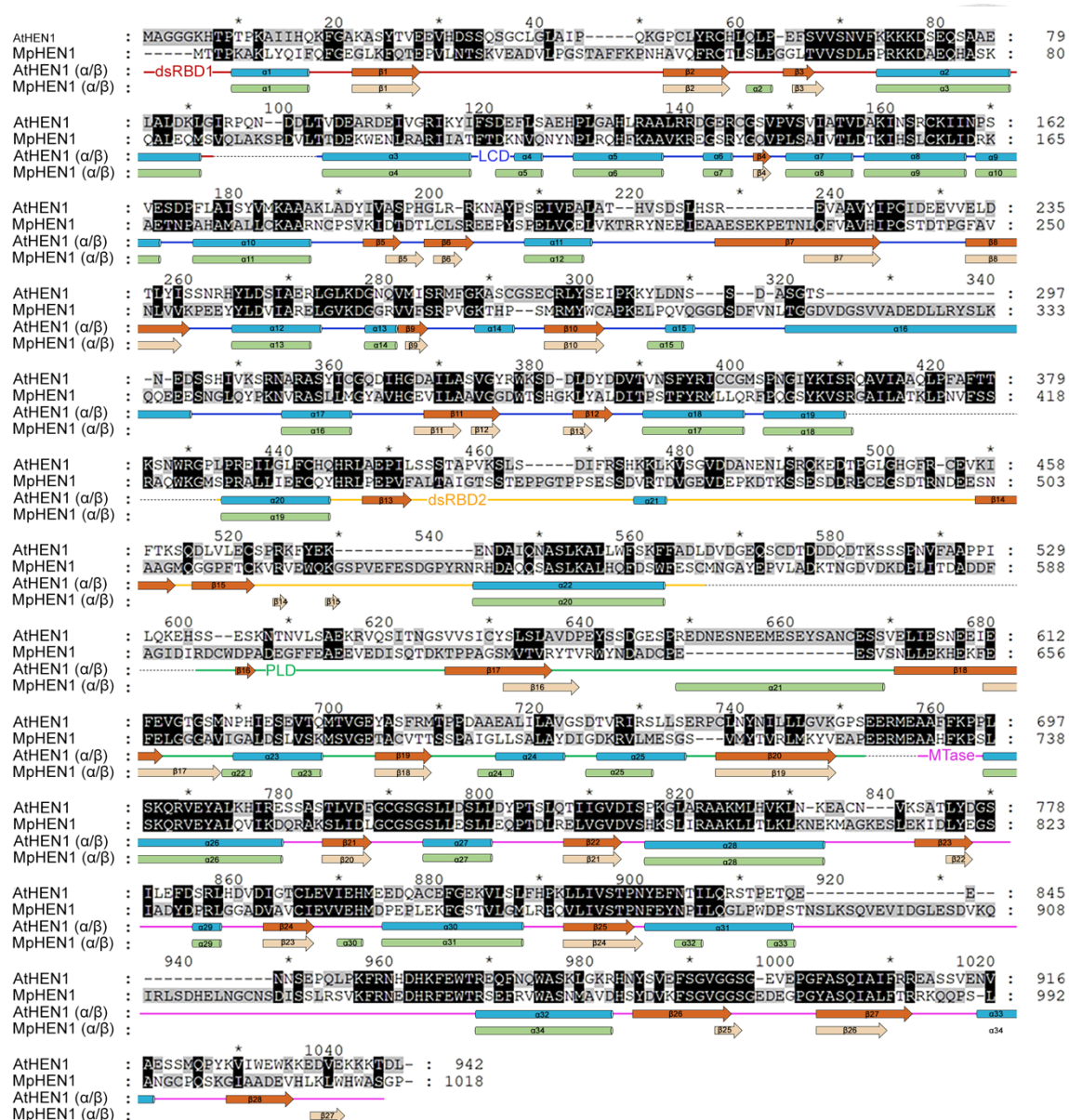


Figure 2.8. The different domains of AtHEN1 and MpHEN1 compared for their α -helix and β -sheet arrangements. α -helix of AtHEN1 and MpHEN1 is shown in blue and green color respectively while β -sheet of AtHEN1 and MpHEN1 is represented in orange and beige respectively among various domains of AtHEN1 and MpHEN1.

(GRMZM2G107457_T01); Sf, *Sphagnum fallax* (Sph-falx0066s0042.1, Sphfalx0001s0228.1); Sl, *Solanum lycopersicum* (Solyc02g070030.2.1); Pt, *Populus trichocarpa* (Potri.001G465500, Potri.011G163600); Gr, *Gossypium raimondii* (Gorai.010G144100); Tc, *Theobroma cacao* (Thecc1EG026937); Cpa, *Carica papaya* (evm.model.supercontig_166.41), Vv, *Vitis vinifera* (GSVIVG01021670001) and *Arabidopsis thaliana*, CHLM (AT4G25080). The bootstrap values are shown above the branches at the nodes. Arrowheads indicate duplicated events.

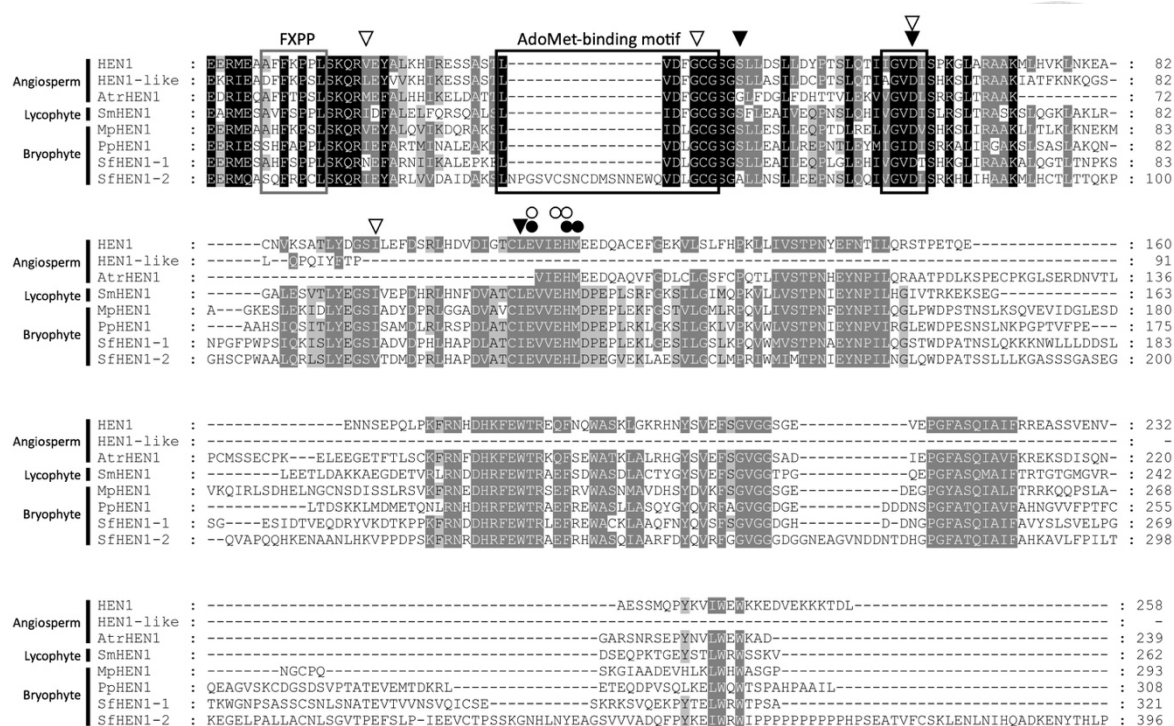


Figure 2.10. MTase domain alignments in several plant species. The arrowheads indicate the SAM-binding residues and dots indicate metal-binding residues. The black and grey boxes mark the AdoMet-binding motif and the FXPP motif, respectively.

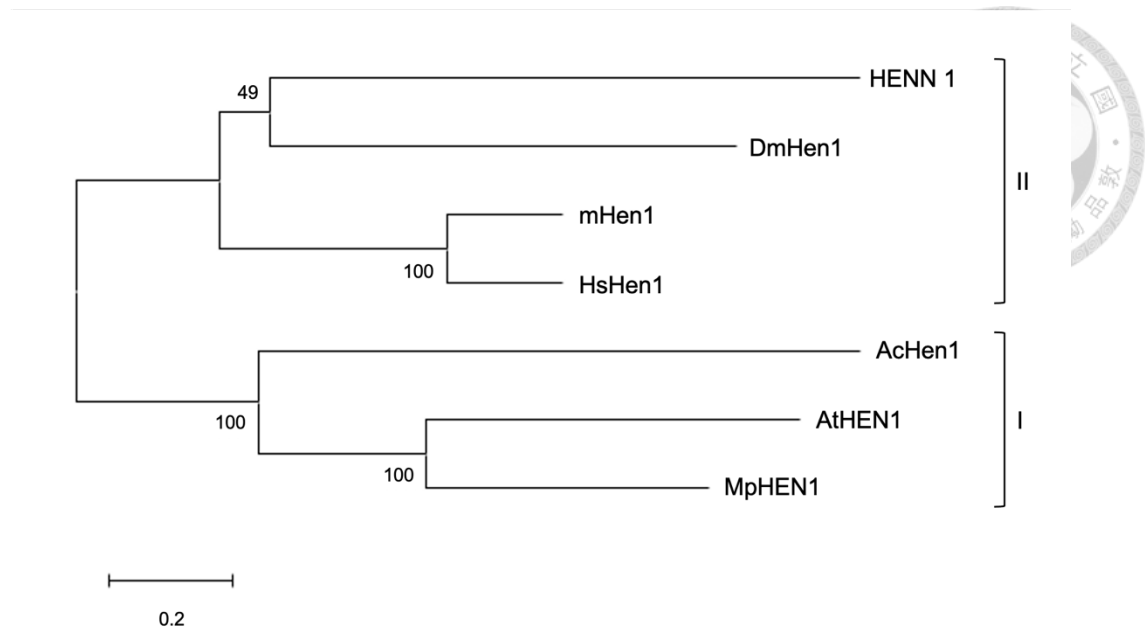


Figure 2.11. Phylogenetic tree of HEN1 and HEN1 orthologs of different species. The phylogram representing the evolutionary relationship between 7 different species of HEN1 or HEN1 orthologs, including *Arabidopsis thaliana* (AtHEN1), *Marchantia polymorpha* (MpHEN1), *Caenorhabditis elegans* (HENN1), *Actinobacteria bacterium* (AcHen1), *Drosophila melanogaster* (DmHen1), *Mus musculus* (mHen1), and *Homo sapiens* (HsHen1). The scale bar presents distance. The numbers on the tree represent the percentage of 10,000 bootstraps.

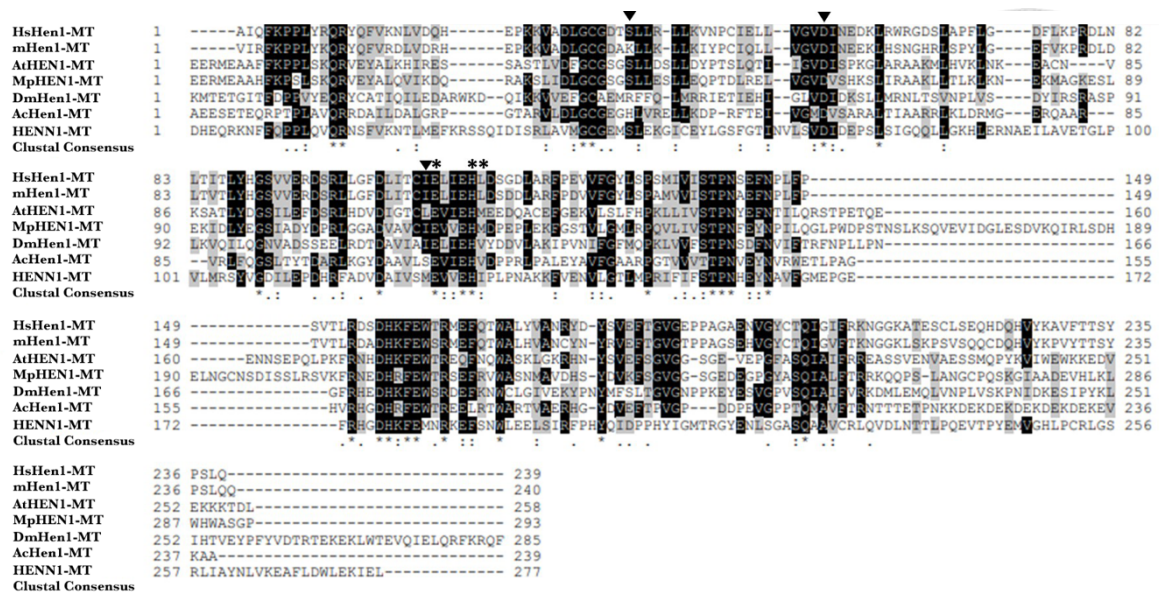
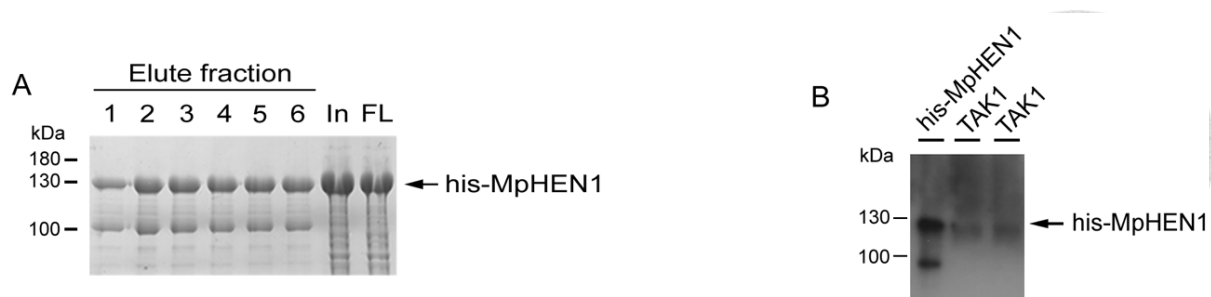
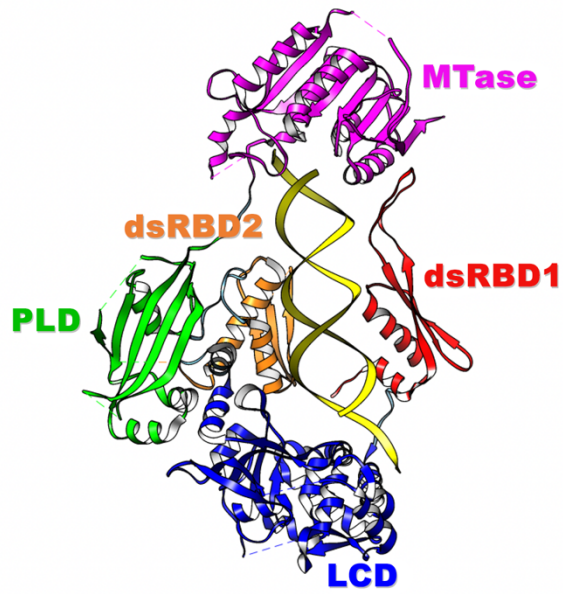


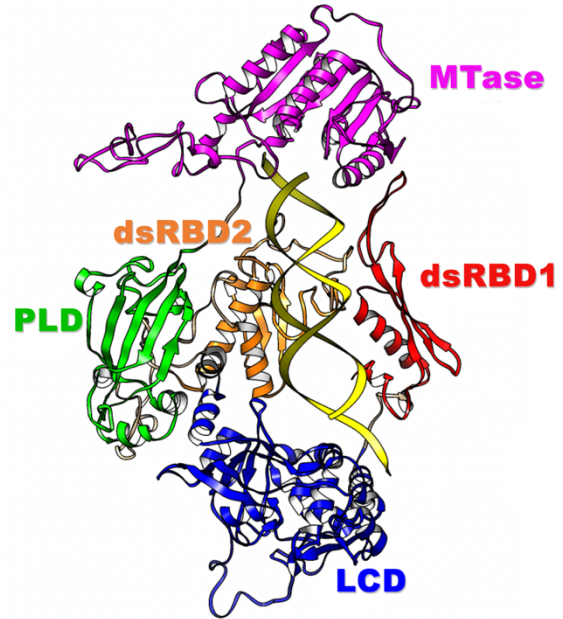
Figure 2.12. The MTase domain comparison between different species. The different MTase domains including *Arabidopsis thaliana* (AtHEN1), *Marchantia polymorpha* (MpHEN1), *Caenorhabditis elegans* (HENN1), *Actinobacteria bacterium* (AcHEN1), *Drosophila melanogaster* (mHen1), *Mus musculus* (mHen1), and *Homo sapiens* (HsHen1). The arrowheads indicate the S-adenosyl-L-methionine binding residues. The Asterisks indicate metal-binding residues.



Appendix figure 2.1. α -MpHEN1 production and efficiency evaluation. **(A)** Expression of the proteins using *E.coli* BL21 (DE3) cells, purified by Fast Protein Liquid Chromatography (FPLC) with His-TrapTM FF, Ni-NTA column of 1ml capacity, and the collected fractions were subjected to 7.5% SDS-PAGE. **(B)** The endogenous MpHEN1 detection for α -MpHEN1 antibody. His-MpHEN1 is the recombinant MpHEN1 while TAK1 is the WT of male *M. polyporpha* were used. Figure credit: Veny Tjita.

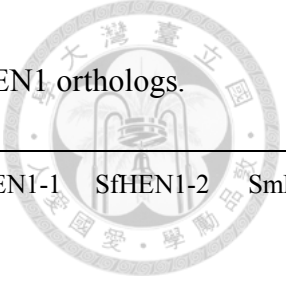
A

**AtHEN1
(3HTX)**

B

**MpHEN1
(modeling)**

Appendix Figure 2.2. AtHEN1 and MpHEN1 homology model. The 3D structure of AtHEN1 and MpHEN1 along with dsRNA is compared. The dsRBD1, LCD, dsRBD2, PLD, and MTase domains on **(A)** AtHEN1 (PDB number: 3HTX) and **(B)** MpHEN1 model are highlighted by red, blue, orange, green, and magenta, respectively. Figure credit: Hao-Ching Wang.

Table 2.1. The similarity and identity of the MTase domains of plant HEN1 orthologs.

Similarity Identity	AtHEN1	AtHEN1- like	AtrHEN1	MpHEN1	PpHEN1	SfHEN1-1	SfHEN1-2	SmHEN1
AtHEN1	-	51.98	65.09	61.88	56.43	54.70	37.37	69.80
AtHEN1-like	50.49	-	49.00	42.32	35.14	31.43	14.10	47.52
AtrHEN1	59.90	46.78	-	57.92	47.52	50.00	28.71	60.39
MpHEN1	54.95	39.35	52.22	-	59.40	63.11	42.32	63.86
PpHEN1	50.00	33.16	42.57	52.97	-	64.35	46.78	63.61
SfHEN1-1	48.51	30.44	44.80	57.17	58.91	-	47.27	58.66
SfHEN1-2	29.95	11.63	23.26	35.64	37.37	39.85	-	38.61
SmHEN1	62.62	44.80	54.20	57.17	56.43	52.47	30.69	-

Table 2.2. The similarity and identity of the different MTase domains.

Similarity	Identity							
		HENN1	AcHen1	DmHen1	AtHEN1	MpHEN1	HsHen1	mHen1
	HENN1	--	13%	25%	28%	23%	25%	24%
	AcHen1	21%	--	18%	18%	19%	19%	20%
	DmHen1	43%	27%	--	26%	22%	30%	31%
	AtHEN1	43%	18%	26%	--	42%	32%	30%
	MpHEN1	35%	28%	39%	57%	--	29%	29%
	HsHen1	37%	27%	47%	46%	41%	--	78%
	mHen1	39%	28%	47%	46%	45%	91%	--

Chapter 3.



HC-Pro suppresses the methyltransferase activity of HEN1

3.1. Abstract

The investigation of viral suppressors helps us to understand the crosstalk between virus and the host plant. This also helps us to unveil the mechanism of hidden molecular gene silencing pathway. The P1/HC-Pro of *Potyvirus* is the first discovered suppressor, however much of the molecular mechanism remained unfathomed. Previous studies based on various Potyviral HC-Pro have shown that HC-Pro binds to small RNA and HEN1, inhibiting the methyltransferase activity of the latter. Although, the P1 does not shown to have any role in HEN1 inhibition however, it enhances the production of HC-Pro and eventually helps in the suppression ability. In this study, we report that TuMV HC-Pro^R inhibits AtHEN1 activity both in vivo as well as in vitro through the FRNK motif by physical interaction, but the HC-Pro^R does not bind with the sRNA. Arabidopsis is the host of TuMV but to our surprise the HC-Pro^R also found to inhibit the *Marchantia polymorpha* HEN1 (MpHEN1) which belongs to bryophyte and is not a conventional host of TuMV.

3.2. Introduction

Small RNAs, such as miRNAs and siRNAs, are important components of an evolutionarily conserved RNA-based gene regulation system found in fungi, plants, and animals, and implicated in a wide range of biological processes ranging from development to antiviral defenses [8, 9, 57, 92, 213-217]. The presence of dsRNA or ssRNAs with stem-loop structures initiates the silencing pathway, which is triggered by the presence of 21- to 24-nt small RNAs, such as siRNAs, miRNAs, and others, which are incorporated into an RNA-induced silencing complex (RISC) to promote sequence-specific cleavage or translation arrest of transcripts of complementary sequences [8, 9, 101, 218-220, 221, 222-224].

Regulation of cellular transcripts, driving heterochromatin formation and transposon transcriptional suppression, processing of noncoding RNA precursors that affect developmental timing and leaf polarity, and stress regulation are all endogenous activities of RNA silencing [34, 218, 220, 223, 225, 226]. Because it is activated by structured RNAs or dsRNAs produced during the replication cycles of different kinds of viruses and subviral pathogens, RNA silencing is also a natural defensive system against viruses [8, 92, 161, 213, 215, 227, 228]. Viruses are both inducers and targets of RNA silencing, but they've also developed techniques to combat it [130, 229, 230]. Silencing suppression is a typical feature of plant viruses, and suppressor proteins are thought to be pathogenicity determinants that are required for successful acculturation. Silencing suppressor proteins, which are found in almost all viruses, have a great deal of structural and sequence variety, which has been described as an evolutionary convergence toward a common functional need [230]. The existence of genetic diversity impacting fitness is a pre-requisite for natural selection to operate. Using solely potyviruses as a model, it was discovered that two amino acid substitutions in the clover yellow vein virus's HC-Pro suppressor are sufficient to diminish symptom severity and viral accumulation [231]. In the plum pox virus HC-Pro, a single mutation produced a similar result

[232]. Also, alterations in the conserved motifs of the ZYMV HC-Pro resulted in weaker viruses on the native host squash, as well as the potential to trigger hypersensitive responses in other local lesion hosts [167]. Overall, viral suppressor proteins are likely to be subjected to significant selection pressures in order to achieve optimal host adaptation, since a successful infection relies on a delicate balance between the host silencing response and viral counter-defense mechanisms [233].

TuMV is a single-stranded positive-sense RNA virus that belongs to the genus *Potyvirus* and the family Potyviridae [234, 235]. Polyprotein processing converts a single open reading frame into 11 mature viral proteins. The HC-Pro is known to serve a variety of roles in the viral infection cycle, with some of these roles being localized to distinct areas of the protein [236]. The C-terminus is a papain-like proteinase that catalyzes autoproteolytic cleavage from the polyprotein and helps the virus spread from cell to cell [125, 160, 237, 238]. HC-Pro has also been discovered to be a suppressor of PTGS and to interfere with the activity of miRNA [148, 164].

The HC-Pro protein is separated into three regions on a schematic level: A N-terminal portion linked to aphid transmission, a C-terminal region linked to proteinase and RNA silencing suppressor activity, and a middle region linked to a variety of activities, including RSS activity [165, 241]. The middle region of mature HC-Pro comprises multiple motifs that are highly conserved across all potyviruses, including the FRNK box at amino acid positions 179 to 182, which is linked to the severity of ZYMV symptoms [166]. The FRNK box mutation to FINK reduces the intensity of symptoms in the leaves of numerous cucurbit species without impacting viral accumulation or infectivity, and this mutation has been exploited for use in cross-protection. These findings suggest that the Arg in the HC-Pro FRNK motif plays a key role in mild strain-mediated cross-protection. In another study using TuMV the authors demonstrated that Tu-GK, which has an Arg182Lys substitution in HC-Pro (HC-Pro^K) and

causes symptomless infection in *Arabidopsis thaliana* (Col-0) plants and moderate infection in *Arabidopsis dcl2/4* mutant plants [171]. Tu-GK offered complete cross-protection against Tu-GR infection in both Col-0 and *dcl2/4* mutant plants, according to their findings [171].

In *Arabidopsis*, a methyltransferase called HEN1 methylates the 2-OH of the 3'-terminal nucleotide of miRNAs and siRNAs [19, 42, 150, 151]. The relevance of miRNA methylation in plants is shown in the reduced accumulation and variability in size of miRNAs, as well as the loss of miRNA function in *hen1* mutants [34, 82, 212, 242]. The addition of one to five U residues to the 3' ends of small RNAs by a new uridylation activity targeting the 3' ends of unmethylated miRNAs and siRNAs causes the size increase of small RNAs in the *hen1-1* mutant [42]. As a result, one of the functions of small RNA methylation is to protect the 3' ends of small RNAs from uridylation activity.

Lozsa et al. 2008 studied the *Nicotiana benthamiana* plants infected with viruses producing RSS, the p19 protein of CIRV and HC-Pro of TEV, they analyzed the 3' modification of silencing-related small RNAs and they found that CIRV had only a little effect on viral siRNA 3' modification, but TEV significantly inhibited si/miRNA 3' modification [174]. In another study, the authors demonstrated that RSS of beet yellows virus 21 kDa protein (p21), the tomato bushy stunt virus 19 kDa protein (p19), and the TuMV silencing suppressor, P1/HC-Pro interfere with the methylation of miRNA [185]. Further Jamous et al. demonstrated that ZYMV HC-Pro directly binds and inhibits the methyltransferase activity of HEN1 [152].

3.3. Materials and methods

3.3.1. Plant growth conditions

This study included seeds from *Arabidopsis thaliana* ecotype Columbia (Col-0), *PI/HC-Pro^R*, and *PI/HC-Pro^K* plants [171], as well as the *hen1-8/hesol-1* double mutant [89]. The 35S promoter-driven *HA-AtHEN1* gene (*35Spro:HA-AtHEN1*) was created and introduced into Col-0 plants to overexpress HEN1 and generate *HA-AtHEN1* plants. In addition, the 35S promoter-driven *PI/HC-Pro^R* gene and *35Spro:HA-AtHEN1* gene were introduced into Col-0 to produce the *PI/HC-Pro^R/HA-AtHEN1* plant, and the 35S promoter-driven *PI/HC-Pro^K* gene and *35Spro:HA-AtHEN1* plant was introduced into Col-0 to generate the *PI/HC-Pro^K/HA-AtHEN1* plant. After surface sterilization, the seeds were plated on Murashige and Skoog (MS) medium. Antibiotics that are appropriate according to the transgenic resistant lines, MS plates were employed. The plants were kept in a growth room with 16 h light/8 h darkness, 20 to 25 °C.

Marchantia polymorpha, wild types Takaragaike-1 (male accession) and Takaragaike-2 (female accession) were employed. On half-strength Gamborg's B5 medium containing 1% agar and MES 2- (N morpholino) ethanesulfonic, either *M. polymorpha* gemma or thallus were developed and maintained.

3.3.2. Mechanical inoculation of virus

Both recombinant viruses, TuGK (milder strain) and TuGR (severe strain) were propagated from DNA-infectious clones. Aliquots of 20 µl were applied onto the pre-carborundum dusted leaves of *Chenopodium quinoa* using sterilized mortar-pestle. At

7 days post inoculation (dpi), the fluorescent microscopy used to examine the establishment of the infection of each virus on the inoculated leaves exploiting the GFP signal. The single infected lesion was then picked and transferred to *N.benthamiana* for amplification and the viral pathogenicity was evaluated at 7 dpi using fluorescent microscopy followed by Western blot.

The 2.5 weeks old Col-0 were later mechanically inoculated using infected leaf's sample of *N.benthamiana* mixed with 3ml of virus inoculation KPB buffer 0.05 M (pH 7.5). At 7 dpi the challenged plants were monitored under fluorescent microscopy and Western blot.

3.3.3. Fluorescent microscopy

GFP fluorescence of TuGK and TuGR infected plants were monitored using a fluorescent microscopy (Nikon 80i, Nikon, Melville, NY, USA). 40X magnification is used to capture the images.

3.3.4. Western blot

10-20 mg of the plant tissue was crushed adding 100-200 μ l of $1 \times$ PBS (1:10). Equal amount i.e., 1:1 v/v of $2 \times$ sample buffer (2% SDS, 10% glycerol, 1% β -mercaptoethanol, 0.005% bromophenol blue, 50 mM Tris-HCl, pH 6.8) mixed with the crushed plant tissue and cooked for 10 mins at 100 °C. Rest of the procedure remained same as mentioned in section 2.3.4 of this thesis.

3.3.5. In vivo and in vitro methylation assay

The wild-type Col-0 was infected with TuGR (severe strain) and TuGK (milder strain) for the in vivo methylation experiment. The infected tissues were utilized for total RNA extraction 10 dpi. A spectrophotometer was used to measure the RNA, and 30 µg/10 µL was employed in the experiment. For in vitro methylation assay, the preparation remained same as described in section 2.3.5.

3.3.6. In vitro pull down and in vivo IP

2 µg bait (GST-HC-Pro^R or GST-HC-Pro^K) and 2 µg prey (his-AtHEN1) proteins were mixed in 1 mL binding buffer (50 mM Tris-HCl, pH 7.5, 100 mM NaCl, 0.2 % glycerol, 0.6 % Triton X-100, 0.5 mM β-mercaptoethanol) for in vitro pull-down. After 2 hours at 25°C, the reaction mixture was incubated for another 2 hours with Glutathione Sepharose 4B resin beads (GE Healthcare, Chicago, IL, USA) before being washed six times with the washing buffer (50 mM Tris-HCl, pH 7.5, 100 mM NaCl, 0.6 % Triton X-100). Western blotting with α-His or α-GST antibodies were used to examine the pulled-down proteins.

For in vivo IP, 1-week-old (1 g) P1/HC-Pro^R/HA-AtHEN1 or P1/HC-Pro^K/HA-AtHEN1 seedlings were homogenized in 1 mL IP buffer (25 mM Tris-HCl, pH 7.5, 150 mM NaCl, 1 mM EDTA, 5 % glycerol, 1 % NP-40), then centrifuged for 10 minutes at 4 °C. In this investigation, the IgG of α -HA was employed for the in vivo IP. A mixture of cleaned Protein A-Agarose beads (50 µL suspension each IP reaction) (Santa Cruz, Dallas, TX, USA), IgG (30 µL per IP reaction), and the lysate were used to perform IP. The IP reaction was kept at 4°C for 3 hours with moderate mixing. The beads were pulled down by centrifugation at 300 g, and the unspecific binding was rinsed twice

with 0.3 mL IP buffer and suspended with 0.3 mL IP buffer. Western blotting and small RNA extraction were done with the IP elutes.



3.3.7. EMSA


Rio's procedure for the electrophoresis mobility shift assay (EMSA) was followed [243]. Purified protein (1 μ g) was incubated with 32 P-labeled synthetic miRNA/miRNA* duplex for 1 hour at 4°C in a binding buffer (40 mM Tris-HCl, pH 8.0, 30 mM KCl, 1 mM MgCl₂, 0.01 % NP40, 1 mM DTT). The EMSA experiment was performed on a 4.2 % native polyacrylamide gel (acrylamide:bisacrylamide = 80:1). For further investigation, the gel was subjected to X-ray film at -80 °C.

3.3.8. β -elimination and northern blot

The procedure remained same as explained in section 2.3.6.

3.4. Results

3.4.1. TuGK and TuGR virus inoculation and titre check



To study the in vivo methylation status of miRNA in *Arabidopsis thaliana* (At) we inoculated the Col-0 plant with TuGK which is a milder strain of TuMV and TuGR which is the severe strain of the same. At first, we used *Chenopodium Quinoa* plants followed by *Nicotiana benthamiana* (Nb) for virus inoculation, which is relatively easy to inoculate and to select for further mechanistic studies in Arabidopsis. The phenotypic appearances were photographed at 7 dpi (Figure 3.1 and 3.3). Based on symptom development, at 7 dpi the inoculated plants were examined under fluorescence microscopy as both the milder and severe strains of TuMV are carrying a *GFP* gene (denoted as TuGK and TuGR) (Figure 3.2 and 3.4). Furthermore, the Western blot analysis showed the presence of TuMV coat protein (TuCP) depicting the presence of the virus in the inoculated plants (Figure 3.5).

3.4.2. HEN1 activity is inhibited by the TuMV HC-Pro suppressor

Yu et al. (2006) found that in transgenic Arabidopsis expressing the TuMV *HC-Pro* gene (*HC-Pro* plant), miRNA methylation is suppressed, suggesting that HC-Pro may limit HEN1 function [185]. As a result, we assessed the state of endogenous miRNA methylation in TuGR and TuGK infected Col-0 plants 14 days after infection. Upon β -elimination, the findings showed that the miR159 in mock and TuGK infected plants remained 100% methylated, however the methylation status in TuGR was decreased to 65% (Figure. 3.6), suggesting that the wild type of HC-Pro can suppress HEN1 methylation in miRNA. *PI/HC-Pro^R* and *PI/HC-Pro^K* plants produced comparable findings. The *PI/HC-Pro^R* plant prevented miRNA methylation, but the

PI/HC-Pro^K plant, like Col-0 plants, exhibited normal miRNA methylation (Appendix figure 3.1.A).

Both TAK1 and Col-0 contain completely methylated miRNA *in vivo*, showing that MpHEN1 may fulfill the same methylation role in *M. polymorpha* as it does in *Arabidopsis*, according to our β -elimination experiment (Appendix figure 3.1.B). We discovered a smear of lower molecular weight bands in the *hen1/hesol* mutant, indicating that exoribonucleases such as SDN are facilitating truncation or degradation of miRNAs (Appendix figure 3.1.B) [90]. miRNA methylation was partially inhibited in the *PI/HC-Pro^R* plant by 47%. (Appendix figure 3.1.B). Overall, the findings suggest that HEN1s in *M. polymorpha* and *Arabidopsis* have similar fundamental behavior.

3.4.3. HC-Pro^R suppresses the activity of the HEN1, *in vitro*.

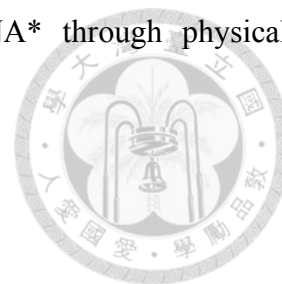
The *in vitro* HC-Pro-mediated HEN1 inhibition experiment was then performed. The findings revealed that increasing the GST-HC-Pro^R to his-AtHEN1 ratio has a positive correlation with its inhibitory impact on his-AtHEN1's methylation property (Figure. 3.7.A and 3.7.B). Surprisingly, GST-HC-Pro^R reduced the activity of MpHEN1 in a dose-dependent manner as well (Figure. 3.7.C and 3.7.D). Because *Arabidopsis* is a TuMV host plant, its silencing suppressor HC-Pro is anticipated to have an inhibitory effect on methylation [185, 219]. While *M. polymorpha*, a basal land plant, is not a TuMV host, but the GST-HC-Pro^R is able to suppress the his-MpHEN1 activity (Figure. 3.7.C and 3.7.D), suggesting that structural similarities between the two HEN1s may be the reason that HC-Pro^R can interact and inhibit. In conclusion, the *in vitro* findings indicated that HC-Pro^R without P1 was capable of aiding miRNA methylation suppression activity.

3.4.4. HC-Pro^R interacts with HEN1 and inhibits miRNA methylation.

The purified GST-tagged recombinant HC-Pro^{R/K} demonstrated excellent expression (Appendix figure 3.2.A). GST-HC-Pro^R had a 5- to 6-fold greater his-AtHEN1 pull-down signal than GST-HC-Pro^K, according to in vitro physical interaction data (Appendix figure 3.2.B, lower panel). In vivo co-immunoprecipitation (co-IP) studies were performed using *PIHC-Pro^R/HA-AtHEN1* and *PIHC-Pro^K/HA-AtHEN1* plants. According to the co-IP results, HC-Pro^R physically interacts with HA-AtHEN1, however no interaction signal between HC-Pro^K and HA-AtHEN1 was seen (Appendix figure 3.2.C). These findings showed that the FRNK motif's Arg is required for strong AtHEN1 binding affinity.

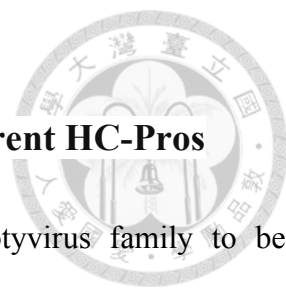
The his-AtHEN1 protein showed significant miRNA duplex binding signals in the EMSA. Although, the miRNA/miRNA* signals did not show any shift in HC-Pro^R or HC-Pro^K (Appendix figure 3.3.A). A positive control for RNA binding was Sigma 70 (an RNA-binding protein) (Appendix figure 3.3.A). We investigated whether HC-Pro^R influences AtHEN1-miRNA duplex binding to learn more about the interaction between HC-Pro^R and AtHEN1 in terms of RNA binding. According to the EMSA data, HC-Pro^R substantially decreased AtHEN1's miRNA duplex-binding ability in a dose-dependent manner (Appendix figure 3.3.B). Only high amounts of HC-Pro^K (0.4 µg) interfered marginally with the HEN1's capacity to bind miRNA/miRNA* (Appendix figure 3.3.B), suggesting that HC-Pro^K cannot bind AtHEN1 effectively and interfere with AtHEN1's RNA-binding activity. Indeed, an in vitro pull-down test revealed that HC-Pro^K still had a minor (0.2- to 0.3-fold) interaction with AtHEN1 (Appendix figure 3.2.B). In summary, HC-Pro^R prevents HEN1-miRNA/miRNA* binding by inhibiting

AtHEN1's methyltransferase activity towards miRNA/miRNA* through physical contact.



3.5. Discussion

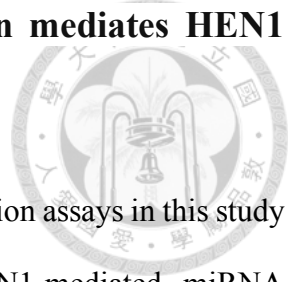
3.5.1. Variation in suppression activity among different HC-Pros



P1/HC-Pro is the first viral suppressor from the potyvirus family to be discovered. TuMV, ZYMV, and TEV, the three most extensively studied HC-Pros have demonstrated their suppression ability in plant [106, 152, 168, 171, 219]; however, there are still distinctions between the three HC-Pros. For example, using the EMSA test, Leibman et al. (2011) established that HC-Pro isolated from ZYMV-infected squash possesses sRNA-binding capacity [244]. Furthermore, Ruiz et al. (2015) investigated the sRNA obtained from a TuMV-infected plant, and the sRNA profile revealed that vsiRNAs may co-immunoprecipitate with HC-Pro, implying that vsiRNAs are sequestered by HC-Pro during TuMV infection [189]. However, our in vitro EMSA results showed that recombinant GST-HC-Pro^R did not have the capacity to bind sRNA duplexes. As a result, we hypothesize that purified HC-Pro from virus-infected plants may contaminate other viral or host proteins that may aid sRNA binding to HC-Pro.

Furthermore, Hu et al. (2020) found that TuMV's P1/HC-Pro can cause AGO1 degradation, but P1/HC-Pro of ZYMV and TEV had no effect on AGO1 stability [106]. Another interesting finding is that TuGR, but not TuGK, inhibits AtHEN1's methylation capability, demonstrating the importance of the FRNK motif's arginine in TuMV HC-Pro [171]. In the instance of ZYMV, only several amino acid alterations entirely eliminated the virus's capacity to inhibit transgenic Arabidopsis [152]. In light of these findings, we propose that HC-Pros from various potyviruses interact different proteins in the silencing pathway in unique ways, each of which has to be investigated further individually.

3.5.2. HC-Pro alone, without any accessory protein mediates HEN1 inhibition

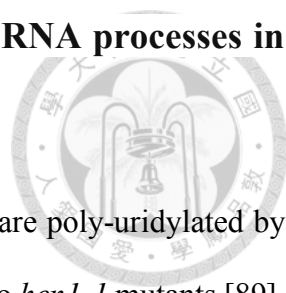


The in vitro and in vivo HC-Pro^R-mediated HEN1 inhibition assays in this study revealed that HC-Pro^R alone is capable of inhibiting HEN1-mediated miRNA methylation without the involvement of P1. Several investigations have shown, however, that HC-Pro alone is insufficient to display the morphological and molecular defects; P1 and HC-Pro must collaborate to produce the optimal gene silencing suppression, as P1 boosts HC-Pro's suppression activity [106, 145, 168, 171, 245-247]. According to recent studies, the P1s of TEV and PVY enhance the translation of their respective P1/HC-Pro [106, 243, 248]. Given this, we hypothesize that, while TuMV P1 does not directly affect HEN1 methylation, it may promote HC-Pro amplification, thereby promoting HEN1 inhibition.

3.5.3. TuMV HC-Pro also can inhibit bryophyte HEN1

Although *M. polymorpha*, a basal land plant, is not a TuMV host, the GST-HC-Pro^R suppressed his-MpHEN1 activity in a dose-dependent manner, in a manner very similar to how it inhibited his-AtHEN1, indicating that HC-Pro^R could interact with MpHEN1, which would require more experimental validations. Our alignment result supported this hypothesis, showing that the HEN1 protein of both species contains substantially conserved peptide sequences in diverse domains, particularly the MTase domain. Targeting such sequences would also be interesting for studying the interacting pattern between viral HC-Pro and the plant's HEN1.

3.5.4. Silencing suppressors interfere with distinct sRNA processes in different ways



Previous research has shown that unmethylated miRNAs are poly-uridylated by HESO1/URT1, resulting in heterogeneous miRNA sizes, similar to *hen1-1* mutants [89]. Plants infected with the oilseed rape mosaic tobamovirus (ORMV) have heterogeneous sizes of unmethylated miRNAs or siRNAs, indicating that ORMV infection may suppress HEN1 function, resulting in polyuridylation [58]. TuMV-infected Col-0 and *PI/HC-Pro^R* plants both did not have such a heterogeneous size of miRNAs, suggesting that the HC-Pro-mediated HEN1 suppression is distinct from ORMV. These findings add to the growing body of evidence that silencing suppressors interact with the different sRNA modification steps, as well as the fact that not all silencing suppressors function the same way.

3.6. Figures and legends

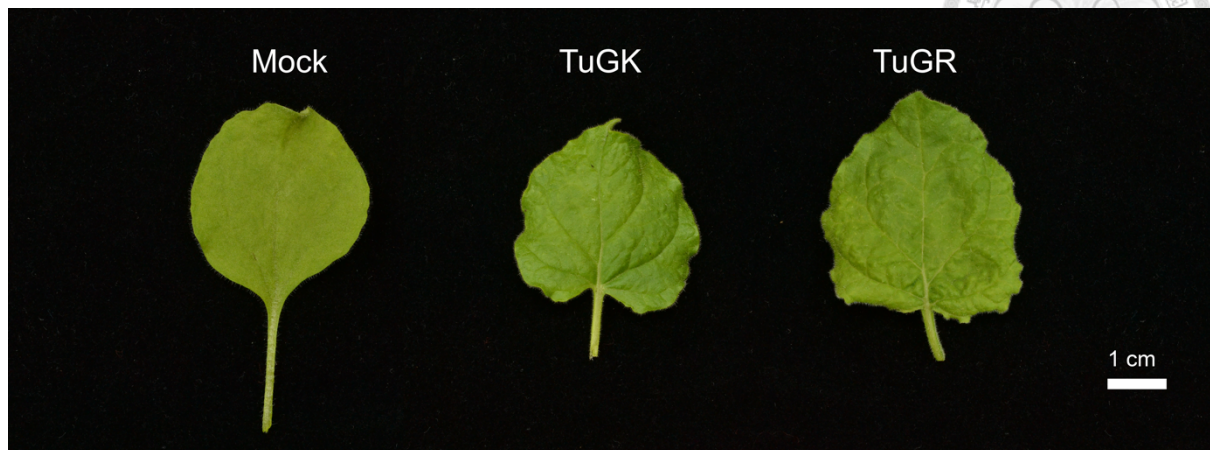


Figure 3.1. Phenotype of leaves observed at 7 dpi. The Nb plants were observed for phenotypic differences upon TuMV virus infection at 7 dpi. Mock represents the non-infected, wild type leaf while the TuGK and TuGR represent the leaves infected with the mutant and the wild strain of TuMV respectively. Bar, 1cm.

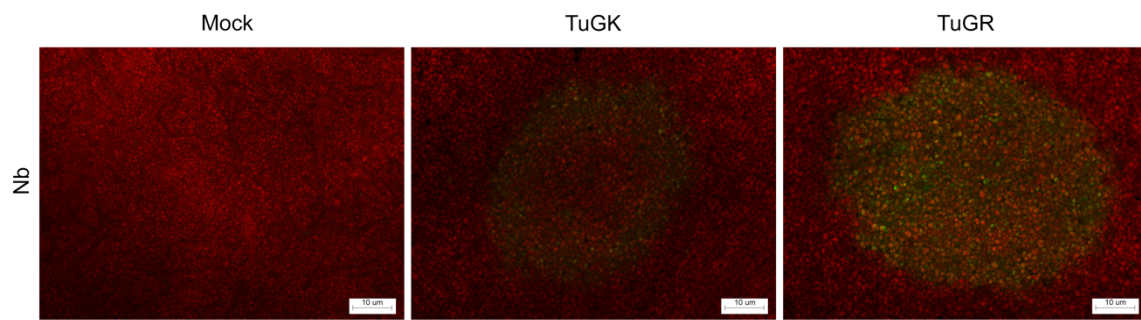


Figure 3.2. Fluorescence microscopy image of the infected plants at 7 dpi. The Nb plants were observed for their GFP signals at 7 dpi of TuMV infection. Mock is the non-infected leaf. Milder strain, TuGK and severe strain TuGR were used for infection. Bar, 10 μ m.

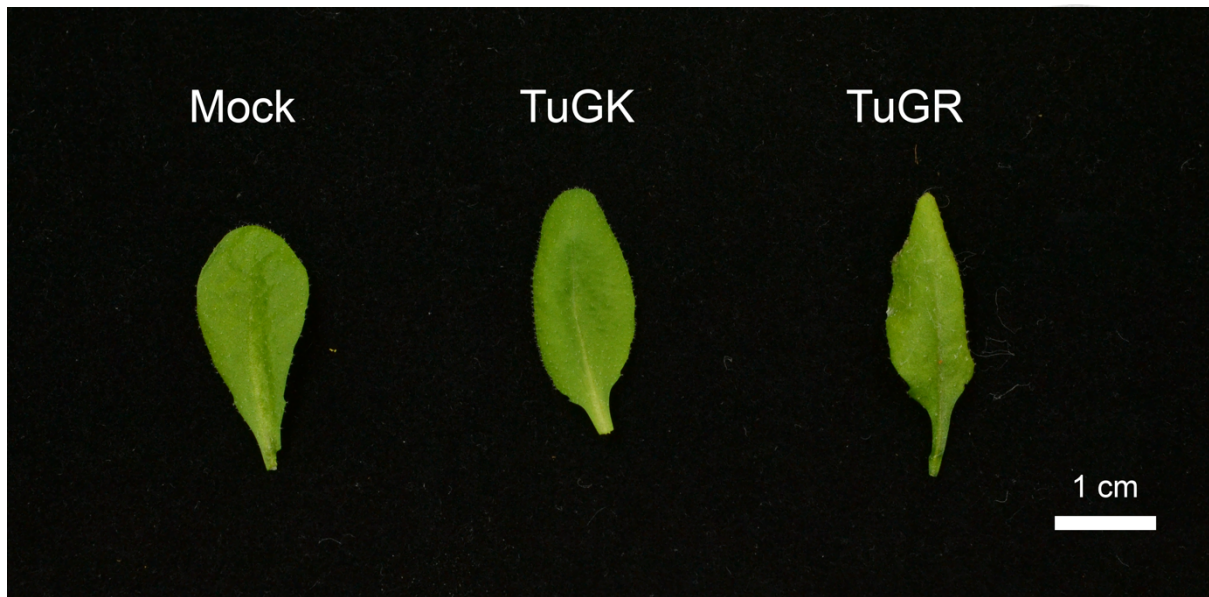


Figure 3.3. Phenotype of leaves observed at 7 dpi. The At (Col-0) plants were observed for phenotypic differences upon TuMV virus infection at 7 dpi. Mock represents the non-infected, wild type leaf while the TuGK and TuGR represent the leaves infected with the mutant and the wild strain of TuMV respectively. Bar, 1cm.

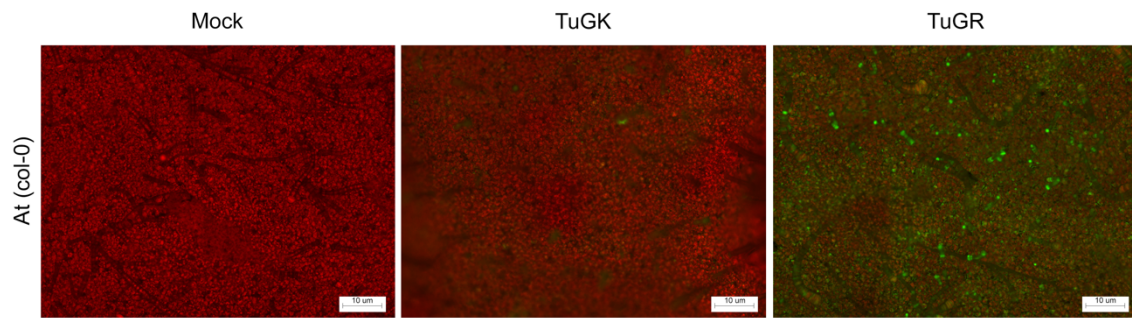


Figure 3.4. Fluorescence microscopy image of the infected plants at 7 dpi. The At (Col-0) plants were observed for their GFP signals at 7 dpi of TuMV infection. Mock is the non-infected leaf. Milder strain, TuGK and severe strain TuGR were used for infection. Bar, 10 μm.

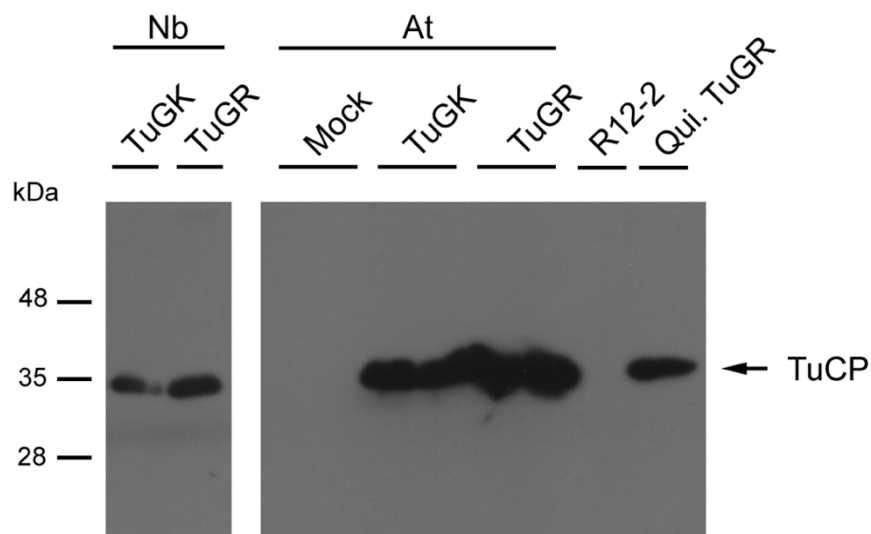


Figure 3.5. The TuMV coat protein (TuCP) detection in infected plants. Western blot analysis for the TuCP was done in both Nb and At (Col-0) plants infected with TuGK (milder strain) and TuGR (severe strain) of TuMV. Mock represents the non-infected sample. R12-2 is used as negative control while *Chenopodium Quinoa* TuGR (Qui. TuGR) is used as positive control.

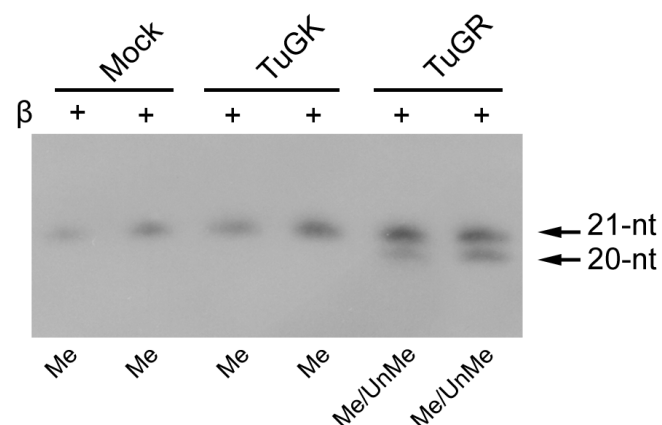


Figure 3.6. TuMV HC-Pro mediated HEN1 methyltransferase activity inhibition. At (Col-0) infected with milder strain, TuGK and wilder stain, TuGR of TuMV and checked for in vivo miR159. The state of miRNA methylation in 1-week-old plants was investigated using oxidation/ β -elimination followed by small-RNA northern blotting. The methylated miRNA is represented by Me at the 21-nt location and the sample having a mix of both methylated and unmethylated is represented by Me/UnMe.

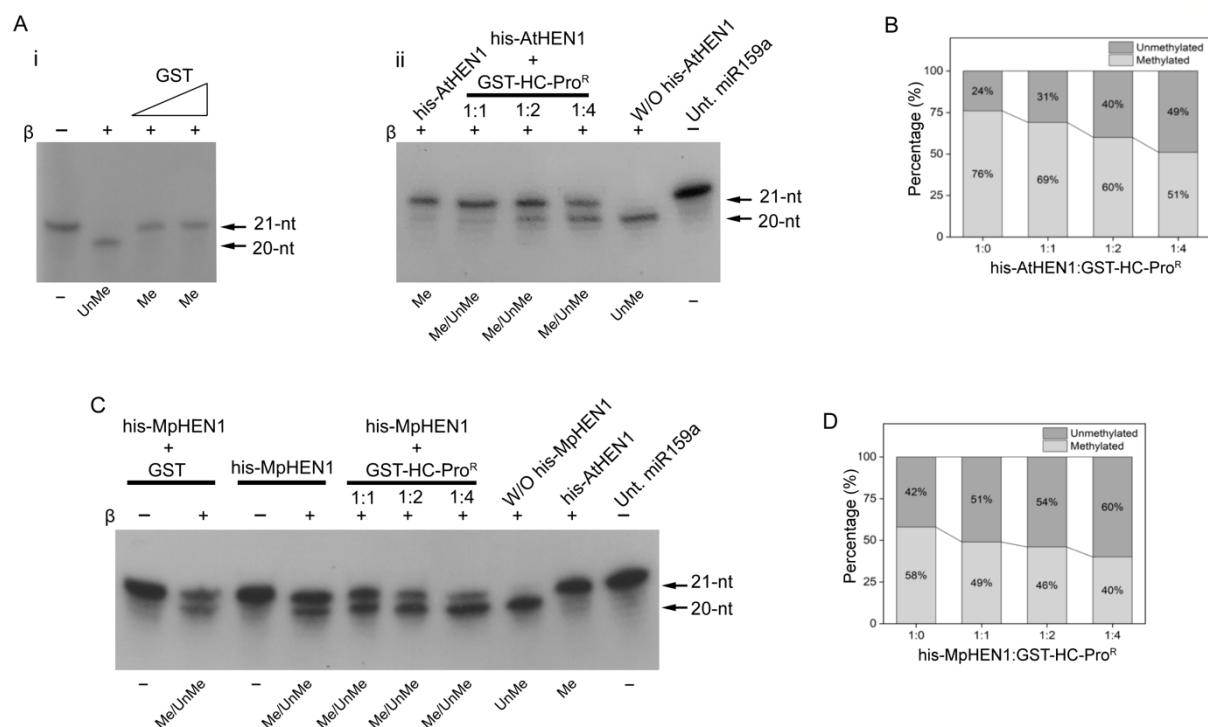
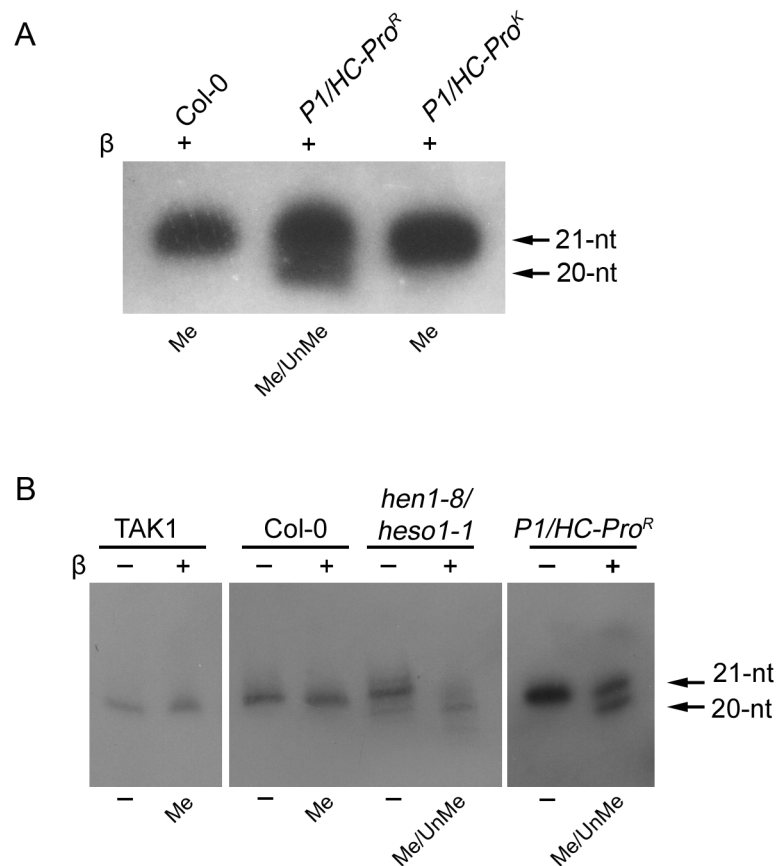


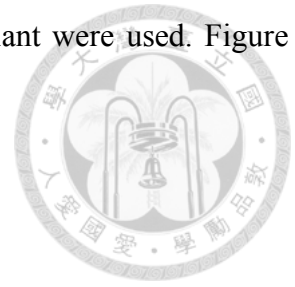
Figure 3.7. The in vitro HC-Pro mediated HEN1 methyltransferase activity inhibition.

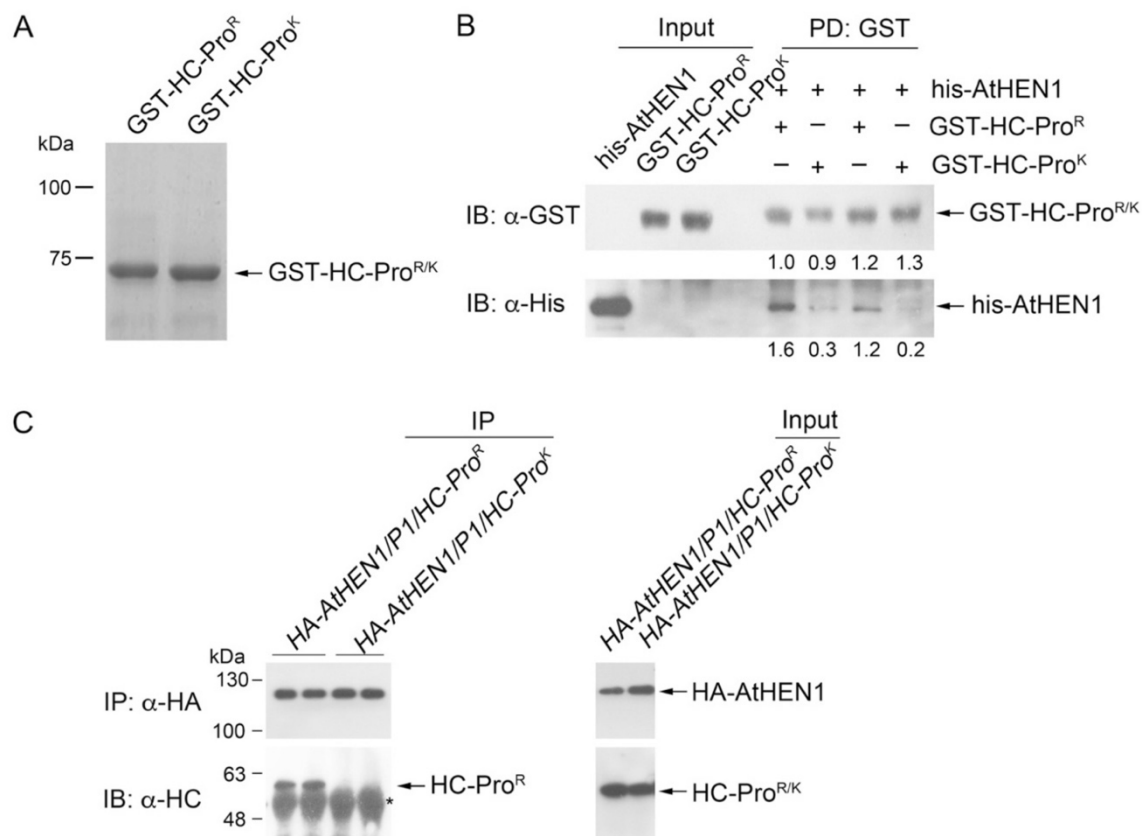
(A) The HC-Pro^R-mediated his-AtHEN1 inhibition assay. (i) The GST was used as negative control. (ii) The increasing ratio of GST-HC-Pro^R vs. AtHEN1 was performed. (B) Graph depicting quantification of the inhibitory effect of GST-HC-Pro^R on methyltransferase activity of AtHEN1. (C) The HC-Pro^R-mediated his-MpHEN1 inhibition assay. The increasing ratio of GST-HC-Pro^R vs. MpHEN1 was performed. (D) Graph depicting quantification of the inhibitory effect of GST-HC-Pro^R on methyltransferase activity of MpHEN1. Synthetic miR159a was used in these in vitro assays. The methylated miRNA is represented by Me at the 21-nt location, whereas the unmethylated miRNA is represented by UnMe at the 20-nt position. – symbolizes untreated samples located at the 21-nt position. The sample having a mix of both methylated and unmethylated is represented by Me/UnMe. Untreated miR159a is abbreviated as Unt. miR159a.



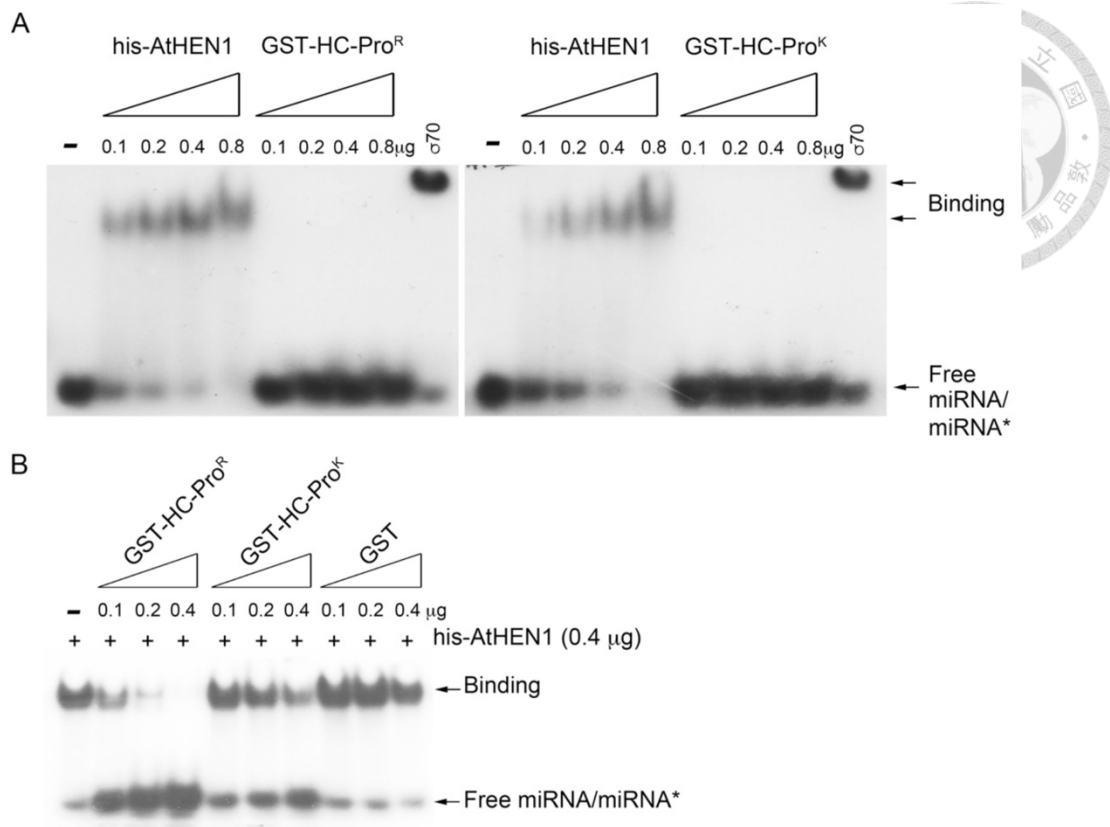
doi: 10.6342/NTU202201363

the *HEN1*, and *HES01* double mutant. *PI/HC-Pro^R*, *PI/HC-Pro^R* plant were used. Figure credit: Pin-Chun Lin (A) and Veny Tjita (B).





Appendix Figure 3.2. Interaction between HC-Pro^R and AtHEN1 in vitro and in vivo. (A) The GST-HC-Pro^{R/K} SDS-PAGE reveals the predicted protein size as a band of about 75 kDa. **(B)** GST-HC-Pro^R, GST-HC-Pro^K, and his-AtHEN1 interaction assessment in vitro pull-down experiment. **(C)** An in vivo co-IP experiment was used to investigate the binding activity of GST-HC-Pro^R or GST-HC-Pro^K to HA-AtHEN1. * Antibody heavy chain. Figure credit: Pin-Chun Lin.



Appendix Figure 3.3. The HC-Pro^{R/K} and the miRNA/miRNA* binding assay. (A) EMSA to investigate the capacity of GST-HC-Pro^R or GST-HC-Pro^K and his-AthEN1 to bind miRNA/miRNA*. **(B)** In vitro competition assay as increasing GST-HC-Pro^{R/K} ratio. Sigma 70 is used as positive control. Figure credit: Pin-Chun Lin.

Chapter 4.

Conclusion and future direction



4.1. Overview

This dissertation was based on studying the HEN1 characteristics evaluation in angiosperm and bryophyte. The two HEN1s methylation activity and structural similarities were focused. Furthermore, this dissertation contains study regarding suppression mechanism by which HC-Pro of TuMV inhibits HEN1 methyltransferase activity.

4.2. Angiosperm and bryophyte HEN1 characteristics study

In chapter 2, we produced α -AtHEN1 belonging to angiosperm and α -MpHEN1 belonging to bryophyte where the α -AtHEN1 showed cross-reactivity for recombinant MpHEN1. Further, we demonstrated that both HEN1s possess the methyltransferase activity and strictly uses duplex RNA for methylation. Both the strands of miRNA get methylated under HEN1 mediated methyltransferase activity. The MTase domain of the two HEN1s holds highest amino acid identity compared with the other domains of the two. The proposed MpHEN1 model found comparable to the AtHEN1. The phylogenetic tree of HEN1 orthologs of plants suggested that the HEN1 function in plants is conserved throughout evolution while the phylogenetic tree between species of various kingdom gave us idea that methyltransferase of animal kingdom is far related than the methyltransferase of plants implying functional difference among HEN1 of diverse kingdom.

4.3. HC-Pro suppressing HEN1 methyltransferase activity studies

In chapter 3, we demonstrated successful recombinant virus, TuGK (milder strain) and TuGR (severe strain) inoculation onto *Arabidopsis*. Further, the *Arabidopsis* HEN1 methyltransferase activity found to be inhibited under TuGR and the inhibition found to be interaction based. However, the milder strain TuGK which only possesses single amino acid substitution in the FRNK motif of TuMV HC-Pro loses the inhibition as well as interaction with AtHEN1. Interestingly, we found HC-Pro^R inhibiting *M. polymorpha* HEN1 as well highlighting possibility of similar interaction and inhibition patterns between TuMV HC-Pro^R and both the HEN1s. Based on our study, we propose a working hypothesis for HC-Pro^R-mediated HEN1 inhibition. In healthy plants, the HEN1 facilitates the methylation of miRNA/miRNA* and siRNA duplexes (Fig. 4.1, panel i). In the TuGR infected plants, the HC-Pro^R interacts and inhibits the HEN1, resulting in lesser sRNA duplexes methylation (Fig. 4.1, panel ii) although in contrast, the HC-Pro^K of TuGK loses the HEN1 interaction and inhibition potential; thus, the HEN1 still can bind the sRNA duplexes and effectuate the methylation activity of plant's RNA silencing regulation (Fig. 4.1, panel iii).

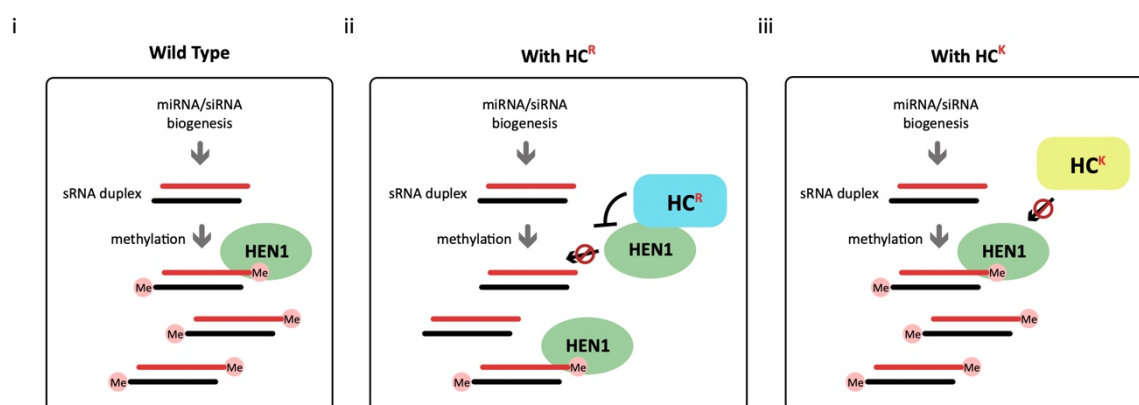


Figure 4.1. The working hypothesis for TuMV HC-Pro^R-mediated HEN1 inhibition. RNA silencing suppression pathway in (i) wild-type healthy plant, (ii) TuGR-infected plants, and (iii) TuGK- infected plants.

4.4. Future directions

4.4.1. HEN1 and TuMV HC-Pro interaction studies



As per our current study we have found that AtHEN1 and TuMV HC-Pro have physical interaction with each other and have indicated the significance of FRNK motif of the HC-Pro in the stable interaction. Furthermore, it may be worthwhile to study the interaction pattern between AtHEN1 and HC-Pro. AtHEN1 has five different domains facilitating corresponding functions, it would be interesting to discover which domain/domains interact with HC-Pro to answer how the methyltransferase activity gets inhibited under HC-Pro influence. For this, we may use the five different fragments of the AtHEN1 as we have produced in this study with the HC-Pro. To study its protein-protein interaction behavior several techniques can be exploited like co-immunoprecipitation and pull-down assay as mentioned in this thesis or Yeast two-hybrid screening (Y2H) system as mentioned by Baranauske et al. 2015 where they studied the interaction of HEN1 with HYL1 and DCL1 proteins [249]. Our early *in silico* data depicts that the HC-Pro through its FRNK motif makes physical interaction with the MTase domain of the AtHEN1. Hence, we hypothesize that through this interaction the methyltransferase activity might get inhibited and AtHEN1 eventually loses its function (Figure 4.2.A). Other possible mechanism of inhibition could be interaction and binding of the TuMV HC-Pro to the dsRBDs, occupying the site of the substrate binding and hence inhibiting the duplex RNA interaction with the HEN1 (Figure 4.2.B) as supported by our EMSA data (Appendix figure 3.3.B).

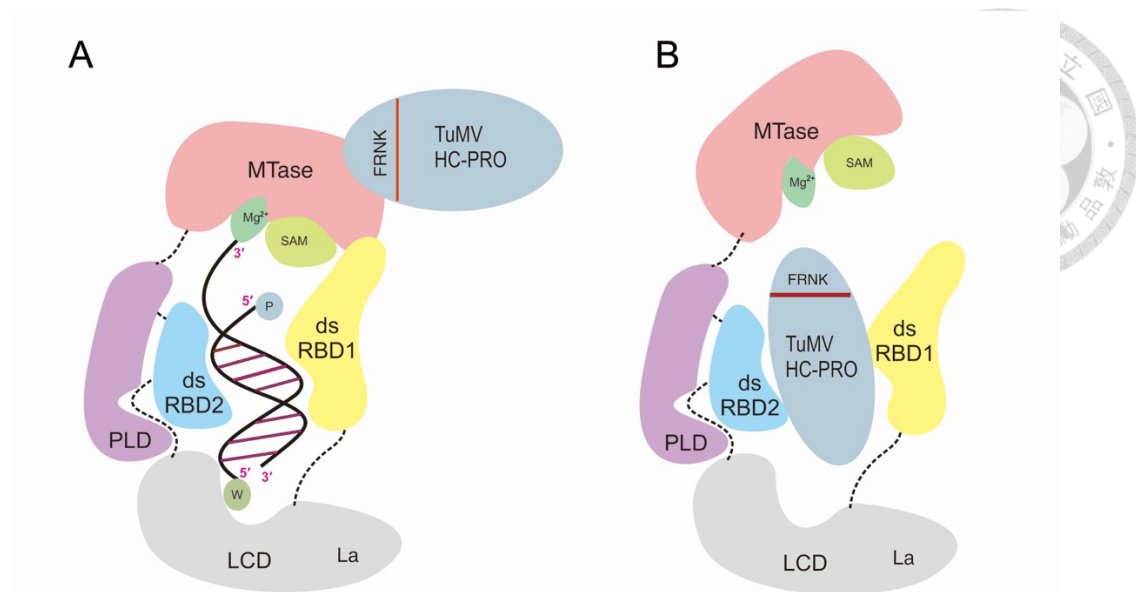
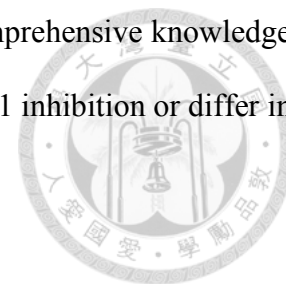


Figure 4.2. Hypothetical models depicting possible interaction pattern between AtHEN1 and TuMV HC-Pro. (A) The TuMV HC-Pro through its FRNK motif would interact with the MTase domain of AtHEN1 inhibiting the methyltransferase activity of the latter protein. (B) The TuMV HC-Pro would interact with the dsRBDs of AtHEN1 leading to blockage of the site for the duplex sRNA binding.

4.4.2. HEN1 inhibition studies under various potyviral HC-Pros

As we have discussed in this thesis before (section 3.5.1) various potyviral HC-Pro has distinct mechanistic behavior. Adding to this knowledge, a recent study from our lab demonstrated that TuMV P1/HC-Pro particularly triggered AGO1 posttranslational degradation. However, the P1/HC-Pro of ZYMV and TEV doesn't cause AGO1 degradation, suggesting that AGO1 degradation does not take place in all potyvirus and not all potyviral P1/HC-Pro behaves in the same way [106]. Considering this diversity in behavior of different potyviral HC-Pro it will be further interesting to study the HEN1 inhibition property of different potyviral HC-Pro. For this, we can use

the similar approach as have used in this thesis and can get comprehensive knowledge of whether diverse potyviral HC-Pro has similar effect on HEN1 inhibition or differ in their HEN1 inhibition property.



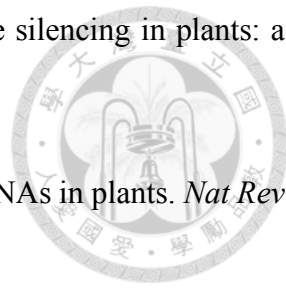
4.4.3. Virus derived siRNA methylation status evaluation

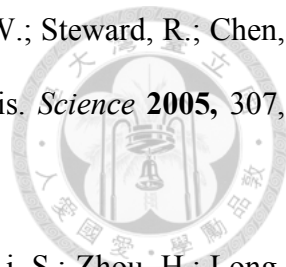
Upon infecting the host, the virus generates virus derived siRNA (vsiRNA) as discussed in section 1.1.2. of this thesis. The HEN1 is known to methylate the host small RNA however, methylation status of vsiRNA is yet to be evaluated. As in this thesis we have discussed the host's (Arabidopsis) miRNA methylation status under virus (TuMV) attack (section 3.4.2), further this study can shed light on the methylation status of vsiRNA. For this, we can immunoprecipitate the AGO and extract the AGO associated viral RNA. β -elimination and northern blot techniques can further be used to analyze the methylation status of the vsiRNA. This study will broaden our knowledge to understand if HEN1 has any bias towards methylating the host small RNA or can methylate any small RNA irrespective of its origin.

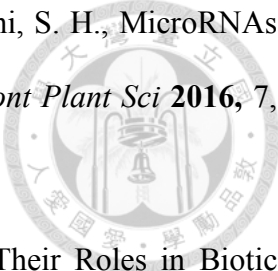
References

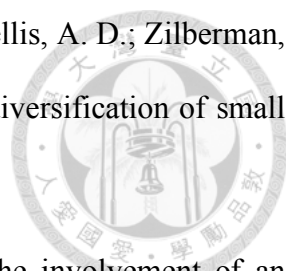


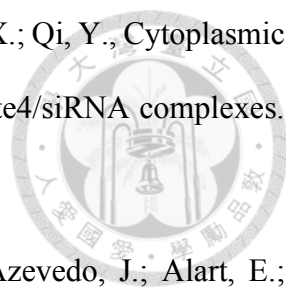
1. Matzke, M. A.; Matzke, A. J.; Pruss, G. J.; Vance, V. B., RNA-based silencing strategies in plants. *Curr Opin Genet Dev* **2001**, 11, (2), 221-7.
2. Kooter, J. M.; Matzke, M. A.; Meyer, P., Listening to the silent genes: transgene silencing, gene regulation and pathogen control. *Trends Plant Sci* **1999**, 4, (9), 340-347.
3. Waterhouse, P. M.; Graham, M. W.; Wang, M. B., Virus resistance and gene silencing in plants can be induced by simultaneous expression of sense and antisense RNA. *Proc Natl Acad Sci U S A* **1998**, 95, (23), 13959-64.
4. Han, H., RNA Interference to Knock Down Gene Expression. *Methods Mol Biol* **2018**, 1706, 293-302.
5. Napoli, C.; Lemieux, C.; Jorgensen, R., Introduction of a Chimeric Chalcone Synthase Gene into Petunia Results in Reversible Co-Suppression of Homologous Genes in trans. *Plant Cell* **1990**, 2, (4), 279-289.
6. Fire, A.; Xu, S.; Montgomery, M. K.; Kostas, S. A.; Driver, S. E.; Mello, C. C., Potent and specific genetic interference by double-stranded RNA in *Caenorhabditis elegans*. *Nature* **1998**, 391, (6669), 806-11.
7. Fagard, M.; Vaucheret, H., (TRANS)GENE SILENCING IN PLANTS: How Many Mechanisms? *Annu Rev Plant Physiol Plant Mol Biol* **2000**, 51, 167-194.
8. Waterhouse, P. M.; Wang, M. B.; Lough, T., Gene silencing as an adaptive defence against viruses. *Nature* **2001**, 411, (6839), 834-42.
9. Voinnet, O., RNA silencing: small RNAs as ubiquitous regulators of gene expression. *Curr Opin Plant Biol* **2002**, 5, (5), 444-51.

- 
10. Zhang, X.; Zhu, Y.; Wu, H.; Guo, H., Post-transcriptional gene silencing in plants: a double-edged sword. *Sci China Life Sci* **2016**, 59, (3), 271-6.
 11. Borges, F.; Martienssen, R. A., The expanding world of small RNAs in plants. *Nat Rev Mol Cell Biol* **2015**, 16, (12), 727-41.
 12. Axtell, M. J., Classification and comparison of small RNAs from plants. *Annu Rev Plant Biol* **2013**, 64, 137-59.
 13. Yu, Y.; Jia, T.; Chen, X., The 'how' and 'where' of plant microRNAs. *New Phytol* **2017**, 216, (4), 1002-1017.
 14. Wang, J.; Mei, J.; Ren, G., Plant microRNAs: Biogenesis, Homeostasis, and Degradation. *Front Plant Sci* **2019**, 10, 360.
 15. Zielezinski, A.; Dolata, J.; Alaba, S.; Kruszka, K.; Pacak, A.; Swida-Barteczka, A.; Knop, K.; Stepień, A.; Bielewicz, D.; Pietrykowska, H.; Sierocka, I.; Sobkowiak, L.; Lakomiak, A.; Jarmolowski, A.; Szweykowska-Kulinska, Z.; Karłowski, W. M., mirEX 2.0 - an integrated environment for expression profiling of plant microRNAs. *BMC Plant Biol* **2015**, 15, 144.
 16. Knop, K.; Stepień, A.; Barciszewska-Pacak, M.; Taube, M.; Bielewicz, D.; Michalak, M.; Borst, J. W.; Jarmolowski, A.; Szweykowska-Kulinska, Z., Active 5' splice sites regulate the biogenesis efficiency of Arabidopsis microRNAs derived from intron-containing genes. *Nucleic Acids Res* **2017**, 45, (5), 2757-2775.
 17. Li, S.; Castillo-González, C.; Yu, B.; Zhang, X., The functions of plant small RNAs in development and in stress responses. *Plant J* **2017**, 90, (4), 654-670.
 18. Rogers, K.; Chen, X., Biogenesis, turnover, and mode of action of plant microRNAs. *Plant Cell* **2013**, 25, (7), 2383-99.

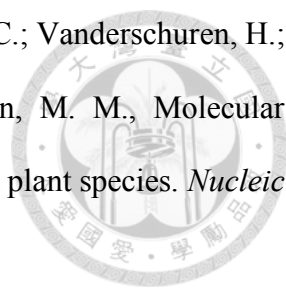
- 
19. Yu, B.; Yang, Z.; Li, J.; Minakhina, S.; Yang, M.; Padgett, R. W.; Steward, R.; Chen, X., Methylation as a crucial step in plant microRNA biogenesis. *Science* **2005**, 307, (5711), 932-5.
 20. Mi, S.; Cai, T.; Hu, Y.; Chen, Y.; Hodges, E.; Ni, F.; Wu, L.; Li, S.; Zhou, H.; Long, C.; Chen, S.; Hannon, G. J.; Qi, Y., Sorting of small RNAs into Arabidopsis argonaute complexes is directed by the 5' terminal nucleotide. *Cell* **2008**, 133, (1), 116-27.
 21. Montgomery, T. A.; Howell, M. D.; Cuperus, J. T.; Li, D.; Hansen, J. E.; Alexander, A. L.; Chapman, E. J.; Fahlgren, N.; Allen, E.; Carrington, J. C., Specificity of ARGONAUTE7-miR390 interaction and dual functionality in TAS3 trans-acting siRNA formation. *Cell* **2008**, 133, (1), 128-41.
 22. Zhu, H.; Hu, F.; Wang, R.; Zhou, X.; Sze, S. H.; Liou, L. W.; Barefoot, A.; Dickman, M.; Zhang, X., Arabidopsis Argonaute10 specifically sequesters miR166/165 to regulate shoot apical meristem development. *Cell* **2011**, 145, (2), 242-56.
 23. Bologna, N. G.; Iselin, R.; Abriata, L. A.; Sarazin, A.; Pumplin, N.; Jay, F.; Grentzinger, T.; Dal Peraro, M.; Voinnet, O., Nucleo-cytosolic Shuttling of ARGONAUTE1 Prompts a Revised Model of the Plant MicroRNA Pathway. *Mol Cell* **2018**, 69, (4), 709-719.e5.
 24. Zhang, B.; You, C.; Zhang, Y.; Zeng, L.; Hu, J.; Zhao, M.; Chen, X., Linking key steps of microRNA biogenesis by TREX-2 and the nuclear pore complex in Arabidopsis. *Nat Plants* **2020**, 6, (8), 957-969.
 25. Dalmadi, Á.; Gyula, P.; Bálint, J.; Szittyá, G.; Havelda, Z., AGO-unbound cytosolic pool of mature miRNAs in plant cells reveals a novel regulatory step at AGO1 loading. *Nucleic Acids Res* **2019**, 47, (18), 9803-9817.

- 
26. Shriram, V.; Kumar, V.; Devarumath, R. M.; Khare, T. S.; Wani, S. H., MicroRNAs As Potential Targets for Abiotic Stress Tolerance in Plants. *Front Plant Sci* **2016**, *7*, 817.
27. Brant, E. J.; Budak, H., Plant Small Non-coding RNAs and Their Roles in Biotic Stresses. *Front Plant Sci* **2018**, *9*, 1038.
28. Guleria, P.; Mahajan, M.; Bhardwaj, J.; Yadav, S. K., Plant small RNAs: biogenesis, mode of action and their roles in abiotic stresses. *Genomics Proteomics Bioinformatics* **2011**, *9*, (6), 183-99.
29. Guo, Q.; Liu, Q.; Smith, N. A.; Liang, G.; Wang, M. B., RNA Silencing in Plants: Mechanisms, Technologies and Applications in Horticultural Crops. *Curr Genomics* **2016**, *17*, (6), 476-489.
30. Dalmay, T.; Hamilton, A.; Rudd, S.; Angell, S.; Baulcombe, D. C., An RNA-dependent RNA polymerase gene in Arabidopsis is required for posttranscriptional gene silencing mediated by a transgene but not by a virus. *Cell* **2000**, *101*, (5), 543-53.
31. Mourrain, P.; Béclin, C.; Elmayan, T.; Feuerbach, F.; Godon, C.; Morel, J. B.; Jouette, D.; Lacombe, A. M.; Nikic, S.; Picault, N.; Ré moué, K.; Sanial, M.; Vo, T. A.; Vaucheret, H., Arabidopsis SGS2 and SGS3 genes are required for posttranscriptional gene silencing and natural virus resistance. *Cell* **2000**, *101*, (5), 533-42.
32. Peragine, A.; Yoshikawa, M.; Wu, G.; Albrecht, H. L.; Poethig, R. S., SGS3 and SGS2/SDE1/RDR6 are required for juvenile development and the production of trans-acting siRNAs in Arabidopsis. *Genes Dev* **2004**, *18*, (19), 2368-79.
33. Vazquez, F.; Vaucheret, H.; Rajagopalan, R.; Lepers, C.; Gascioli, V.; Mallory, A. C.; Hilbert, J. L.; Bartel, D. P.; Crété, P., Endogenous trans-acting siRNAs regulate the accumulation of Arabidopsis mRNAs. *Mol Cell* **2004**, *16*, (1), 69-79.

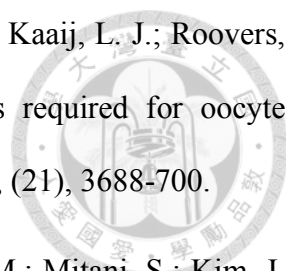
- 
34. Xie, Z.; Johansen, L. K.; Gustafson, A. M.; Kasschau, K. D.; Lellis, A. D.; Zilberman, D.; Jacobsen, S. E.; Carrington, J. C., Genetic and functional diversification of small RNA pathways in plants. *PLoS Biol* **2004**, 2, (5), E104.
35. Yu, D.; Fan, B.; MacFarlane, S. A.; Chen, Z., Analysis of the involvement of an inducible Arabidopsis RNA-dependent RNA polymerase in antiviral defense. *Mol Plant Microbe Interact* **2003**, 16, (3), 206-16.
36. Chan, S. W.; Zilberman, D.; Xie, Z.; Johansen, L. K.; Carrington, J. C.; Jacobsen, S. E., RNA silencing genes control de novo DNA methylation. *Science* **2004**, 303, (5662), 1336.
37. Zilberman, D.; Cao, X.; Jacobsen, S. E., ARGONAUTE4 control of locus-specific siRNA accumulation and DNA and histone methylation. *Science* **2003**, 299, (5607), 716-9.
38. Haag, J. R.; Pikaard, C. S., Multisubunit RNA polymerases IV and V: purveyors of non-coding RNA for plant gene silencing. *Nat Rev Mol Cell Biol* **2011**, 12, (8), 483-92.
39. Feng, S.; Jacobsen, S. E.; Reik, W., Epigenetic reprogramming in plant and animal development. *Science* **2010**, 330, (6004), 622-7.
40. Matzke, M. A.; Kanno, T.; Matzke, A. J., RNA-Directed DNA Methylation: The Evolution of a Complex Epigenetic Pathway in Flowering Plants. *Annu Rev Plant Biol* **2015**, 66, 243-67.
41. Zhang, H.; He, X.; Zhu, J. K., RNA-directed DNA methylation in plants: Where to start? *RNA Biol* **2013**, 10, (10), 1593-6.
42. Li, J.; Yang, Z.; Yu, B.; Liu, J.; Chen, X., Methylation protects miRNAs and siRNAs from a 3'-end uridylation activity in Arabidopsis. *Curr Biol* **2005**, 15, (16), 1501-7.

- 
43. Ye, R.; Wang, W.; Iki, T.; Liu, C.; Wu, Y.; Ishikawa, M.; Zhou, X.; Qi, Y., Cytoplasmic assembly and selective nuclear import of Arabidopsis Argonaute4/siRNA complexes. *Mol Cell* **2012**, 46, (6), 859-70.
44. Pontier, D.; Picart, C.; Roudier, F.; Garcia, D.; Lahmy, S.; Azevedo, J.; Alart, E.; Laudie, M.; Karlowski, W. M.; Cooke, R.; Colot, V.; Voinnet, O.; Lagrange, T., NERD, a plant-specific GW protein, defines an additional RNAi-dependent chromatin-based pathway in Arabidopsis. *Mol Cell* **2012**, 48, (1), 121-32.
45. Allen, E.; Xie, Z.; Gustafson, A. M.; Carrington, J. C., microRNA-directed phasing during trans-acting siRNA biogenesis in plants. *Cell* **2005**, 121, (2), 207-21.
46. Xie, Z.; Allen, E.; Wilken, A.; Carrington, J. C., DICER-LIKE 4 functions in trans-acting small interfering RNA biogenesis and vegetative phase change in Arabidopsis thaliana. *Proc Natl Acad Sci U S A* **2005**, 102, (36), 12984-9.
47. Yoshikawa, M.; Peragine, A.; Park, M. Y.; Poethig, R. S., A pathway for the biogenesis of trans-acting siRNAs in Arabidopsis. *Genes Dev* **2005**, 19, (18), 2164-75.
48. Adenot, X.; Elmayan, T.; Laressergues, D.; Boutet, S.; Bouché, N.; Gasciolli, V.; Vaucheret, H., DRB4-dependent TAS3 trans-acting siRNAs control leaf morphology through AGO7. *Curr Biol* **2006**, 16, (9), 927-32.
49. Hiraguri, A.; Itoh, R.; Kondo, N.; Nomura, Y.; Aizawa, D.; Murai, Y.; Koiwa, H.; Seki, M.; Shinozaki, K.; Fukuhara, T., Specific interactions between Dicer-like proteins and HYL1/DRB-family dsRNA-binding proteins in Arabidopsis thaliana. *Plant Mol Biol* **2005**, 57, (2), 173-88.
50. Cuperus, J. T.; Carbonell, A.; Fahlgren, N.; Garcia-Ruiz, H.; Burke, R. T.; Takeda, A.; Sullivan, C. M.; Gilbert, S. D.; Montgomery, T. A.; Carrington, J. C., Unique

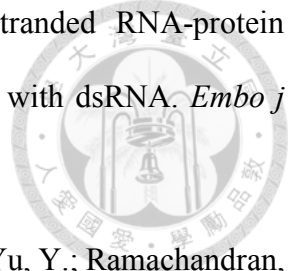
- functionality of 22-nt miRNAs in triggering RDR6-dependent siRNA biogenesis from target transcripts in Arabidopsis. *Nat Struct Mol Biol* **2010**, 17, (8), 997-1003.
51. Chen, H. M.; Chen, L. T.; Patel, K.; Li, Y. H.; Baulcombe, D. C.; Wu, S. H., 22-Nucleotide RNAs trigger secondary siRNA biogenesis in plants. *Proc Natl Acad Sci U S A* **2010**, 107, (34), 15269-74.
52. Fahlgren, N.; Montgomery, T. A.; Howell, M. D.; Allen, E.; Dvorak, S. K.; Alexander, A. L.; Carrington, J. C., Regulation of AUXIN RESPONSE FACTOR3 by TAS3 ta-siRNA affects developmental timing and patterning in Arabidopsis. *Curr Biol* **2006**, 16, (9), 939-44.
53. Johnson, C.; Kasprzewska, A.; Tennessen, K.; Fernandes, J.; Nan, G. L.; Walbot, V.; Sundaresan, V.; Vance, V.; Bowman, L. H., Clusters and superclusters of phased small RNAs in the developing inflorescence of rice. *Genome Res* **2009**, 19, (8), 1429-40.
54. Zhai, J.; Jeong, D. H.; De Paoli, E.; Park, S.; Rosen, B. D.; Li, Y.; González, A. J.; Yan, Z.; Kitto, S. L.; Grusak, M. A.; Jackson, S. A.; Stacey, G.; Cook, D. R.; Green, P. J.; Sherrier, D. J.; Meyers, B. C., MicroRNAs as master regulators of the plant NB-LRR defense gene family via the production of phased, trans-acting siRNAs. *Genes Dev* **2011**, 25, (23), 2540-53.
55. Fei, Q.; Xia, R.; Meyers, B. C., Phased, secondary, small interfering RNAs in posttranscriptional regulatory networks. *Plant Cell* **2013**, 25, (7), 2400-15.
56. Creasey, K. M.; Zhai, J.; Borges, F.; Van Ex, F.; Regulski, M.; Meyers, B. C.; Martienssen, R. A., miRNAs trigger widespread epigenetically activated siRNAs from transposons in Arabidopsis. *Nature* **2014**, 508, (7496), 411-5.
57. Ding, S. W.; Voinnet, O., Antiviral immunity directed by small RNAs. *Cell* **2007**, 130, (3), 413-26.


- 
58. Akbergenov, R.; Si-Ammour, A.; Blevins, T.; Amin, I.; Kutter, C.; Vanderschuren, H.; Zhang, P.; Gruissem, W.; Meins, F., Jr.; Hohn, T.; Pooggin, M. M., Molecular characterization of geminivirus-derived small RNAs in different plant species. *Nucleic Acids Res* **2006**, 34, (2), 462-71.
59. Deleris, A.; Gallego-Bartolome, J.; Bao, J.; Kasschau, K. D.; Carrington, J. C.; Voinnet, O., Hierarchical action and inhibition of plant Dicer-like proteins in antiviral defense. *Science* **2006**, 313, (5783), 68-71.
60. Fusaro, A. F.; Matthew, L.; Smith, N. A.; Curtin, S. J.; Dedic-Hagan, J.; Ellacott, G. A.; Watson, J. M.; Wang, M. B.; Brosnan, C.; Carroll, B. J.; Waterhouse, P. M., RNA interference-inducing hairpin RNAs in plants act through the viral defence pathway. *EMBO Rep* **2006**, 7, (11), 1168-75.
61. Diaz-Pendon, J. A.; Li, F.; Li, W. X.; Ding, S. W., Suppression of antiviral silencing by cucumber mosaic virus 2b protein in Arabidopsis is associated with drastically reduced accumulation of three classes of viral small interfering RNAs. *Plant Cell* **2007**, 19, (6), 2053-63.
62. Qu, F.; Ye, X.; Morris, T. J., Arabidopsis DRB4, AGO1, AGO7, and RDR6 participate in a DCL4-initiated antiviral RNA silencing pathway negatively regulated by DCL1. *Proc Natl Acad Sci U S A* **2008**, 105, (38), 14732-7.
63. Qu, F.; Ye, X.; Hou, G.; Sato, S.; Clemente, T. E.; Morris, T. J., RDR6 has a broad-spectrum but temperature-dependent antiviral defense role in *Nicotiana benthamiana*. *J Virol* **2005**, 79, (24), 15209-17.
64. Schwach, F.; Vaistij, F. E.; Jones, L.; Baulcombe, D. C., An RNA-dependent RNA polymerase prevents meristem invasion by potato virus X and is required for the

- activity but not the production of a systemic silencing signal. *Plant Physiol* **2005**, 138, (4), 1842-52.
65. Donaire, L.; Barajas, D.; Martínez-García, B.; Martínez-Priego, L.; Pagán, I.; Llave, C., Structural and genetic requirements for the biogenesis of tobacco rattle virus-derived small interfering RNAs. *J Virol* **2008**, 82, (11), 5167-77.
66. Wang, X. B.; Wu, Q.; Ito, T.; Cillo, F.; Li, W. X.; Chen, X.; Yu, J. L.; Ding, S. W., RNAi-mediated viral immunity requires amplification of virus-derived siRNAs in *Arabidopsis thaliana*. *Proc Natl Acad Sci U S A* **2010**, 107, (1), 484-9.
67. Dunoyer, P.; Himber, C.; Voinnet, O., DICER-LIKE 4 is required for RNA interference and produces the 21-nucleotide small interfering RNA component of the plant cell-to-cell silencing signal. *Nat Genet* **2005**, 37, (12), 1356-60.
68. Ji, L. H.; Ding, S. W., The suppressor of transgene RNA silencing encoded by Cucumber mosaic virus interferes with salicylic acid-mediated virus resistance. *Mol Plant Microbe Interact* **2001**, 14, (6), 715-24.
69. Xie, Z.; Fan, B.; Chen, C.; Chen, Z., An important role of an inducible RNA-dependent RNA polymerase in plant antiviral defense. *Proc Natl Acad Sci U S A* **2001**, 98, (11), 6516-21.
70. Zhao, Y.; Mo, B.; Chen, X., Mechanisms that impact microRNA stability in plants. *RNA Biol* **2012**, 9, (10), 1218-23.
71. Zhao, Y.; Yu, Y.; Zhai, J.; Ramachandran, V.; Dinh, T. T.; Meyers, B. C.; Mo, B.; Chen, X., The *Arabidopsis* nucleotidyl transferase HESO1 uridylates unmethylated small RNAs to trigger their degradation. *Curr Biol* **2012**, 22, (8), 689-94.

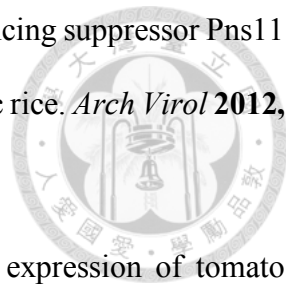
- 
72. Kamminga, L. M.; Luteijn, M. J.; den Broeder, M. J.; Redl, S.; Kaaij, L. J.; Roovers, E. F.; Ladurner, P.; Berezikov, E.; Ketting, R. F., Hen1 is required for oocyte development and piRNA stability in zebrafish. *Embo j* **2010**, 29, (21), 3688-700.
 73. Billi, A. C.; Alessi, A. F.; Khivansara, V.; Han, T.; Freeberg, M.; Mitani, S.; Kim, J. K., The *Caenorhabditis elegans* HEN1 ortholog, HENN-1, methylates and stabilizes select subclasses of germline small RNAs. *PLoS Genet* **2012**, 8, (4), e1002617.
 74. Montgomery, T. A.; Rim, Y. S.; Zhang, C.; Downen, R. H.; Phillips, C. M.; Fischer, S. E.; Ruvkun, G., PIWI associated siRNAs and piRNAs specifically require the *Caenorhabditis elegans* HEN1 ortholog henn-1. *PLoS Genet* **2012**, 8, (4), e1002616.
 75. Kurth, H. M.; Mochizuki, K., 2'-O-methylation stabilizes Piwi-associated small RNAs and ensures DNA elimination in *Tetrahymena*. *Rna* **2009**, 15, (4), 675-85.
 76. Kirino, Y.; Mourelatos, Z., The mouse homolog of HEN1 is a potential methylase for Piwi-interacting RNAs. *Rna* **2007**, 13, (9), 1397-401.
 77. Saito, K.; Sakaguchi, Y.; Suzuki, T.; Suzuki, T.; Siomi, H.; Siomi, M. C., Pimet, the *Drosophila* homolog of HEN1, mediates 2'-O-methylation of Piwi- interacting RNAs at their 3' ends. *Genes Dev* **2007**, 21, (13), 1603-8.
 78. Horwich, M. D.; Li, C.; Matranga, C.; Vagin, V.; Farley, G.; Wang, P.; Zamore, P. D., The *Drosophila* RNA methyltransferase, DmHen1, modifies germline piRNAs and single-stranded siRNAs in RISC. *Curr Biol* **2007**, 17, (14), 1265-72.
 79. Kamminga, L. M.; van Wolfswinkel, J. C.; Luteijn, M. J.; Kaaij, L. J.; Bagijn, M. P.; Sapetschnig, A.; Miska, E. A.; Berezikov, E.; Ketting, R. F., Differential impact of the HEN1 homolog HENN-1 on 21U and 26G RNAs in the germline of *Caenorhabditis elegans*. *PLoS Genet* **2012**, 8, (7), e1002702.

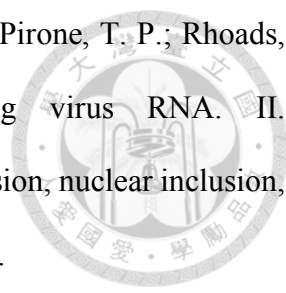
80. Ren, G.; Chen, X.; Yu, B., Uridylation of miRNAs by hen1 suppressor1 in Arabidopsis. *Curr Biol* **2012**, 22, (8), 695-700.
81. Ameres, S. L.; Horwich, M. D.; Hung, J. H.; Xu, J.; Ghildiyal, M.; Weng, Z.; Zamore, P. D., Target RNA-directed trimming and tailing of small silencing RNAs. *Science* **2010**, 328, (5985), 1534-9.
82. Park, W.; Li, J.; Song, R.; Messing, J.; Chen, X., CARPEL FACTORY, a Dicer homolog, and HEN1, a novel protein, act in microRNA metabolism in Arabidopsis thaliana. *Curr Biol* **2002**, 12, (17), 1484-95.
83. Chen, X.; Liu, J.; Cheng, Y.; Jia, D., HEN1 functions pleiotropically in Arabidopsis development and acts in C function in the flower. *Development* **2002**, 129, (5), 1085-94.
84. Tkaczuk, K. L.; Obarska, A.; Bujnicki, J. M., Molecular phylogenetics and comparative modeling of HEN1, a methyltransferase involved in plant microRNA biogenesis. *BMC Evol Biol* **2006**, 6, 6.
85. Huang, Y.; Ji, L.; Huang, Q.; Vassilyev, D. G.; Chen, X.; Ma, J. B., Structural insights into mechanisms of the small RNA methyltransferase HEN1. *Nature* **2009**, 461, (7265), 823-7.
86. Kang, C. B.; Hong, Y.; Dhe-Paganon, S.; Yoon, H. S., FKBP family proteins: immunophilins with versatile biological functions. *Neurosignals* **2008**, 16, (4), 318-25.
87. Tian, B.; Bevilacqua, P. C.; Diegelman-Parente, A.; Mathews, M. B., The double-stranded-RNA-binding motif: interference and much more. *Nat Rev Mol Cell Biol* **2004**, 5, (12), 1013-23.

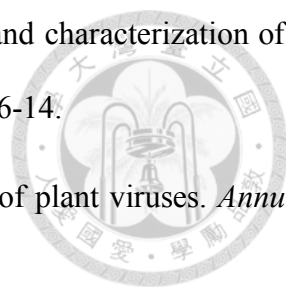
- 
88. Ryter, J. M.; Schultz, S. C., Molecular basis of double-stranded RNA-protein interactions: structure of a dsRNA-binding domain complexed with dsRNA. *Embo j* **1998**, 17, (24), 7505-13.
89. Tu, B.; Liu, L.; Xu, C.; Zhai, J.; Li, S.; Lopez, M. A.; Zhao, Y.; Yu, Y.; Ramachandran, V.; Ren, G.; Yu, B.; Li, S.; Meyers, B. C.; Mo, B.; Chen, X., Distinct and cooperative activities of HESO1 and URT1 nucleotidyl transferases in microRNA turnover in Arabidopsis. *PLoS Genet* **2015**, 11, (4), e1005119.
90. Ramachandran, V.; Chen, X., Degradation of microRNAs by a family of exoribonucleases in Arabidopsis. *Science* **2008**, 321, (5895), 1490-2.
91. Kim, V. N.; Han, J.; Siomi, M. C., Biogenesis of small RNAs in animals. *Nat Rev Mol Cell Biol* **2009**, 10, (2), 126-39.
92. Chen, W.; Liu, M.; Cheng, G.; Yan, W.; Fei, L.; Zheng, Z., RNA silencing: a remarkable parallel to protein-based immune systems in vertebrates? *FEBS Lett* **2005**, 579, (11), 2267-72.
93. Huntzinger, E.; Izaurralde, E., Gene silencing by microRNAs: contributions of translational repression and mRNA decay. *Nat Rev Genet* **2011**, 12, (2), 99-110.
94. Chen, X., Small RNAs and their roles in plant development. *Annu Rev Cell Dev Biol* **2009**, 25, 21-44.
95. Onodera, Y.; Haag, J. R.; Ream, T.; Costa Nunes, P.; Pontes, O.; Pikaard, C. S., Plant nuclear RNA polymerase IV mediates siRNA and DNA methylation-dependent heterochromatin formation. *Cell* **2005**, 120, (5), 613-22.
96. Herr, A. J.; Jensen, M. B.; Dalmay, T.; Baulcombe, D. C., RNA polymerase IV directs silencing of endogenous DNA. *Science* **2005**, 308, (5718), 118-20.

- 
97. Li, C.; Zhang, B., MicroRNAs in Control of Plant Development. *J Cell Physiol* **2016**, 231, (2), 303-13.
98. Wienholds, E.; Plasterk, R. H., MicroRNA function in animal development. *FEBS Lett* **2005**, 579, (26), 5911-22.
99. Ferguson, L. R., RNA silencing: Mechanism, biology and responses to environmental stress. *Mutat Res* **2011**, 714, (1-2), 93-4.
100. Yang, X.; Wang, Y.; Guo, W.; Xie, Y.; Xie, Q.; Fan, L.; Zhou, X., Characterization of small interfering RNAs derived from the geminivirus/betasatellite complex using deep sequencing. *PLoS One* **2011**, 6, (2), e16928.
101. Baulcombe, D., RNA silencing in plants. *Nature* **2004**, 431, (7006), 356-63.
102. Burgyán, J.; Havelda, Z., Viral suppressors of RNA silencing. *Trends Plant Sci* **2011**, 16, (5), 265-72.
103. Sáenz, P.; Salvador, B.; Simón-Mateo, C.; Kasschau, K. D.; Carrington, J. C.; García, J. A., Host-specific involvement of the HC protein in the long-distance movement of potyviruses. *J Virol* **2002**, 76, (4), 1922-31.
104. Azevedo, J.; Garcia, D.; Pontier, D.; Ohnesorge, S.; Yu, A.; Garcia, S.; Braun, L.; Bergdoll, M.; Hakimi, M. A.; Lagrange, T.; Voinnet, O., Argonaute quenching and global changes in Dicer homeostasis caused by a pathogen-encoded GW repeat protein. *Genes Dev* **2010**, 24, (9), 904-15.
105. Young, B. A.; Stenger, D. C.; Qu, F.; Morris, T. J.; Tatineni, S.; French, R., Tritimovirus P1 functions as a suppressor of RNA silencing and an enhancer of disease symptoms. *Virus Res* **2012**, 163, (2), 672-7.

106. Hu, S. F.; Wei, W. L.; Hong, S. F.; Fang, R. Y.; Wu, H. Y.; Lin, P. C.; Sanobar, N.; Wang, H. P.; Sulistio, M.; Wu, C. T.; Lo, H. F.; Lin, S. S., Investigation of the effects of P1 on HC-pro-mediated gene silencing suppression through genetics and omics approaches. *Bot Stud* **2020**, 61, (1), 22.
107. Várallyay, É.; Oláh, E.; Havelda, Z., Independent parallel functions of p19 plant viral suppressor of RNA silencing required for effective suppressor activity. *Nucleic Acids Res* **2014**, 42, (1), 599-608.
108. Siddiqui, S. A.; Sarmiento, C.; Truve, E.; Lehto, H.; Lehto, K., Phenotypes and functional effects caused by various viral RNA silencing suppressors in transgenic *Nicotiana benthamiana* and *N. tabacum*. *Mol Plant Microbe Interact* **2008**, 21, (2), 178-87.
109. Soitamo, A. J.; Jada, B.; Lehto, K., HC-Pro silencing suppressor significantly alters the gene expression profile in tobacco leaves and flowers. *BMC Plant Biol* **2011**, 11, 68.
110. Várallyay, E.; Válczi, A.; Agyi, A.; Burgyán, J.; Havelda, Z., Plant virus-mediated induction of miR168 is associated with repression of ARGONAUTE1 accumulation. *Embo j* **2010**, 29, (20), 3507-19.
111. Chapman, E. J.; Prokhnovsky, A. I.; Gopinath, K.; Dolja, V. V.; Carrington, J. C., Viral RNA silencing suppressors inhibit the microRNA pathway at an intermediate step. *Genes Dev* **2004**, 18, (10), 1179-86.
112. Jay, F.; Wang, Y.; Yu, A.; Taconnat, L.; Pelletier, S.; Colot, V.; Renou, J. P.; Voinnet, O., Misregulation of AUXIN RESPONSE FACTOR 8 underlies the developmental abnormalities caused by three distinct viral silencing suppressors in *Arabidopsis*. *PLoS Pathog* **2011**, 7, (5), e1002035.

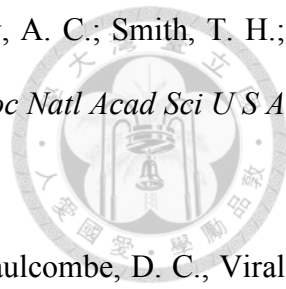
- 
113. Shen, W. J.; Ruan, X. L.; Li, X. S.; Zhao, Q.; Li, H. P., RNA silencing suppressor Pns1 of rice gall dwarf virus induces virus-like symptoms in transgenic rice. *Arch Virol* **2012**, 157, (8), 1531-9.
114. Stav, R.; Hendelman, A.; Buxdorf, K.; Arazi, T., Transgenic expression of tomato bushy stunt virus silencing suppressor P19 via the pOp/LhG4 transactivation system induces viral-like symptoms in tomato. *Virus Genes* **2010**, 40, (1), 119-29.
115. Moreno, A.; Fereres, A., Virus diseases in lettuce in the Mediterranean basin. *Adv Virus Res* **2012**, 84, 247-88.
116. Nicolas, O.; Laliberté, J. F., The complete nucleotide sequence of turnip mosaic potyvirus RNA. *J Gen Virol* **1992**, 73 (Pt 11), 2785-93.
117. Soumounou, Y.; Laliberté, J. F., Nucleic acid-binding properties of the P1 protein of turnip mosaic potyvirus produced in Escherichia coli. *J Gen Virol* **1994**, 75 (Pt 10), 2567-73.
118. Kassanis, B., The transmission of potato aucuba mosaic virus by aphids from plants also infected by potato viruses A or Y. *Virology* **1961**, 13, 93-7.
119. Kassanis, B.; Govier, D. A., New evidence on the mechanism of aphid transmission of potato C and potato aucuba mosaic viruses. *J Gen Virol* **1971**, 10, (1), 99-101.
120. Govier, D. A.; Kassanis, B., A virus-induced component of plant sap needed when aphids acquire potato virus Y from purified preparations. *Virology* **1974**, 61, (2), 420-6.
121. Govier, D. A.; Kassanis, B., Evidence that a component other than the virus particle is needed for aphid transmission of potato virus Y. *Virology* **1974**, 57, (1), 285-6.

- 
122. Hellmann, G. M.; Thornbury, D. W.; Hiebert, E.; Shaw, J. G.; Pirone, T. P.; Rhoads, R. E., Cell-free translation of tobacco vein mottling virus RNA. II. Immunoprecipitation of products by antisera to cylindrical inclusion, nuclear inclusion, and helper component proteins. *Virology* **1983**, 124, (2), 434-44.
123. Thornbury, D. W.; Hellmann, G. M.; Rhoads, R. E.; Pirone, T. P., Purification and characterization of potyvirus helper component. *Virology* **1985**, 144, (1), 260-7.
124. Carrington, J. C.; Cary, S. M.; Parks, T. D.; Dougherty, W. G., A second proteinase encoded by a plant potyvirus genome. *Embo j* **1989**, 8, (2), 365-70.
125. Carrington, J. C.; Freed, D. D.; Sanders, T. C., Autocatalytic processing of the potyvirus helper component proteinase in Escherichia coli and in vitro. *J Virol* **1989**, 63, (10), 4459-63.
126. Oh, C. S.; Carrington, J. C., Identification of essential residues in potyvirus proteinase HC-Pro by site-directed mutagenesis. *Virology* **1989**, 173, (2), 692-9.
127. Carrington, J. C.; Freed, D. D.; Oh, C. S., Expression of potyviral polyproteins in transgenic plants reveals three proteolytic activities required for complete processing. *Embo j* **1990**, 9, (5), 1347-53.
128. Klein, P. G.; Klein, R. R.; Rodríguez-Cerezo, E.; Hunt, A. G.; Shaw, J. G., Mutational analysis of the tobacco vein mottling virus genome. *Virology* **1994**, 204, (2), 759-69.
129. Rojas, M. R.; Zerbini, F. M.; Allison, R. F.; Gilbertson, R. L.; Lucas, W. J., Capsid protein and helper component-proteinase function as potyvirus cell-to-cell movement proteins. *Virology* **1997**, 237, (2), 283-95.
130. Kasschau, K. D.; Carrington, J. C., A counterdefensive strategy of plant viruses: suppression of posttranscriptional gene silencing. *Cell* **1998**, 95, (4), 461-70.

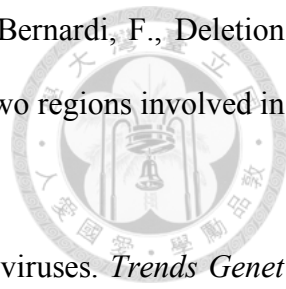
- 
131. Govier, D. A.; Kassanis, B.; Pirone, T. P., Partial purification and characterization of the potato virus Y helper component. *Virology* **1977**, 78, (1), 306-14.
132. Pirone, T. P.; Blanc, S., Helper-dependent vector transmission of plant viruses. *Annu Rev Phytopathol* **1996**, 34, 227-47.
133. Redondo, E.; Krause-Sakate, R.; Yang, S. J.; Lot, H.; Le Gall, O.; Candresse, T., Lettuce mosaic virus pathogenicity determinants in susceptible and tolerant lettuce cultivars map to different regions of the viral genome. *Mol Plant Microbe Interact* **2001**, 14, (6), 804-10.
134. Shi, X. M.; Miller, H.; Verchot, J.; Carrington, J. C.; Vance, V. B., Mutations in the region encoding the central domain of helper component-proteinase (HC-Pro) eliminate potato virus X/potyviral synergism. *Virology* **1997**, 231, (1), 35-42.
135. Wang, Y.; Gaba, V.; Yang, J.; Palukaitis, P.; Gal-On, A., Characterization of Synergy Between Cucumber mosaic virus and Potyviruses in Cucurbit Hosts. *Phytopathology* **2002**, 92, (1), 51-8.
136. Pruss, G.; Ge, X.; Shi, X. M.; Carrington, J. C.; Bowman Vance, V., Plant viral synergism: the potyviral genome encodes a broad-range pathogenicity enhancer that transactivates replication of heterologous viruses. *Plant Cell* **1997**, 9, (6), 859-68.
137. Ballut, L.; Drucker, M.; Pugnière, M.; Cambon, F.; Blanc, S.; Roquet, F.; Candresse, T.; Schmid, H. P.; Nicolas, P.; Gall, O. L.; Badaoui, S., HcPro, a multifunctional protein encoded by a plant RNA virus, targets the 20S proteasome and affects its enzymic activities. *J Gen Virol* **2005**, 86, (Pt 9), 2595-2603.
138. Sahana, N.; Kaur, H.; Basavaraj; Tena, F.; Jain, R. K.; Palukaitis, P.; Canto, T.; Praveen, S., Inhibition of the host proteasome facilitates papaya ringspot virus

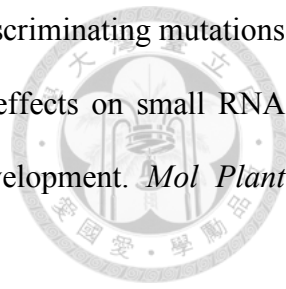
accumulation and proteosomal catalytic activity is modulated by viral factor HcPro. *PLoS One* **2012**, 7, (12), e52546.


139. Valli, A.; Gallo, A.; Calvo, M.; de Jesús Pérez, J.; García, J. A., A novel role of the potyviral helper component proteinase contributes to enhance the yield of viral particles. *J Virol* **2014**, 88, (17), 9808-18.
140. Anandalakshmi, R.; Marathe, R.; Ge, X.; Herr, J. M., Jr.; Mau, C.; Mallory, A.; Pruss, G.; Bowman, L.; Vance, V. B., A calmodulin-related protein that suppresses posttranscriptional gene silencing in plants. *Science* **2000**, 290, (5489), 142-4.
141. Endres, M. W.; Gregory, B. D.; Gao, Z.; Foreman, A. W.; Mlotshwa, S.; Ge, X.; Pruss, G. J.; Ecker, J. R.; Bowman, L. H.; Vance, V., Two plant viral suppressors of silencing require the ethylene-inducible host transcription factor RAV2 to block RNA silencing. *PLoS Pathog* **2010**, 6, (1), e1000729.
142. Ala-Poikela, M.; Goytia, E.; Haikonen, T.; Rajamäki, M. L.; Valkonen, J. P., Helper component proteinase of the genus Potyvirus is an interaction partner of translation initiation factors eIF(iso)4E and eIF4E and contains a 4E binding motif. *J Virol* **2011**, 85, (13), 6784-94.
143. Guo, D.; Spetz, C.; Saarma, M.; Valkonen, J. P., Two potato proteins, including a novel RING finger protein (HIP1), interact with the potyviral multifunctional protein HCpro. *Mol Plant Microbe Interact* **2003**, 16, (5), 405-10.
144. Haikonen, T.; Rajamäki, M. L.; Valkonen, J. P., Interaction of the microtubule-associated host protein HIP2 with viral helper component proteinase is important in infection with potato virus A. *Mol Plant Microbe Interact* **2013**, 26, (7), 734-44.

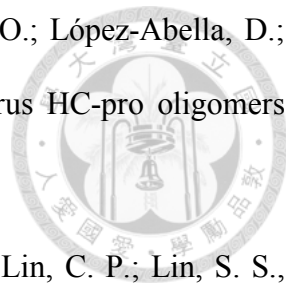
- 
145. Anandalakshmi, R.; Pruss, G. J.; Ge, X.; Marathe, R.; Mallory, A. C.; Smith, T. H.; Vance, V. B., A viral suppressor of gene silencing in plants. *Proc Natl Acad Sci U S A* **1998**, 95, (22), 13079-84.
146. Brigneti, G.; Voinnet, O.; Li, W. X.; Ji, L. H.; Ding, S. W.; Baulcombe, D. C., Viral pathogenicity determinants are suppressors of transgene silencing in *Nicotiana benthamiana*. *Embo j* **1998**, 17, (22), 6739-46.
147. Kasschau, K. D.; Carrington, J. C., Requirement for HC-Pro processing during genome amplification of tobacco etch potyvirus. *Virology* **1995**, 209, (1), 268-73.
148. Shibolet, Y. M.; Haronsky, E.; Leibman, D.; Arazi, T.; Wassenegger, M.; Whitham, S. A.; Gaba, V.; Gal-On, A., The conserved FRNK box in HC-Pro, a plant viral suppressor of gene silencing, is required for small RNA binding and mediates symptom development. *J Virol* **2007**, 81, (23), 13135-48.
149. Lakatos, L.; Csorba, T.; Pantaleo, V.; Chapman, E. J.; Carrington, J. C.; Liu, Y. P.; Dolja, V. V.; Calvino, L. F.; López-Moya, J. J.; Burgyán, J., Small RNA binding is a common strategy to suppress RNA silencing by several viral suppressors. *Embo j* **2006**, 25, (12), 2768-80.
150. Ebhardt, H. A.; Thi, E. P.; Wang, M. B.; Unrau, P. J., Extensive 3' modification of plant small RNAs is modulated by helper component-proteinase expression. *Proc Natl Acad Sci U S A* **2005**, 102, (38), 13398-403.
151. Yang, Z.; Ebright, Y. W.; Yu, B.; Chen, X., HEN1 recognizes 21-24 nt small RNA duplexes and deposits a methyl group onto the 2' OH of the 3' terminal nucleotide. *Nucleic Acids Res* **2006**, 34, (2), 667-75.
152. Jamous, R. M.; Boonrod, K.; Fuellgrabe, M. W.; Ali-Shtayeh, M. S.; Krczal, G.; Wassenegger, M., The helper component-proteinase of the Zucchini yellow mosaic

- virus inhibits the Hua Enhancer 1 methyltransferase activity in vitro. *J Gen Virol* **2011**, 92, (Pt 9), 2222-2226.
153. Ivanov, K. I.; Eskelin, K.; Bašić, M.; De, S.; Lõhmus, A.; Varjosalo, M.; Mäkinen, K., Molecular insights into the function of the viral RNA silencing suppressor HCPro. *Plant J* **2016**, 85, (1), 30-45.
154. Blanc, S.; Ammar, E. D.; Garcia-Lampasona, S.; Dolja, V. V.; Llave, C.; Baker, J.; Pirone, T. P., Mutations in the potyvirus helper component protein: effects on interactions with virions and aphid stylets. *J Gen Virol* **1998**, 79 (Pt 12), 3119-22.
155. Blanc, S.; López-Moya, J. J.; Wang, R.; García-Lampasona, S.; Thornbury, D. W.; Pirone, T. P., A specific interaction between coat protein and helper component correlates with aphid transmission of a potyvirus. *Virology* **1997**, 231, (1), 141-7.
156. Peng, Y. H.; Kadoury, D.; Gal-On, A.; Huet, H.; Wang, Y.; Raccach, B., Mutations in the HC-Pro gene of zucchini yellow mosaic potyvirus: effects on aphid transmission and binding to purified virions. *J Gen Virol* **1998**, 79 (Pt 4), 897-904.
157. Kasschau, K. D.; Cronin, S.; Carrington, J. C., Genome amplification and long-distance movement functions associated with the central domain of tobacco etch potyvirus helper component-proteinase. *Virology* **1997**, 228, (2), 251-62.
158. Cronin, S.; Verchot, J.; Haldeman-Cahill, R.; Schaad, M. C.; Carrington, J. C., Long-distance movement factor: a transport function of the potyvirus helper component proteinase. *Plant Cell* **1995**, 7, (5), 549-59.
159. Maia, I. G.; Bernardi, F., Nucleic acid-binding properties of a bacterially expressed potato virus Y helper component-proteinase. *J Gen Virol* **1996**, 77 (Pt 5), 869-77.

- 
160. Urcuqui-Inchima, S.; Maia, I. G.; Arruda, P.; Haenni, A. L.; Bernardi, F., Deletion mapping of the potyviral helper component-proteinase reveals two regions involved in RNA binding. *Virology* **2000**, 268, (1), 104-11.
161. Voinnet, O., RNA silencing as a plant immune system against viruses. *Trends Genet* **2001**, 17, (8), 449-59.
162. Li, W. X.; Ding, S. W., Viral suppressors of RNA silencing. *Curr Opin Biotechnol* **2001**, 12, (2), 150-4.
163. Mallory, A. C.; Ely, L.; Smith, T. H.; Marathe, R.; Anandalakshmi, R.; Fagard, M.; Vaucheret, H.; Pruss, G.; Bowman, L.; Vance, V. B., HC-Pro suppression of transgene silencing eliminates the small RNAs but not transgene methylation or the mobile signal. *Plant Cell* **2001**, 13, (3), 571-83.
164. Kasschau, K. D.; Carrington, J. C., Long-distance movement and replication maintenance functions correlate with silencing suppression activity of potyviral HC-Pro. *Virology* **2001**, 285, (1), 71-81.
165. Plisson, C.; Drucker, M.; Blanc, S.; German-Retana, S.; Le Gall, O.; Thomas, D.; Bron, P., Structural characterization of HC-Pro, a plant virus multifunctional protein. *J Biol Chem* **2003**, 278, (26), 23753-61.
166. Gal-On, A., A Point Mutation in the FRNK Motif of the Potyvirus Helper Component-Protease Gene Alters Symptom Expression in Cucurbits and Elicits Protection Against the Severe Homologous Virus. *Phytopathology* **2000**, 90, (5), 467-73.
167. Lin, S. S.; Wu, H. W.; Jan, F. J.; Hou, R. F.; Yeh, S. D., Modifications of the Helper Component-Protease of Zucchini yellow mosaic virus for Generation of Attenuated Mutants for Cross Protection Against Severe Infection. *Phytopathology* **2007**, 97, (3), 287-96.

- 
168. Wu, H. W.; Lin, S. S.; Chen, K. C.; Yeh, S. D.; Chua, N. H., Discriminating mutations of HC-Pro of zucchini yellow mosaic virus with differential effects on small RNA pathways involved in viral pathogenicity and symptom development. *Mol Plant Microbe Interact* **2010**, 23, (1), 17-28.
169. Chen, C. C.; Chao, C. H.; Chen, C. C.; Yeh, S. D.; Tsai, H. T.; Chang, C. A., Identification of Turnip mosaic virus Isolates Causing Yellow Stripe and Spot on Calla Lily. *Plant Dis* **2003**, 87, (8), 901-905.
170. Niu, Q. W.; Lin, S. S.; Reyes, J. L.; Chen, K. C.; Wu, H. W.; Yeh, S. D.; Chua, N. H., Expression of artificial microRNAs in transgenic *Arabidopsis thaliana* confers virus resistance. *Nat Biotechnol* **2006**, 24, (11), 1420-8.
171. Kung, Y. J.; Lin, P. C.; Yeh, S. D.; Hong, S. F.; Chua, N. H.; Liu, L. Y.; Lin, C. P.; Huang, Y. H.; Wu, H. W.; Chen, C. C.; Lin, S. S., Genetic analyses of the FRNK motif function of Turnip mosaic virus uncover multiple and potentially interactive pathways of cross-protection. *Mol Plant Microbe Interact* **2014**, 27, (9), 944-55.
172. Burd, C. G.; Dreyfuss, G., Conserved structures and diversity of functions of RNA-binding proteins. *Science* **1994**, 265, (5172), 615-21.
173. Fuellgrabe, M. W.; Boonrod, K.; Jamous, R.; Moser, M.; Shibolet, Y.; Krczal, G.; Wassenegger, M., Expression, purification and functional characterization of recombinant Zucchini yellow mosaic virus HC-Pro. *Protein Expr Purif* **2011**, 75, (1), 40-5.
174. Lózsá, R.; Csorba, T.; Lakatos, L.; Burgyán, J., Inhibition of 3' modification of small RNAs in virus-infected plants require spatial and temporal co-expression of small RNAs and viral silencing-suppressor proteins. *Nucleic Acids Res* **2008**, 36, (12), 4099-107.

- 
175. Dolja, V. V.; Herndon, K. L.; Pirone, T. P.; Carrington, J. C., Spontaneous mutagenesis of a plant potyvirus genome after insertion of a foreign gene. *J Virol* **1993**, 67, (10), 5968-75.
176. Dolja, V. V.; McBride, H. J.; Carrington, J. C., Tagging of plant potyvirus replication and movement by insertion of beta-glucuronidase into the viral polyprotein. *Proc Natl Acad Sci U S A* **1992**, 89, (21), 10208-12.
177. Dolja, V. V.; Hong, J.; Keller, K. E.; Martin, R. R.; Peremyslov, V. V., Suppression of potyvirus infection by coexpressed closterovirus protein. *Virology* **1997**, 234, (2), 243-52.
178. Atreya, C. D.; Pirone, T. P., Mutational analysis of the helper component-proteinase gene of a potyvirus: effects of amino acid substitutions, deletions, and gene replacement on virulence and aphid transmissibility. *Proc Natl Acad Sci U S A* **1993**, 90, (24), 11919-23.
179. Dunoyer, P.; Lecellier, C. H.; Parizotto, E. A.; Himber, C.; Voinnet, O., Probing the microRNA and small interfering RNA pathways with virus-encoded suppressors of RNA silencing. *Plant Cell* **2004**, 16, (5), 1235-50.
180. Mallory, A.; Vaucheret, H., Form, function, and regulation of ARGONAUTE proteins. *Plant Cell* **2010**, 22, (12), 3879-89.
181. Várallyay, E.; Havelda, Z., Unrelated viral suppressors of RNA silencing mediate the control of ARGONAUTE1 level. *Mol Plant Pathol* **2013**, 14, (6), 567-75.
182. Torres-Barceló, C.; Daròs, J. A.; Elena, S. F., Compensatory molecular evolution of HC-Pro, an RNA-silencing suppressor from a plant RNA virus. *Mol Biol Evol* **2010**, 27, (3), 543-51.

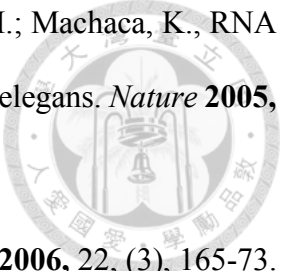
- 
183. Ruiz-Ferrer, V.; Boskovic, J.; Alfonso, C.; Rivas, G.; Llorca, O.; López-Abella, D.; López-Moya, J. J., Structural analysis of tobacco etch potyvirus HC-pro oligomers involved in aphid transmission. *J Virol* **2005**, 79, (6), 3758-65.
184. Lin, Y. Y.; Fang, M. M.; Lin, P. C.; Chiu, M. T.; Liu, L. Y.; Lin, C. P.; Lin, S. S., Improving initial infectivity of the Turnip mosaic virus (TuMV) infectious clone by an mini binary vector via agro-infiltration. *Bot Stud* **2013**, 54, (1), 22.
185. Yu, B.; Chapman, E. J.; Yang, Z.; Carrington, J. C.; Chen, X., Transgenically expressed viral RNA silencing suppressors interfere with microRNA methylation in Arabidopsis. *FEBS Lett* **2006**, 580, (13), 3117-20.
186. Hafrén, A.; Üstün, S.; Hochmuth, A.; Svenning, S.; Johansen, T.; Hofius, D., Turnip Mosaic Virus Counteracts Selective Autophagy of the Viral Silencing Suppressor HCpro. *Plant Physiol* **2018**, 176, (1), 649-662.
187. Poque, S.; Wu, H. W.; Huang, C. H.; Cheng, H. W.; Hu, W. C.; Yang, J. Y.; Wang, D.; Yeh, S. D., Potyviral Gene-Silencing Suppressor HCPro Interacts with Salicylic Acid (SA)-Binding Protein 3 to Weaken SA-Mediated Defense Responses. *Mol Plant Microbe Interact* **2018**, 31, (1), 86-100.
188. Zheng, H.; Yan, F.; Lu, Y.; Sun, L.; Lin, L.; Cai, L.; Hou, M.; Chen, J., Mapping the self-interacting domains of TuMV HC-Pro and the subcellular localization of the protein. *Virus Genes* **2011**, 42, (1), 110-6.
189. Garcia-Ruiz, H.; Carbonell, A.; Hoyer, J. S.; Fahlgren, N.; Gilbert, K. B.; Takeda, A.; Giampetruzzi, A.; Garcia Ruiz, M. T.; McGinn, M. G.; Lowery, N.; Martinez Baladejo, M. T.; Carrington, J. C., Roles and programming of Arabidopsis ARGONAUTE proteins during Turnip mosaic virus infection. *PLoS Pathog* **2015**, 11, (3), e1004755.

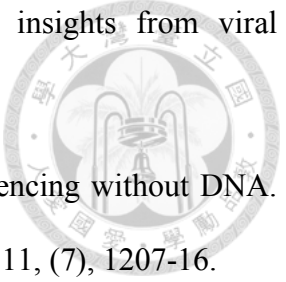
190. Sahana, N.; Kaur, H.; Jain, R. K.; Palukaitis, P.; Canto, T.; Praveen, S., The asparagine residue in the FRNK box of potyviral helper-component protease is critical for its small RNA binding and subcellular localization. *J Gen Virol* **2014**, 95, (Pt 5), 1167-1177.
191. Yu, B.; Bi, L.; Zhai, J.; Agarwal, M.; Li, S.; Wu, Q.; Ding, S. W.; Meyers, B. C.; Vaucheret, H.; Chen, X., siRNAs compete with miRNAs for methylation by HEN1 in Arabidopsis. *Nucleic Acids Res* **2010**, 38, (17), 5844-50.
192. Zhai, J.; Zhao, Y.; Simon, S. A.; Huang, S.; Petsch, K.; Arikiti, S.; Pillay, M.; Ji, L.; Xie, M.; Cao, X.; Yu, B.; Timmermans, M.; Yang, B.; Chen, X.; Meyers, B. C., Plant microRNAs display differential 3' truncation and tailing modifications that are ARGONAUTE1 dependent and conserved across species. *Plant Cell* **2013**, 25, (7), 2417-28.
193. Plotnikova, A.; Baranauskė, S.; Osipenko, A.; Klimašauskas, S.; Vilkaitis, G., Mechanistic insights into small RNA recognition and modification by the HEN1 methyltransferase. *Biochem J* **2013**, 453, (2), 281-90.
194. Vilkaitis, G.; Plotnikova, A.; Klimasauskas, S., Kinetic and functional analysis of the small RNA methyltransferase HEN1: the catalytic domain is essential for preferential modification of duplex RNA. *Rna* **2010**, 16, (10), 1935-42.
195. Kirino, Y.; Mourelatos, Z., 2'-O-methyl modification in mouse piRNAs and its methylase. *Nucleic Acids Symp Ser (Oxf)* **2007**, (51), 417-8.
196. Vagin, V. V.; Sigova, A.; Li, C.; Seitz, H.; Gvozdev, V.; Zamore, P. D., A distinct small RNA pathway silences selfish genetic elements in the germline. *Science* **2006**, 313, (5785), 320-4.
197. Jain, R.; Shuman, S., Bacterial Hen1 is a 3' terminal RNA ribose 2'-O-methyltransferase component of a bacterial RNA repair cassette. *Rna* **2010**, 16, (2), 316-23.

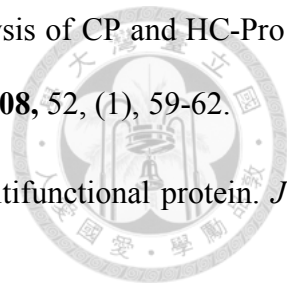
198. Mui Chan, C.; Zhou, C.; Brunzelle, J. S.; Huang, R. H., Structural and biochemical insights into 2'-O-methylation at the 3'-terminal nucleotide of RNA by Hen1. *Proc Natl Acad Sci U S A* **2009**, 106, (42), 17699-704.
199. Bowman, J. L.; Kohchi, T.; Yamato, K. T.; Jenkins, J.; Shu, S.; Ishizaki, K.; Yamaoka, S.; Nishihama, R.; Nakamura, Y.; Berger, F.; Adam, C.; Aki, S. S.; Althoff, F.; Araki, T.; Arteaga-Vazquez, M. A.; Balasubramanian, S.; Barry, K.; Bauer, D.; Boehm, C. R.; Briginshaw, L.; Caballero-Perez, J.; Catarino, B.; Chen, F.; Chiyoda, S.; Chovatia, M.; Davies, K. M.; Delmans, M.; Demura, T.; Dierschke, T.; Dolan, L.; Dorantes-Acosta, A. E.; Eklund, D. M.; Florent, S. N.; Flores-Sandoval, E.; Fujiyama, A.; Fukuzawa, H.; Galik, B.; Grimanelli, D.; Grimwood, J.; Grossniklaus, U.; Hamada, T.; Haseloff, J.; Hetherington, A. J.; Higo, A.; Hirakawa, Y.; Hundley, H. N.; Ikeda, Y.; Inoue, K.; Inoue, S. I.; Ishida, S.; Jia, Q.; Kakita, M.; Kanazawa, T.; Kawai, Y.; Kawashima, T.; Kennedy, M.; Kinose, K.; Kinoshita, T.; Kohara, Y.; Koide, E.; Komatsu, K.; Kopischke, S.; Kubo, M.; Kyojuka, J.; Lagercrantz, U.; Lin, S. S.; Lindquist, E.; Lipzen, A. M.; Lu, C. W.; De Luna, E.; Martienssen, R. A.; Minamino, N.; Mizutani, M.; Mizutani, M.; Mochizuki, N.; Monte, I.; Mosher, R.; Nagasaki, H.; Nakagami, H.; Naramoto, S.; Nishitani, K.; Ohtani, M.; Okamoto, T.; Okumura, M.; Phillips, J.; Pollak, B.; Reinders, A.; Rövekamp, M.; Sano, R.; Sawa, S.; Schmid, M. W.; Shirakawa, M.; Solano, R.; Spunde, A.; Suetsugu, N.; Sugano, S.; Sugiyama, A.; Sun, R.; Suzuki, Y.; Takenaka, M.; Takezawa, D.; Tomogane, H.; Tsuzuki, M.; Ueda, T.; Umeda, M.; Ward, J. M.; Watanabe, Y.; Yazaki, K.; Yokoyama, R.; Yoshitake, Y.; Yotsui, I.; Zachgo, S.; Schmutz, J., Insights into Land Plant Evolution Garnered from the *Marchantia polymorpha* Genome. *Cell* **2017**, 171, (2), 287-304.e15.
200. Komatsu, A.; Terai, M.; Ishizaki, K.; Suetsugu, N.; Tsuboi, H.; Nishihama, R.; Yamato, K. T.; Wada, M.; Kohchi, T., Phototropin encoded by a single-copy gene mediates

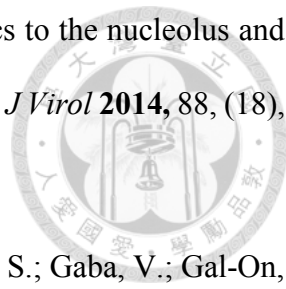
- chloroplast photorelocation movements in the liverwort *Marchantia polymorpha*. *Plant Physiol* **2014**, 166, (1), 411-27.
201. Ueda, M.; Kuniyoshi, T.; Yamamoto, H.; Sugimoto, K.; Ishizaki, K.; Kohchi, T.; Nishimura, Y.; Shikanai, T., Composition and physiological function of the chloroplast NADH dehydrogenase-like complex in *Marchantia polymorpha*. *Plant J* **2012**, 72, (4), 683-93.
202. You, C.; Cui, J.; Wang, H.; Qi, X.; Kuo, L. Y.; Ma, H.; Gao, L.; Mo, B.; Chen, X., Conservation and divergence of small RNA pathways and microRNAs in land plants. *Genome Biol* **2017**, 18, (1), 158.
203. Lin, P. C.; Lu, C. W.; Shen, B. N.; Lee, G. Z.; Bowman, J. L.; Arteaga-Vazquez, M. A.; Liu, L. Y.; Hong, S. F.; Lo, C. F.; Su, G. M.; Kohchi, T.; Ishizaki, K.; Zachgo, S.; Althoff, F.; Takenaka, M.; Yamato, K. T.; Lin, S. S., Identification of miRNAs and Their Targets in the Liverwort *Marchantia polymorpha* by Integrating RNA-Seq and Degradome Analyses. *Plant Cell Physiol* **2016**, 57, (2), 339-58.
204. Lin, S. S.; Bowman, J. L., MicroRNAs in *Marchantia polymorpha*. *New Phytol* **2018**, 220, (2), 409-416.
205. Waterhouse, A.; Bertoni, M.; Bienert, S.; Studer, G.; Tauriello, G.; Gumienny, R.; Heer, F. T.; de Beer, T. A. P.; Rempfer, C.; Bordoli, L.; Lepore, R.; Schwede, T., SWISS-MODEL: homology modelling of protein structures and complexes. *Nucleic Acids Res* **2018**, 46, (W1), W296-w303.
206. Wang, Y.; Xu, L.; Thilmony, R.; You, F. M.; Gu, Y. Q.; Coleman-Derr, D., PIECE 2.0: an update for the plant gene structure comparison and evolution database. *Nucleic Acids Res* **2017**, 45, (D1), 1015-1020.

207. Huerta-Cepas, J.; Serra, F.; Bork, P., ETE 3: Reconstruction, Analysis, and Visualization of Phylogenomic Data. *Mol Biol Evol* **2016**, 33, (6), 1635-8.
208. Price, M. N.; Dehal, P. S.; Arkin, A. P., FastTree: computing large minimum evolution trees with profiles instead of a distance matrix. *Mol Biol Evol* **2009**, 26, (7), 1641-50.
209. Peng, L.; Zhang, F.; Shang, R.; Wang, X.; Chen, J.; Chou, J. J.; Ma, J.; Wu, L.; Huang, Y., Identification of substrates of the small RNA methyltransferase Hen1 in mouse spermatogonial stem cells and analysis of its methyl-transfer domain. *J Biol Chem* **2018**, 293, (26), 9981-9994.
210. Schmid, M. W.; Giraldo-Fonseca, A.; Rövekamp, M.; Smetanin, D.; Bowman, J. L.; Grossniklaus, U., Extensive epigenetic reprogramming during the life cycle of *Marchantia polymorpha*. *Genome Biol* **2018**, 19, (1), 9.
211. Zhao, S.; Liu, M. F., Mechanisms of microRNA-mediated gene regulation. *Sci China C Life Sci* **2009**, 52, (12), 1111-6.
212. Boutet, S.; Vazquez, F.; Liu, J.; Béclin, C.; Fagard, M.; Gratias, A.; Morel, J. B.; Crété, P.; Chen, X.; Vaucheret, H., Arabidopsis HEN1: a genetic link between endogenous miRNA controlling development and siRNA controlling transgene silencing and virus resistance. *Curr Biol* **2003**, 13, (10), 843-8.
213. Ratcliff, F.; Harrison, B. D.; Baulcombe, D. C., A similarity between viral defense and gene silencing in plants. *Science* **1997**, 276, (5318), 1558-60.
214. Baulcombe, D., RNA silencing. *Trends Biochem Sci* **2005**, 30, (6), 290-3.
215. Ding, S. W.; Li, H.; Lu, R.; Li, F.; Li, W. X., RNA silencing: a conserved antiviral immunity of plants and animals. *Virus Res* **2004**, 102, (1), 109-15.

- 
216. Wilkins, C.; Dishongh, R.; Moore, S. C.; Whitt, M. A.; Chow, M.; Machaca, K., RNA interference is an antiviral defence mechanism in *Caenorhabditis elegans*. *Nature* **2005**, 436, (7053), 1044-7.
217. Kim, V. N.; Nam, J. W., Genomics of microRNA. *Trends Genet* **2006**, 22, (3), 165-73.
218. Hammond, S. M.; Caudy, A. A.; Hannon, G. J., Post-transcriptional gene silencing by double-stranded RNA. *Nat Rev Genet* **2001**, 2, (2), 110-9.
219. Kasschau, K. D.; Xie, Z.; Allen, E.; Llave, C.; Chapman, E. J.; Krizan, K. A.; Carrington, J. C., P1/HC-Pro, a viral suppressor of RNA silencing, interferes with Arabidopsis development and miRNA unction. *Dev Cell* **2003**, 4, (2), 205-17.
220. Bartel, D. P., MicroRNAs: genomics, biogenesis, mechanism, and function. *Cell* **2004**, 116, (2), 281-97.
221. Pfeffer, S.; Zavolan, M.; Grässer, F. A.; Chien, M.; Russo, J. J.; Ju, J.; John, B.; Enright, A. J.; Marks, D.; Sander, C.; Tuschl, T., Identification of virus-encoded microRNAs. *Science* **2004**, 304, (5671), 734-6.
222. Buchon, N.; Vaury, C., RNAi: a defensive RNA-silencing against viruses and transposable elements. *Heredity (Edinb)* **2006**, 96, (2), 195-202.
223. Brodersen, P.; Voinnet, O., The diversity of RNA silencing pathways in plants. *Trends Genet* **2006**, 22, (5), 268-80.
224. Chapman, E. J.; Carrington, J. C., Specialization and evolution of endogenous small RNA pathways. *Nat Rev Genet* **2007**, 8, (11), 884-96.
225. Carrington, J. C.; Ambros, V., Role of microRNAs in plant and animal development. *Science* **2003**, 301, (5631), 336-8.

- 
226. Voinnet, O., Induction and suppression of RNA silencing: insights from viral infections. *Nat Rev Genet* **2005**, 6, (3), 206-20.
227. Ratcliff, F. G.; MacFarlane, S. A.; Baulcombe, D. C., Gene silencing without DNA. rna-mediated cross-protection between viruses. *Plant Cell* **1999**, 11, (7), 1207-16.
228. Lecellier, C. H.; Voinnet, O., RNA silencing: no mercy for viruses? *Immunol Rev* **2004**, 198, 285-303.
229. Voinnet, O.; Pinto, Y. M.; Baulcombe, D. C., Suppression of gene silencing: a general strategy used by diverse DNA and RNA viruses of plants. *Proc Natl Acad Sci U S A* **1999**, 96, (24), 14147-52.
230. Li, F.; Ding, S. W., Virus counterdefense: diverse strategies for evading the RNA-silencing immunity. *Annu Rev Microbiol* **2006**, 60, 503-31.
231. Yambao, M. L.; Yagihashi, H.; Sekiguchi, H.; Sekiguchi, T.; Sasaki, T.; Sato, M.; Atsumi, G.; Tacahashi, Y.; Nakahara, K. S.; Uyeda, I., Point mutations in helper component protease of clover yellow vein virus are associated with the attenuation of RNA-silencing suppression activity and symptom expression in broad bean. *Arch Virol* **2008**, 153, (1), 105-15.
232. González-Jara, P.; Atencio, F. A.; Martínez-García, B.; Barajas, D.; Tenllado, F.; Díaz-Ruíz, J. R., A Single Amino Acid Mutation in the Plum pox virus Helper Component-Proteinase Gene Abolishes Both Synergistic and RNA Silencing Suppression Activities. *Phytopathology* **2005**, 95, (8), 894-901.
233. Moissiard, G.; Voinnet, O., Viral suppression of RNA silencing in plants. *Mol Plant Pathol* **2004**, 5, (1), 71-82.
234. Chung, B. Y.; Miller, W. A.; Atkins, J. F.; Firth, A. E., An overlapping essential gene in the Potyviridae. *Proc Natl Acad Sci U S A* **2008**, 105, (15), 5897-902.

- 
235. Shi, M. L.; Li, H. Y.; Schubert, J.; Zhou, X. P., Sequence analysis of CP and HC-Pro genes of Turnip mosaic virus isolates from China. *Acta Virol* **2008**, 52, (1), 59-62.
236. Maia, I. G.; Haenni, A.; Bernardi, F., Potyviral HC-Pro: a multifunctional protein. *J Gen Virol* **1996**, 77 (Pt 7), 1335-41.
237. Urcuqui-Inchima, S.; Walter, J.; Drugeon, G.; German-Retana, S.; Haenni, A. L.; Candresse, T.; Bernardi, F.; Le Gall, O., Potyvirus helper component-proteinase self-interaction in the yeast two-hybrid system and delineation of the interaction domain involved. *Virology* **1999**, 258, (1), 95-9.
238. Vargason, J. M.; Szittyá, G.; Burgyán, J.; Hall, T. M., Size selective recognition of siRNA by an RNA silencing suppressor. *Cell* **2003**, 115, (7), 799-811.
239. Reed, J. C.; Kasschau, K. D.; Prokhnevsky, A. I.; Gopinath, K.; Pogue, G. P.; Carrington, J. C.; Dolja, V. V., Suppressor of RNA silencing encoded by Beet yellows virus. *Virology* **2003**, 306, (2), 203-9.
240. Silhavy, D.; Molnár, A.; Lucioli, A.; Szittyá, G.; Hornyik, C.; Tavazza, M.; Burgyán, J., A viral protein suppresses RNA silencing and binds silencing-generated, 21- to 25-nucleotide double-stranded RNAs. *Embo j* **2002**, 21, (12), 3070-80.
241. Varrelmann, M.; Maiss, E.; Pilot, R.; Palkovics, L., Use of pentapeptide-insertion scanning mutagenesis for functional mapping of the plum pox virus helper component proteinase suppressor of gene silencing. *J Gen Virol* **2007**, 88, (Pt 3), 1005-1015.
242. Han, M. H.; Goud, S.; Song, L.; Fedoroff, N., The Arabidopsis double-stranded RNA-binding protein HYL1 plays a role in microRNA-mediated gene regulation. *Proc Natl Acad Sci U S A* **2004**, 101, (4), 1093-8.

- 
243. Martínez, F.; Daròs, J. A., Tobacco etch virus protein P1 traffics to the nucleolus and associates with the host 60S ribosomal subunits during infection. *J Virol* **2014**, 88, (18), 10725-37.
244. Leibman, D.; Wolf, D.; Saharan, V.; Zelcer, A.; Arazi, T.; Yoel, S.; Gaba, V.; Gal-On, A., A high level of transgenic viral small RNA is associated with broad potyvirus resistance in cucurbits. *Mol Plant Microbe Interact* **2011**, 24, (10), 1220-38.
245. Rajamäki, M. L.; Kelloniemi, J.; Alminante, A.; Kekarainen, T.; Rabenstein, F.; Valkonen, J. P., A novel insertion site inside the potyvirus P1 cistron allows expression of heterologous proteins and suggests some P1 functions. *Virology* **2005**, 342, (1), 88-101.
246. Valli, A.; Martín-Hernández, A. M.; López-Moya, J. J.; García, J. A., RNA silencing suppression by a second copy of the P1 serine protease of Cucumber vein yellowing ipomovirus, a member of the family Potyviridae that lacks the cysteine protease HCPro. *J Virol* **2006**, 80, (20), 10055-63.
247. Pasin, F.; Shan, H.; García, B.; Müller, M.; San León, D.; Ludman, M.; Fresno, D. H.; Fátýol, K.; Munné-Bosch, S.; Rodrigo, G.; García, J. A., Absciscic Acid Connects Phytohormone Signaling with RNA Metabolic Pathways and Promotes an Antiviral Response that Is Evaded by a Self-Controlled RNA Virus. *Plant Commun* **2020**, 1, (5).
248. Tena Fernández, F.; González, I.; Doblas, P.; Rodríguez, C.; Sahana, N.; Kaur, H.; Tenllado, F.; Praveen, S.; Canto, T., The influence of cis-acting P1 protein and translational elements on the expression of Potato virus Y helper-component proteinase (HCPro) in heterologous systems and its suppression of silencing activity. *Mol Plant Pathol* **2013**, 14, (5), 530-41.

249. Baranauskė, S.; Mickutė, M.; Plotnikova, A.; Finke, A.; Venclovas, Č.; Klimašauskas, S.; Vilkaitis, G., Functional mapping of the plant small RNA methyltransferase: HEN1 physically interacts with HYL1 and DICER-LIKE 1 proteins. *Nucleic Acids Res* **2015**, 43, (5), 2802-12.
250. Wieczorek, P.; & Obrepalska-Stęplowska, A.; Suppress to survive—implication of plant viruses in PTGS. *Plant Molecular Biology Reporter* **2015**, 33(3), 335-346.
251. Sanobar, N.; Lin, P.C.; Pan, Z.J.; Fang, R.Y.; Tjita, V.; Chen, F.F.; Wang, H.C.; Tsai, H.L.; Wu, S.H.; Shen, T.L. and Chen, Y.H., Investigating the viral suppressor HC-pro inhibiting small RNA methylation through functional comparison of HEN1 in angiosperm and bryophyte. *Viruses* **2021**, 13(9), p.1837.